ABSTRACT

MZYK, PHILIP CHRISTOPHER. Effects of Hypoxia and Iron Chelation on the Metabolism of the Amyloid Precursor Protein in Retinal Pigmented Epithelial Cells. (Under the direction of Dr. Mary McGahan).

Two common pathogenic stimuli, altered oxygen concentration and iron availability, change the intricate interrelationship between iron and the metabolism of the amyloid precursor protein (APP) in the retinal pigmented epithelium (RPE) of the eye, causing disruptive effects on cellular metabolism. In hypoxia, both APP and iron are depleted. When iron is deficient APP is not properly processed for full functionality. Crucially, APP is metabolized into active metabolites, one of which helps to regulate cellular iron levels. Our recent findings have led us to focus on the interrelationship of hypoxia, iron, and APP within the RPE. Here, we further characterized how APP is altered by changes in both iron and oxygen metabolism, as well as by changes in their levels in primary, cultured RPE cells. Additionally, we identified a novel role for APP in photoreceptor phagocytosis.

First, we studied how hypoxia altered the levels, localization, and secretion of APP from polarized and non-polarized RPE. We found that intracellular levels of APP are decreased in hypoxic conditions. In order to determine how hypoxia caused a decrease in APP levels in RPE cells, we studied if it affected the synthesis or degradation of APP. We found that hypoxia decreased APP's synthesis, but not its degradation.

Hypoxia also caused a change in directional secretion of APP, with a dramatic decrease (92%) in apical secretion. Three dimensional quantitative fluorescence imaging of APP in fixed, polarized RPE cells showed that APP localization is substantially affected by hypoxia. APP almost completely disappeared from the apical surface which is in agreement with the directional secretion data.

In order to determine the mechanism by which APP is directionally secreted we studied an intracellular protein transporter, retromer, responsible for membrane localization. Like APP, retromer levels are greatly decreased in hypoxic conditions. Knockdown of retromer with siRNA also decreased the secretion of APP from the RPE. Therefore, it is likely that retromer participates in the movement of APP to its proper location in RPE cells. These projects provided novel insight into the mechanisms by which hypoxia was altering APP synthesis, localization, and section from the RPE.

APP undergoes extensive glycosylation in a highly orchestrated post-translational process. Iron chelation was utilized to study the effects of altered iron metabolism on APP glycosylation. Our studies revealed that a decrease in iron levels causes APP glycosylation to be significantly altered. Specifically, the terminal glycan sialic acid is likely either not added or removed when the iron content of the cell is lowered. This finding demonstrates that the maturation of APP may be iron dependent.

Lastly, we investigated a functional role for APP in RPE cells. Normally, the RPE phagocytose photoreceptor outer segments. APP has characteristics of cell surface receptors and adhesion molecules. Therefore, we hypothesized that APP may participate in the phagocytic process. We designed a study in which siRNA was used to knockdown APP in RPE cells, and then fed those cells photoreceptor outer segments. We found that APP knockdown decreased the ability of the RPE to phagocytosis photoreceptor outer segments. These results demonstrate a novel role for APP in the metabolism of photoreceptors and demonstrate that APP may act as a cellular receptor or adhesion molecule. Therefore, a hypoxia induced decreased in APP levels on the apical surface of the RPE could have serious effects on one of the RPE's critical roles in the visual pathway.

Effects of Hypoxia and Iron Chelation on the Metabolism of the Amyloid Precursor Protein in Retinal Pigmented Epithelial Cells

by
Philip Christopher Mzyk

A dissertation submitted to the Graduate Faculty of
North Carolina State University
in partial fulfillment of the
requirements for the degree of
Doctor of Philosophy

Comparative Biomedical Sciences

Raleigh, North Carolina

2018

APPROVED BY:

_____	_____
Dr. Mary McGahan Committee Chair	Dr. Samuel Jones
_____	_____
Dr. Nanette Nascone-Yoder	Dr. Brian Gilger
_____	
Dr. Freya Mowat	

DEDICATION

To my family, for never saying I couldn't.

To my wife, for always making sure that I could.

BIOGRAPHY

Born in Germany, but raised in North Carolina, Philip has always been curious about the way that science can tell the story of how life works. This curiosity led him to pursue a PhD after receiving his bachelor's degree in zoology from NC State University in 2012. Being born three months early, Philip has always wondered how the body is able to overcome such a large loss in its developmental timeline. For Philip, this loss was most apparent in his vision, so when he was offered the chance to pursue a PhD in the lab of Dr. Chris McGahan studying the mechanisms of ocular diseases, he knew it was a good fit for his background. Outside of his research, Philip enjoys all forms of cooking, reading, and getting to spend time with his wife and pets.

ACKNOWLEDGMENTS

I have had quite an adventure while completing this degree. I have a new appreciation for what it means to be a scientist, and that is in large part to the many people that have helped me to reach this point.

First, I have to say a heartfelt thank you to my mentor, *Dr. Chris McGahan* for taking me into her lab when I was just an undergraduate. You have shown me not only how to be a scientist, but to also remember that every achievement within a lab comes from the entire team working together. Your effort in taking the time to really improve my writing will be a tremendous benefit that I will be able to utilize throughout my scientific career. I will never forget your favorite line that, "The data is the data!" That always reminds me that no matter how an experiment turns out, you have to interpret the data as it stands, and look at the whole picture, not just what you want to see. You took the time to make sure that not only my science was taken care of, but that I too was always doing okay, and that has always meant a lot to me.

Next, I have to thank all of the lab members that I have had the privilege to work beside: *Dr. Steve Nagar*, *Jill Harned*, and *Dr. Margaret Goralska*. Steve, you always listened when I needed to talk out an experiment, and I swear that I planned so many experiments during our endless talks within the office! Your passion for cooking and gardening helped me to focus on life outside of the lab too, and for that I am very thankful. Jill, you always knew exactly how I needed to fine tune an experiment to get it back on track. Your willingness to always share your tips and tricks helped me so much in my bench work, not to mention it avoided so much frustration on my part knowing that I wasn't the first to have a problem on any number of protocols. Margaret, I still remember coming in early my first summer in the lab when you taught me how to do Westerns. You joked that now that I knew how they worked, that I might

get stuck doing them all the time, and that certainly came true! All of you helped to shape the scientist I am today, and for that I am forever grateful.

To my committee members, *Dr. Sam Jones, Dr. Freya Mowat, Dr. Brian Gilger,* and *Dr. Nanette-Nascone Yoder*, thank you all for helping me to craft the story behind my science, and ensuring that I always asked more questions about my work to keep pushing it forward.

I am very thankful to *Dr. Michael Bereman* and his lab for providing their expert support in analyzing my mass spectroscopy samples. Their effort helped us to look at our experiments in a new light beyond the capabilities that our lab alone could undertake.

To my family, your endless support along this journey has been more helpful than you can ever know. I don't think any of us knew exactly what I was getting into when I started all of this, but I know your encouragement has helped so much during it all.

Lastly, to my wife who knows exactly what it takes to finish this degree! Your persistence in telling me that I could do it, coupled with your tremendous love and support during all of my experiments and the long writing process made all of this that much better. Plus, the ability to always be able to go pet a cute baby animal was a major perk when life was just getting a little too crazy.

TABLE OF CONTENTS

LIST OF FIGURES

Appendix 2 - Mass Spectrometry and Lectin Blotting for Analysis of APP Glycosylation

CHAPTER 1

A Review of the Literature Regarding Ocular Physiology, Iron and Oxygen Metabolism, and the Amyloid Precursor Protein

Overview

Age-related macular degeneration (AMD) is the main cause of irreversible vision loss in the elderly, accounting for about half of the newly registered cases of blindness in the developed world. Unfortunately, the pathologic mechanisms underlying AMD are incompletely understood. However, in AMD there is dysregulation of the metabolism of both iron and the amyloid precursor protein (APP). Iron is an essential trace element which is important in retinal physiology for proper enzyme function and it is vital for cellular respiration. APP and its byproducts have been implicated in the progression of AMD. In addition, within the eye, the retina has varied iron and oxygen levels, both of which can be altered in pathological conditions. Importantly, iron and APP metabolism are interrelated in a feedback loop; iron regulates APP synthesis and its glycosylation, and APP in turn regulates iron levels in cells.

A deeper mechanistic understanding of the connection between iron and APP metabolism is the basis of this dissertation as it is essential to understand these critical aspects of ocular pathology. The premise of this work is that two common pathogenic stimuli, altered oxygen concentration and iron availability, change the intricate interrelationship between iron and APP metabolism in the retinal pigmented epithelium (RPE), causing disruptive effects on cellular function. In hypoxia, iron is depleted, while iron levels increase in response to iron overload in the RPE. We have also found that APP is depleted in hypoxia and is not properly processed for full functionality when iron is deficient. Results from this work will provide information critical to the development of new treatments for diseases in which iron and APP play key roles, with the ultimate disposition of APP and its reciprocal effects on iron metabolism to be the subject of future work.

Anatomy of the Eye: Focusing on the Retinal Pigmented Epithelium

The eye is responsible for turning light into an electrical signal that can be interpreted by the brain. The exterior of the eye is covered by the cornea, which acts as a protective membrane for the eye, as well as providing roughly 75% of the focusing power of the eye (Figure 1.1). Behind the cornea is the anterior segment of the eye, which is filled with aqueous humor, a fluid which helps to maintain the intraocular pressure of the eye. Next comes the lens, which provides the remaining focusing power of the eye. Following the lens is the posterior chamber, which is filled with vitreous humor, which also maintains intraocular pressure. At the back of the posterior chamber is the retina (Figure 1.2). The retina is responsible for converting the focused light of the eye into the electrical signals that are transmitted to the brain via the optic nerve. The retina sits atop the retinal pigmented epithelium (RPE) which maintains a basement membrane called Bruch's membrane. This membrane separates the RPE and retina from the choroidal vasculature of the eye. The work within this dissertation focuses specifically on the physiology of the RPE.

The RPE is a highly specialized monolayer of heavily pigmented, tight junctional, polarized cells (Figure 1.3). The RPE makes up the outer blood retinal barrier. This barrier is formed by the tight junctions comprised primarily of the zonulae occludentes [1, 2]. These tight junctions regulate the flow of ions into and out of the eye and prevent diffusion of large toxic molecules from the choroidal capillaries to the photoreceptors of the neural retina above. They also separate the apical and basolateral domains of the RPE, allowing for the appropriate polarized movement of substrates into and out of the retina. The inner blood retinal barrier is formed by the zonula occludentes between endothelial cells of the retinal circulation in species like dogs and humans that have a retinal vasculature.

A myriad of sorting signals determine where proteins travel within the RPE. Apical sorting signals are usually found within a protein's glycans, segments of the protein bound within the membrane, or their C terminal domain [3]. Some common apical sorting signals seen within the RPE are glycosylphosphatidylinisotol (GPI) anchors, N- or O- glycans, or dynein binding sites [4]. Basolateral sorting signals are usually short, simple peptide motifs found in the C terminal domain [3]. Common basolateral sorting signals in the RPE are tyrosine or dileucine motifs [4].

One example of how the RPE regulates polarity is seen by how the RPE ensures that fluid is continually transported out of the subretinal space. This movement of fluid away from the subretinal space towards the choroid allows the RPE to maintain a negative hydrostatic pressure within the subretinal space [4]. This pressure is necessary for the adhesion of the photoreceptor outer segments to the apical villi and surface of the RPE. Without this tight adhesion, retinal detachment can occur, resulting in vision loss [5].

The RPE also has one of its major ion transporters, the sodium potassium ATPase pump, located apically instead of the usual basal localization that this pump assumes in other epithelial cells [6]. This change in localization is thought to aid in phototransduction with the photoreceptors. During phototransduction, the photoreceptors require a large amount of sodium to properly function, and the apically located sodium potassium pump is able to provide this necessary ion [7].

For another example of how the RPE controls and, in stressed states, can enhance polarization, specifically basolateral localization and secretion, consider how the RPE upregulates the production of the potent antioxidant glutathione when placed under oxidative stress by ensuring that the amino acid glutamate is secreted basolaterally. Under normal

conditions, glutamate is preferentially secreted basolaterally. RPE cells contain the X_c^- antiporter, which exchanges glutamate for cysteine. Cystine is reduced in cells to cysteine, the rate limiting amino acid for glutathione synthesis. Therefore, when the RPE secretes glutamate, it is accompanied by an exchange for cystine causing an increase in production of the essential intracellular antioxidant, glutathione [8]. Because the RPE routinely are exposed to high levels of free radicals as seen with POS phagocytosis, production of glutathione is very beneficial for the RPE. Under oxidative stress, the RPE cause the polarization of glutamate secretion in the basolateral direction to be significantly increased. Therefore increased secretion of glutamate from the basolateral surface would provide an advantage by increasing the production of glutathione when the RPE is being stressed. The above example shows how the RPE is able to internally control its contents through the proper polarized localization and secretion of glutamate. The RPE also ensures the proper polarized transport of numerous other components, such as moving glucose apically for energy metabolism to the photoreceptors and removing excess lactic acid basolaterally [9, 10].

The basolateral membrane of the RPE connects with the highly specialized and multilayered Bruch's membrane. Bruch's membrane is synthesized and maintained by the RPE and the underlying choroidal vasculature [11]. Bruch's membrane is a crucial component of the retina, as a permeable Bruch's membrane allows for nutrients, metabolites and oxygen exchange between the capillaries and the retina [12].

Age-Related Macular Degeneration

Age-related macular degeneration (AMD) is a progressive neurodegeneration of the retina, specifically within the macula [13]. The macula is the area of the retina responsible for visual acuity and color vision, so degeneration of this area leads to severe vision loss. Besides

age and genetics, multiple risk factors exist that have been linked to AMD susceptibility, including obesity, hypertension, atherosclerosis and smoking [14]. These factors have been shown to contribute to the key process that results in vision loss in AMD, namely the gradual impairment of the RPE [15].

Two forms of AMD occur. The more prevalent form is the dry form of AMD, where sub-RPE deposits called drusen form under the RPE, and ultimately disrupt the RPE monolayer, leading to RPE and photoreceptor apoptosis [13]. Drusen formation increases the distance between the choroid and the retina. This causes a reduced flow of oxygen from the choroid to the retina, resulting in a hypoxic environment for the RPE and photoreceptors [16]. Drusen is partially composed of APP byproducts [14]. As such, APP dysregulation may contribute to AMD progression. Additionally, iron has been found in higher levels in both the RPE and photoreceptors of those with AMD [17].

The second form of AMD is called the wet form, because it involves the neovascularization of vessels that break through the RPE, again ultimately leading to vision loss. Hypoxia is also believed to play a role in the progression of the wet form of AMD. Choroidal ischemia, resulting in decreased blood flow to the retina, is a prognostic indicator for wet AMD [16]. Hypoxia inducible factor, which is upregulated in hypoxic conditions, is present in higher amounts in wet AMD, as is vascular endothelial growth factor, which is also stimulated by hypoxic conditions [18]. Lastly, empirical data shows that when compared to non-AMD patients, the ability of the retina to extract oxygen from retinal vessels is lowered in patients with the wet form of AMD [16].

The Visual Cycle: The Relationship between Photoreceptors and the RPE

Photoreceptors (shown in figures 1.2 and 1.3) are specialized neurons at the back of the retina where photons of light are detected in the initial steps of the visual cycle [19]. The light sensitive photoreceptors of the retina interdigitate with the apical microvilli of the RPE. The RPE participates in the visual cycle and is responsible not only for the nutrition of photoreceptors but also for the proper phagocytosis and turnover of photoreceptor outer segments (POS) [20]. The interaction between the RPE and photoreceptors is critical for visual function.

The purpose of the retina is to convert photochemical transductions into nerve impulses that can be created and transmitted along the visual pathway to the brain for higher cortical processing (Figure 1.4). This pathway relies on the retina and its multiple layers for its functionality. For phototransduction to begin, light must first reach the retina. To do so, light is focused through the cornea after which it is further focused through the lens. This focused wave of light, which is comprised of photons, passes through the clear vitreous humor and is next absorbed by the photoreceptors of the retina. Within the photoreceptors, light isomerizes the 11-*cis*-retinal chromophore of rhodopsin to its all-*trans*-retinal isomer. This photoisomerization is the initial and only light dependent reaction in the phototransduction cascade, with its end product being the conversion of light into an electrical signal that is processed into a visual signal [21].

Once rhodopsin is isomerized to its all-*trans* state, it loses its light sensitivity, and must be converted back into 11-*cis*-retinal. This reisomerization of rhodopsin from its *trans* state back to its *cis* state is a key component of the visual cycle. This reisomerization can occur because 20 to 40 photoreceptor cells project towards and interdigitate with each RPE cell [22]. This close

contact allows the all-*trans* form of rhodopsin to move into the RPE, where reisomerization occurs. Without this reisomerization in the RPE, phototransduction would not be able to take place.

After *trans*-retinol is taken up by the neighboring RPE, it is esterified by lecithin:retinol acyltransferase (LRAT). This esterification allows all-*trans* retinol to serve as the substrate for the crucial RPE65 enzyme within the RPE. The iron dependent RPE65 enzyme is then able to catalyze the conversion of all-*trans*-retinal into 11-*cis*-retinol, which is further oxidized within the RPE into 11-*cis*-retinal. 11-*cis*-retinal is then moved back into the photoreceptors, where it is able to couple to opsin and form rhodopsin, which can then participate in the phototransduction cascade again [23]. If the RPE65 enzyme does not function properly within the RPE, toxic levels of *trans*-retinol can build up within the RPE since it cannot be reduced to its *cis* form. As such, the phototransduction cascade cannot occur, leading to retinal degenerations such as AMD and ultimate loss of vision [22, 23].

The intricate relationship between the RPE and photoreceptors explained above in the visual cycle is crucial for vision as well as the protection of the retina. Though retinals are extremely well suited for signaling the arrival of a photon and inducing phototransduction, they are also very sensitive to oxidation and are thus extremely toxic [24]. Additionally, if the RPE is damaged and POS cannot be properly phagocytosed, then the RPE will have a buildup of large levels of POS that it cannot properly degrade. This excess POS buildup will lead to rapid photoreceptor degeneration and vision loss since the RPE cannot properly function [25]. This interplay of RPE and photoreceptor cells creates a rich environment for oxidative damage as it has high lipid, oxygen and iron content. Even during the regular phagocytosis of POS free radicals are released into the RPE. However, the RPE is able to mitigate the harmful effects

from these free radicals, by employing its pigment granules to absorb excess light, especially blue light, as well as enzymatic and non-enzymatic anti-oxidants to remove excess free radicals and other deleterious byproducts [26].

Blue light is a short wavelength light that induces retinal damage by generating reactive oxygen species. These reactive oxygen species have been shown to damage the photoreceptor outers segments, as well as stall cellular proliferation, and harm the mitochondria within the RPE [26]. Blue light absorption by the RPE is critical because blue light causes the greatest damage to the retina when compared against all other types of light within the visible spectrum. Since light must pass through the entire retina to reach the photoreceptors (see figure 1.2), the RPE pigment prevents the return of excess light into the photoreceptive layer of the retina and ultimately helps to quench harmful light derived reactive oxygen species. Specifically, the pigment within the RPE is able to reduce the amount of blue light that interacts with the retina by 40% due to the presence of carotenoids in the RPE pigment [26]. These carotenoids interact with free radicals and prevent lipid peroxidation by taking the energy generated from the free radicals and transferring it into the carotenoid where it cannot be utilized in harmful cellular reactions [26]. Additionally, carotenoids are known to act synergistically with other antioxidants, such as vitamin C, and their activity is enhanced in the low oxygen environments that the retina is in under normal physiological conditions [26].

Iron Metabolism

Iron is a trace metal essential for many specific enzymatic processes as well as being utilized in other metabolic functions; some of which are oxygen transport, DNA synthesis (as a cofactor for ribonucleotide reductase), and electron transport [27]. In eukaryotic organisms, over 1000 different iron-dependent proteins have been identified [28]. Iron primarily exists in two

oxidation states, ferrous (Fe^{2+}) and ferric (Fe^{3+}) [29]. Single electron exchanges convert one form to the other. Iron has many key functions that are only recently being discovered, such as the control of glutamate secretion (an excitotoxic neurotransmitter in the brain and the retina) and glutathione levels (a strong antioxidant) in cells [8, 30]. The retina and the RPE contain all of the iron regulatory proteins thus far discovered. Importantly, as discussed earlier, a key enzyme in the visual cycle, RPE65, is an iron dependent enzyme [31]. When the iron binding sites on the RPE65 enzyme are mutated, RPE65 activity can be greatly reduced and, in some circumstances, even abolished, severely affecting normal visual function [22].

Even though iron is essential for proper cellular functions, iron can also catalyze damaging free radical reactions by creating reactive oxygen species (ROS), and therefore its levels are highly regulated. ROS play a fundamental role in the pathophysiology of dozens of diseases and the iron-catalyzed formation of ROS is a major player in these processes [32]. Within the eye, ROS participate in tissue damage which contributes to many diseases including cataractogenesis, diseases of the cornea, retinal degeneration, diabetic retinopathy, glaucoma, photoreceptor damage, and age-related macular degeneration [17, 33-38]. The pathway to ROS formation can begin when the oxygen radical superoxide is produced from oxidized reactions in the mitochondria and other redox reactions in cells. Superoxide is detoxified by superoxide dismutase which results in the formation of hydrogen peroxide. In the presence of ferrous iron (Fe^{2+}) hydrogen peroxide can form the highly reactive and damaging hydroxyl radical ($^{\cdot}OH$), a ROS. It is crucial to understand how the RPE regulates its iron content, and how iron metabolism is dysregulated under pathological circumstances, unleashing its potent ability to cause oxidative damage and other deleterious effects.

In the blood, ferric iron (Fe^{3+}) is primarily bound to the glycoprotein transferrin (Tf), which has two iron binding sites. Under normal physiological conditions, these two iron binding sites are normally not both occupied by iron but have a high affinity for it [39]. This high iron affinity gives Tf a very potent antioxidant ability, as unbound Tf will readily bind any free iron. In mice with retinal degeneration (rd10 mice), Tf has been shown to prevent photoreceptor degeneration and Tf levels are increased in AMD retinas [40, 41]. Within the intraocular fluids (IOFs) of the eye, Tf is found in high concentrations, because it is made and secreted by many ocular tissues, including the RPE [42]. Once iron is bound to Tf, it is unable to catalyze free radical formation [42, 43]. However, during ocular inflammation, Tf becomes saturated with iron and non-transferrin bound iron accumulates in the IOFs making it available to catalyze free radical reactions or for uptake by the retina and other ocular tissues [44]. Uptake from non-Tf bound iron sources is not tightly regulated compared to Tf-bound iron, therefore increasing the potential for cellular iron overload [45].

Transferrin receptors (TfR) are found on the cell surface and in clathrin coated membrane pits where they have a high affinity for diferric Tf (Figure 1.5). After a TfR binds Tf, it is internalized by endocytosis into an endosome. RPE cells have TfRs on both the basolateral and apical surfaces and can take up iron from either side [46]. Once Tf is internalized, the resulting endosomes become acidified through the actions of a proton dependent ATPase, which actively moves H^+ into the endosome to lower the pH. Iron is released from Tf due to this acidic environment, converted from ferric to ferrous iron, and removed from the endosome by the proton-metal symporter divalent metal transporter (DMT1) to the cytoplasm for transport to sites of storage or utilization. The TfR is then recycled back to the cell surface [29].

Iron can also be taken up in the form of heme, a breakdown product of hemoglobin, which is present in tissues after hemorrhage. Heme is then further metabolized intracellularly, with iron released for use by the cell or storage in the iron storage protein ferritin. However, iron storage capacity can be overwhelmed and the excess iron can cause damage.

Once inside the cytoplasm either through TfR endocytosis or heme internalization, iron can be utilized for the assembly of iron-sulfur clusters, maturation of various non-heme iron enzymes, stored in ferritin, or exported out of the cell [47]. The ubiquitous iron storage protein ferritin is a multimeric protein containing 24 subunits of two types, heavy (H) and light (L), which are present in tissue specific ratios. Each ferritin molecule is capable of storing 4,500 atoms of iron, making ferritin extremely effective at binding excess free iron within the cell.

The only protein responsible for iron efflux from cells so far identified is ferroportin (FPN). This essential protein needs the presence of a ferroxidase to convert the ferrous iron found intracellularly to the ferric form that is needed for binding to the extracellular Tf. Ceruloplasmin and hephaestin are ferroxidases that convert iron to its ferric form and with FPN remove iron from cells and allow it to bind Tf for transport away from the cell. RPE cells primarily express FPN on the basolateral membrane. FPN levels are regulated by the hormone hepcidin. Hepcidin is a negative regulator of FPN. It removes FPN from the cellular membrane via endocytosis and targets it for degradation. This negative regulation is triggered when intracellular iron levels are low. By removing FPN from the membrane, hepcidin decreases secretion of iron from the cell, enabling maintenance of proper intracellular iron levels. Dysregulation of hepcidin, FPN, or FPN's associated ferroxidases leads to retinal degeneration [48-50].

Once iron is taken up into cells, or is released from storage in ferritin or from proteins of which it is an essential component, it transits through a pool called labile cell iron (LCI) [51]. Very little is known about this process, since there are currently no acceptable tools available for its study. Iron chaperones, fluorescent iron probes and chelators have been utilized, but there has been little progress made to directly measure how LCI or the actual movement of iron around the cell between compartments is regulated. Additionally, there are intracellular source-dependent pools of iron, further complicating the understanding of intracellular iron metabolism [52]. Importantly, iron acutely controls the synthesis of its own regulatory and storage proteins at the translational level through the iron controlled binding of an iron regulatory protein (IRP) to an iron responsive element (IRE) in the untranslated region of ferritin or the transferrin receptor (Figure 1.6) [53]. In addition to the regulation of ferritin synthesis at the translational level, the ratio of the H:L chains of ferritin is regulated by differences in half-life and secretion for each chain [54, 55]. Due to this control of iron regulatory and storage proteins, the measurements of these proteins are used as surrogates to estimate whether the LCI increases or decreases in size. As an example, excess iron in cells is associated with an increase in ferritin concentration. This is a result of the cell synthesizing more ferritin to bind the excess iron and prevent ROS damage.

Cells can inappropriately sequester iron in intracellular compartments or in the iron storage protein ferritin. This can appear to be iron overload when total iron is measured or tissue sections stained with Perl's stain [37]. Because the cells sense that LCI is lowered in these iron overload situations, responses that are similar to iron depletion are upregulated. For example, cells can respond by increasing iron uptake and decreasing efflux. Unfortunately, this can result in a vicious cycle of increased iron uptake and inappropriate storage in organelles; this excess

iron can catalyze oxidative damage. However, it can also cause cellular responses that are similar to iron depletion, such as those caused by iron chelators.

Use of chelators is an accepted means of treating systemic iron overload and is promising for treatment of localized iron overload (regional siderosis; as occurs in the heart, brain and retina) [37, 56-58]. The major concern in these cases is loss of iron from unaffected tissues and the resulting side effects. The iron chelator Dp44mT is cell permeant and extremely effective at binding iron and removing it from cells. Deferiprone (DFP) is used clinically for systemic siderosis and has been used successfully for treatment of experimental retinal iron overload in mice [59]. Specifically, a hepcidin knockout mouse model was used to test whether treatment with DFP could help mitigate the effects of sustained retinal iron overload. In the hepcidin knockout model, DFP was able to protect against retinal and RPE degeneration [59]. The protective effects of DFP may be due to the fact that, unlike Dp44mT, DFP, in addition to its iron chelating ability, can donate chelated iron to Tf. This recycled iron can then be redistributed to other cells or tissues, decreasing damage due to chelator induced iron deficiency. Additionally, DFP has been shown to have no retinal toxicity and it has a low affinity for iron. This low affinity for iron allows DFP to avoid binding iron that is tightly bound in physiologically necessary locations and lets DFP remove free or loosely bound iron that has the potential to cause oxidative damage [59].

Hypoxia and Oxidative Stress in the Eye

Oxygen is crucial for energy production by oxidative phosphorylation, but it is also a necessary requirement for other cellular functions, such as intracellular signaling, gene expression and cell survival [60-62]. Because of this, even minuscule changes in the cellular oxygen environment throughout the body can have drastic effects on cell metabolism, function,

and viability [63]. The retina is one of the most metabolically active tissues of the body [7]. The retina uses oxygen more rapidly than other tissues due to the high-energy demanding task of providing and sustaining a highly sensitive and efficient system for the conversion of light energy into a neuronal signal that can be interpreted by the brain [64, 65]. In the retina, the highest levels of oxygen (at an average of 50 mmHg) are found at the choroid, at the back of the eye (Figure 1.7) [7]. Oxygen levels fall dramatically moving from the back of the eye at the choroid towards the vitreous, with a noticeable decrease in oxygen levels of an average of 5 mmHg at the photoreceptors. This rapid change in the oxygen level near the photoreceptors demonstrates the high metabolic activity of the photoreceptors, especially since the area of the highest oxygen levels at the choroid are so close to the photoreceptors [66]. Moving past the photoreceptors, oxygen levels rise slightly to 15 mmHg due to the retinal vasculature that is behind the photoreceptors, until falling again to almost 2mmHg. This decrease in oxygen levels is due to the avascular nature of the middle of the retina. Once at the edge of the retina beside the vitreous body, oxygen levels rise to 25 mmHg because of the proximity of the superficial retinal capillary bed that can deliver oxygen to this final layer of the retina [66]. Overall, the oxygen sources for the metabolism of the retina comes from the two main vascular supplies of the eyes, the choroidal circulation under the RPE and the main retinal artery [67]. The choroidal circulation nourishes the RPE and the photoreceptors, while the retinal circulation provides oxygen and nutrients to the inner retina. If either of these sources of oxygen are disrupted, ocular damage due to oxidative stress can occur, resulting in numerous ocular diseases, such as proliferative diabetic retinopathy, glaucoma, and AMD [68].

Hypoxia is defined as an oxygen level below the level normally found in a specific cell, tissue, or organism, and it is a cause of oxidative stress to cells [28, 68]. Hypoxia occurs when

the normal vascular circulation is disrupted and it results in the transcriptional control of dozens of proteins, including most of the known iron-regulatory proteins (Figure 1.8) [69]. Oxidative stress due to hypoxia occurs in cells when they are exposed to ischemic conditions that are present in a variety of disease states, including ocular diseases [70]. Importantly, hypoxia can dramatically affect iron metabolism as iron regulates the hypoxic response and hypoxia alters levels of iron regulatory and storage proteins [28]. The activity of the transcription factor, hypoxia inducible factor-1 (HIF1) is regulated by both oxygen and iron. HIF1 is a dimer consisting of the constitutively produced nuclear HIF1β and the highly regulated cytoplasmic HIF1α. Under normoxic conditions and in the presence of iron, HIF1α is targeted for degradation by the proteasome [71, 72]. Under hypoxic or low iron conditions, HIF1α moves to the nucleus where it forms a dimer with HIF1β producing active HIF1. HIF1 controls the transcription of dozens of genes, including most of the iron regulatory and storage proteins. Importantly, even under normoxic conditions iron chelators can prevent HIF1α degradation which underscores the dominant role played by iron in the regulation of HIF activity. Overall, hypoxia causes oxidative damage to cells due to disruption of normal mitochondrial function, ultimately leading to increased mitochondrial ROS production [28].

As discussed above, the retina has varied oxygen levels throughout its multiple layers, and those levels of oxygenation can all be considered hypoxic when compared to ambient oxygen levels. Therefore, when designing studies for this dissertation, we evaluated the oxygen levels at which the RPE specifically show signs of oxidative stress by monitoring the levels of HIF-1α. HIF-1α is upregulated under hypoxic conditions in the RPE [42]. These studies allowed us to determine the experimental levels of oxygen necessary for the RPE to truly be considered to be under hypoxic conditions. This work was done by exposing retinal pigmented

epithelial cells to hypoxic oxygen concentrations ranging from 0.5% to 21% oxygen. ELISA assays were used to determine HIF-1α levels. It was found that hypoxic conditions at 0.5% O_2 upregulated the levels of HIF-1α, and this upregulation was sustained over 24 hours, while normoxic conditions at 21% O_2 did not cause an increase in HIF-1α levels (Figure 1.9). These studies provided the rational for carrying out the hypoxic studies within this dissertation at 0.5% O_2, and the normoxic studies at 21% O_2.

Hypoxia also downregulates hepcidin levels (see iron metabolism section), which in turn raises ferroportin levels in cells. Additionally, hypoxia up-regulates transferrin receptor and transferrin levels, which can lead to increased intracellular iron levels in cells. [28, 73-75]. These changes in cellular iron metabolism due to hypoxia can also directly affect glutamate production and secretion, as explained in the RPE physiology section [8, 30]. Since glutamate is an essential neurotransmitter for both the brain and the retina, its levels are highly regulated. High levels of apical glutamate secretion from the RPE can cause excitotoxic damage to the retina, leading to visual defects [76]. This damage can occur during an ischemic event, such as a stroke or instances of retinal hypoxia, where large amounts of glutamate are secreted from cells. Importantly, this secretion of glutamate in hypoxic conditions is iron dependent. When iron chelators are applied to cells in hypoxic conditions, glutamate secretion from these cells decreases. Conversely, in iron-deficient anemic rats, significantly lower glutamate is secreted into the serum, and impaired behavioral function is observed [77]. These examples illustrate the importance of proper regulation of glutamate levels in maintaining normal physiological function.

For a specific example of the effects of hypoxia on iron metabolism in the eye, consider iron efflux from RPE cells. Under normoxic conditions, iron efflux from polarized RPE cells is

greater in the basolateral direction. However, under hypoxic conditions efflux in the basolateral direction is markedly increased when compared to normoxic conditions [78]. This shows that while hypoxia can have deleterious effects on the cellular metabolism in the eye, the RPE are able to divert potentially damaging excess iron away from the retina and back to the choroidal circulation under conditions of hypoxia. This can provide protection against iron-induced free radical damage.

While polarized secretion is normal in the presence of an intact barrier system, it is important to understand that the blood ocular barrier is often disrupted in ocular disease, thereby adding another layer of dysfunction which may contribute to disease pathogenesis [78]. One example of the negative effects that can occur when the polarity of the blood ocular barrier is disrupted can be seen by examining the polarization of pigment epithelium derived factor (PEDF). PEDF is highly expressed in the retina, where it serves as a neurotrophic factor and angiogenesis inhibitor [79, 80]. Multiple studies have shown that PEDF is secreted from the apical surface of the RPE, where it provides neurotrophic support to the photoreceptors and maintains a non-angiogenic retinal environment [81-83]. Disrupting the polarity of PEDF by causing it to be secreted basolaterally can promote vascularization of the retina, while simultaneously decreasing the ability of photoreceptors to functions properly [81]. Additionally, dysregulated expression of PEDF plays a role in the pathogenesis of late-stage AMD.

Amyloid Precursor Protein

Roughly ten years ago, the amyloid precursor protein (APP), was proposed to have ferroxidase activity. Due to the likely involvement of APP in ocular pathologies, such as AMD, and because iron and APP reciprocally regulate one another, we pursued the connection between iron and APP. APP is ubiquitously expressed and produces amyloid beta (Aβ), which is a key

component of the plaques present in Alzheimer's disease. Aβ is also found in drusen (an extracellular conglomerate of proteins, lipids, carbohydrates, iron, and other cellular components that lies beneath the RPE) and is associated with age-related macular degeneration (AMD) [84, 85]. APP has three main isoforms. APP_{695} is found only in the brain, whereas APP_{751} and APP_{770} are found throughout the body [86]. The various isoforms may be identified using antibodies to their specific domains; APP_{751} has a Kunitz-type protease inhibitor (KPI) domain and APP_{770} has both a KPI and an OX-2 homology (OX-2) domain [87].

Regardless of the isoform, APP is cleaved in either one of two pathways: the amyloidogenic pathway, which produces Aβ, or the non-amyloidogenic pathway (Figure 1.10). The amyloidogenic pathway begins with β-secretase cleavage. This cleavage occurs primarily within the *trans*-Golgi network, though some does occur at the cell membrane and within endosomes. In either case, the soluble APPβ (sAPPβ) ectodomain is produced. γ-secretase then cleaves off functional Aβ [88].

The non-amyloidogenic pathway, which is found primarily at the cell membrane, is initiated when APP is first cleaved by α-secretase. This cleaves off part of the Aβ domain of APP, preventing formation of functional Aβ, and produces the large ectodomain soluble APP alpha (sAPPα), which can be secreted. In both pathways, the small C-terminal fragment, APP intracellular domain (AICD) is produced when γ–secretase cleavage occurs [87].

RPE cells constitutively express APP and the secretases responsible for its processing [89]. The amyloidogenic byproduct Aβ likely causes toxicity both within the RPE and when secreted, and contributes to AMD progression. In RPE cells, Aβ has been shown to reduce mitochondrial redox potential as well as increase production of ROS [90]. Additionally, Aβ causes an increase in the neovascularization within the choroid by upregulating vascular

endothelial growth factor, ultimately contributing to late stage AMD [89]. The RPE's proximity to drusen buildup within the underlying Bruch's membrane implicates the RPE as the likely source for the increased Aβ deposits seen in AMD. This is bolstered by the finding that Aβ immunoreactivity is seen within the cytoplasm of RPE cells [91]. The deposition of Aβ may cause local inflammation, leading to the buildup of drusen, RPE atrophy, and ultimately photoreceptor cell death. As a therapeutic target for the buildup of Aβ, it has been shown that anti-Aβ antibodies do offer some protection against the retinal degeneration seen in a mouse model of AMD [92]. Non-amyloidogenic byproducts of APP are implicated in cell development, growth, survival and repair, as well in iron metabolism [93-95].

As mentioned above, APP was identified as a ferroxidase over ten years ago, with the ability to convert ferrous iron to its ferric form for cellular export. APP was proposed to have ferroxidase activity similar to that of ceruloplasmin. Specifically, APP was said to have an iron binding site within its E2 domain, and this site was proposed to have homology with the ferroxidase site found on ferritin [96]. This ferroxidase activity was believed to be present for both the full length and soluble forms of APP. Knockdown of APP with siRNA caused iron retention, while adding exogenous APP caused an increase in iron export [96]. It is important to note that these early findings also revealed that APP had major interactions with ferroportin, and as such facilitated iron export from cells [96]. However, the original studies claiming that APP had ferroxidase activity were contested. Specifically, it was shown that the kinetic measurements of the ferroxidase activity of the peptide of APP that was said to have ferroxidase activity were incorrectly obtained and calculated [97]. When the proposed ferroxidase sites were compared against the correct kinetic parameters, it was found that APP did not possess ferroxidase activity above baseline kinetic measurements [97]. Furthermore, when studies were

done against the E2 domain on native APP and not an isolated peptide, it was also found that no ferroxidase activity was present [98].

Studies were later done that discovered that, while APP does not have ferroxidase activity, the soluble form of APP, sAPPα, does have the ability to stabilize the iron exporter ferroportin [94, 95]. In the presence of iron sAPPα was shown to stabilize ferroportin in HEK293T cells, primary neuronal cultures, and brain endothelial cells [47, 94, 95]. This ability to stabilize ferroportin was localized to the E2 domain on the soluble form of APP, but it was now shown that the E2 domain had the ability to target ferroportin specifically, and not the ability to exhibit ferroxidase activity that was originally claimed. By stabilizing ferroportin, sAPPα may regulate iron levels within the RPE and prevent the harmful effects of iron overload. Additionally APP mRNA also has an iron-regulatory element (IRE) [99]. IREs are RNA stem loops that control the translation of iron regulatory proteins, including APP, and thus balance cellular iron storage and transport. Addition of exogenous iron increases APP translation in RPE cells [100]. Thus, more sAPPα can be produced which can stabilize ferroportin and increase removal of excess iron from the cell. Additionally, another complex within the iron pathway, DMT1, has been implicated in APP processing. Knockdown of DMT1 by siRNA resulted in a significant decrease in APP and its cleavage product Aβ; this further supports the hypothesis that iron influences synthesis and/or processing of APP [101]. Overall, the potential ability to aid in iron export may be why APP and its byproducts have been shown to have an iron regulatory component.

Aside from these activities involved in iron metabolism, APP also has a role in maintaining inner retinal circuitry and rod and cone pathways [102]. Therefore, its apical

secretion from polarized RPE cells could be of paramount importance due to their close relationship with the photoreceptors.

It is important to note that in patients with AMD, increased iron is found in the RPE [103]. In this situation, the ability of iron to upregulate the production of APP, and then utilize that extra APP to stabilize ferroportin in an attempt to clear the excess iron from the RPE may not be sufficient to decrease the intracellular levels of iron. Overall, APP, as an iron regulatory protein, may be upregulated by elevated iron levels, but chronic iron overload may increase the byproducts of APP processing, leading to generation of Aβ. Therefore, an iron induced increase in APP levels may be a cellular response to try and offset the elevated iron levels, but in the process may contribute to the pathology of AMD through generation of excess harmful APP byproducts, such as Aβ.

Intracellular localization of APP and iron regulatory proteins by retromer

Polarized localization and secretion of proteins is a complex, multistep process. Such localization is mediated by multiple helper proteins and signaling motifs on individual proteins that are moved to specific locations. Once such regulator of polarized protein movement is retromer. Retromer is a multimeric protein complex found in the cytosol that is involved in the polarized transport of proteins [104-106]. Retromer transports proteins from endosomes to the trans-Golgi network or to the cell surface [107]. With respect to iron regulation, retromer transports DMT1, Tf, TfR, and APP [108-110]. Loss of retromer impairs transferrin-mediated iron uptake with accumulation of transferrin in early endosomes causing anemia in vertebrates [109]. Cells that have retromer knocked down with siRNA and are then treated with iron chelators have decreased transferrin function, as retromer cannot retrieve transferrin from the early endosomes to recycle it back to the cell surface. Retromer also recycles DMT1 from

endosomes to the trans-Golgi network and DMT1 co-localizes with TfR-positive endosomes. Loss of retromer function therefore impairs the ability of DMT1 to be localized to endosomes where iron needs to be released into the cytoplasm from within the endosome. In addition to protein transport, retromer is needed for rhodopsin recycling within photoreceptors, and loss of retromer function leads to photoreceptor degradation due to the improper localization of rhodopsin within photoreceptors such that it cannot be recycled and used within the visual transduction cascade properly [111] This improper localization of rhodopsin ultimately leads to toxic buildup of rhodopsin within photoreceptors, which causes stress and degradation of the photoreceptors.

Retromer's ability to recognize cargo is still poorly understood [112]. Specific subunits (Vps35 and Vps26) of retromer interact with cargo, and these subunits bind to the cytoplasmic domain of their specific cargos [108, 113, 114]. Mutations in the specific sorting motif of the cytoplasmic domain of DMT1 greatly impair its recruitment into retromer. Importantly, retromer can transport APP throughout the cell and shuttle APP away from key cleavage enzymes, limiting production of Aβ [115, 116].

Additionally, retromer properly localizes the SorLA protein, which is a protein found in the trans-Golgi network that slows the release of APP, thereby controlling the amount of APP that can be processed into Aβ by keeping APP within the TGN [113]. When retromer levels are decreased within the cell, SorLA does not localize correctly, and more Aβ is generated [113]. SorLA and retromer are both decreased in Alzheimer's patients, implying that loss of retromer plays a role in the pathogenesis of Alzheimer's and perhaps AMD [117, 118].

Retromer also regulates the polarized movement of APP from the trans-Golgi network to apical or basolateral surfaces for secretion. When retromer levels are decreased, Aβ levels are

shown to increase [119]. This increase in Aβ is seen both intracellularly and in the amount of Aβ that are secreted. Therefore, retromer may be responsible for facilitating the interaction between APP and β-secretase, which is responsible for the production of the Aβ byproduct of APP. This is important because Aβ is found in drusen present in AMD, suggesting a link between retromer deregulation and Aβ accumulation in AMD. APP and Tf have been shown to co-localize during endocytic transport within the cell however the significance of this is not known [116]. As previously mentioned, when APP trafficking to the cell surface is impaired or altered, iron accumulation within the cell occurs.

Glycosylation of iron regulatory proteins and APP

While it is recognized that glycans play a major role in human disease, glycoprotein synthesis and structure is understudied. The glycosylation of proteins begins with a cotranslational process in the endoplasmic reticulum (ER) with the addition of sugars and movement of proteins through the Golgi apparatus where a complex and finely orchestrated removal and addition of glycans occurs. Thus, post-translationally modified proteins can be recognized and moved to their proper intracellular, plasma membrane or secretory vesicle location. Glycosylation plays a pivotal role in this critical function.

The functional properties of glycans in glycoproteins can be divided into two main categories: structural and modulatory functions; and the recognition of glycans by other molecules and proteins. Glycans help to control cell to cell, cell to matrix and cell to molecule interactions, and are involved in many important processes in complex organisms, including the assembly and development of multicellular organs. They act as signals that determine how the glycoproteins are processed within the cell and which compartments they are targeted to.

Additionally, intracellular glycans can function as molecular switches, toggling cellular functions on and off [120].

Two main forms of glycosylation exist, N- and O- glycosylation. N-glycosylation generally beings as a covalent bond on an asparagine, and O-glycosylation beings as a covalent bond on a proteins serine or threonine [120]. An important distinction between these two main types of glycosylation is that O-glycosylation occurs only after protein translation, whereas N-glycosylation can occur before a protein is fully translated [120]. Both N- and O-glycosylation are important for APP function, and glycosylation is implicated in the correct functionality of the iron transport protein transferrin [121].

Protein glycosylation is essential to proper protein folding and movement to the cell membrane for insertion or secretion. It is also essential for the polarized placement of many proteins in epithelial cells [122]. It has recently been recognized that glycosylation plays an important role in angiogenesis which, when dysregulated, can have devastating effects on virtually all ocular tissues due to the ability of the newly formed blood vessels to break through the retina, causing widespread oxidative damage and cellular death [123]. Oxidative stress is also known to alter protein glycosylation. Specifically, protein glycosylation can be altered when the sugar metabolism within cells is disrupted as cells adapt to the anaerobic state caused by hypoxia [124]. Under hypoxic conditions, the activity of glucosaminyltransferases is vastly reduced [125]. This means that glucosaminyltransferases, the enzymes that are necessary for the addition of sugars during glycosylation, are not able to function at their normal capacity, thus lowering the ability of the cell to properly glycosylate its proteins. Within the eye, improper protein glycosylation has been shown to be causative factor of diabetic retinopathy.

An example of how glycosylation effects a proteins function is seen with the iron regulator proteins transferrin (Tf), which transports iron extracellularly, and its receptor, transferrin receptor (TfR). Glycosylation of TfR increases its affinity for Tf by ten-fold and is required for targeting of TfR to the membrane [126, 127]. The affinity of iron for Tf is decreased when Tf is desialylated. Over 50% of proteins are glycosylated, so it is not surprising that APP itself is a heavily glycosylated protein [128]. However, little is known about how glycosylation effects APP's intracellular movement.

The glycosylation pathway of APP is well documented [120]. APP glycosylation begins in the ER with the first addition of simple sugars. After this initial addition of sugars, APP moves on to be processed through the various compartments of the Golgi apparatus. There is significant posttranslational modification of APP as it transits through the Golgi to the endosomes. These modifications result in a heavily glycosylated mature APP which is the form that is secreted. The mature form of APP has an outer coat of glycans covered with sialic acid. Addition of sialic acid to the outer most sugars is believed to protect them from removal. The majority of APP undergoes O-glycosylation with a terminal glycan addition of sialic acid. APP that is not O-glycosylated undergoes N-glycosylation, and no sialic acid is added. Post-translationally modified proteins can then be recognized and moved to their proper intracellular, plasma membrane, or secretory vesicle locations.

Once properly glycosylated, APP is cleaved by either α- or β-secretase to release soluble APP (sAPPα or β, respectively). γ-secretase then acts on the remaining protein to release Aβ. The processing pathway taken by APP through the maturation process determines which route it takes. The importance of glycosylation for APP's functional localization is illustrated by the finding that the membrane protein TMEM59 causes a decrease in APP glycosylation, or

maturation of APP [129]. This results in sequestration of APP in the Golgi and its inability to move to the membrane for processing to soluble APP (sAPP) and Aβ. O-glycosylation has been shown to promote the plasma membrane localization of APP, which enhances the non-amyloidogenic processing of APP [130]. Increased sialylation of APP in Neuro-2a cells caused a 2-3 fold increase in the secretion of Aβ and sAPP [131]. Overall, changes in the glycosylation of APP alters its subcellular distribution, and may cause APP to be processed incorrectly, leading to multiple disease states [132].

APP's Potential Role in Photoreceptor Phagocytosis

As explained in the RPE physiology section, the apical villi of the RPE heavily interdigitate with the photoreceptors that are directly above the RPE. Diurnal synchronized phagocytosis of photoreceptor outer segments (POS) shed daily by photoreceptor cells is an essential task of the RPE. Deficiencies in this phagocytosis of POS cause retinal degeneration in animal models [20]. For POS to be phagocytosed, they must be recognized and internalized by the RPE. This internalization pathway has been well studied. Two of the key components involved in the phagocytosis of POS are the α5βv integrin complex and the Mer tyrosine kinsase (MerTK). In brief, during POS phagocytosis, the α5 and βv integrins dimerize to form the α5βv complex [20]. This complex anchors itself within the apical membrane of the RPE and recognizes POS that are ready to be phagocytosed. This recognition activates MerTk, and once activated, MerTK aids in the engulfment of the POS. Additionally, another receptor within the apical membrane of the RPE, CD36, is able to recognize oxidized phospholipids on POS and can aid in the recognition of POS [20].

All of these functions for POS recognition have features that are shared with APP. APP can dimerize with itself through the formation of high affinity disulfide bridges, as well as lower

affinity binding through heparin binding domains found within its E1 and E2 domains [133]. This dimerization is similar to that seen with the formation of the α5βv integrin complex. The cytosolic domain of APP possesses several conserved sequences that are responsible for numerous protein to protein interactions. Notable within these sequences are two sequences that are responsible for the endocytosis and internal trafficking of proteins [133]. Such endocytic signals are also found on MerTk [20]. Due to these similarities, it may be possible that APP can act as an enhancer, or a receptor, for POS during their phagocytosis.

Concluding Remarks

Age related macular degeneration in the retina is an increasingly common ocular disease which causes significant morbidity and has an enormous health care cost. Pathologic mechanisms underlying this disease are incompletely understood. However, in this disease it is known that there is dysregulation of the metabolism of both iron and APP. Importantly, as explained above, APP and iron metabolism work in tandem. Changes in iron metabolism affect APP production and secretion, and changes in APP can also alter the ability of the cell to process and secrete iron. Because of this intricate relationship between iron and APP, it is proposed that iron and APP are critical interconnected components of the pathogenesis of ocular disease conditions. However, studies up to this point have only began to understand the mechanistic components of the interrelated control of APP and iron metabolism. When the RPE cellular pathology is altered, specifically by changing the levels of oxygen, iron, and APP availability, the ability for the RPE to properly function is severely impaired, leading to ocular disease such as APP. Therefore, the hypothesis of this proposal is that common pathogenic stimuli in the forms of hypoxia and iron chelation are able to alter the interrelationship between iron and APP metabolism in the RPE. These detrimental stimuli will lead to disruptive effects on cell

metabolism. To investigate this hypothesis, the RPE will be studied under states of hypoxia and iron chelation, while investigating the changes in the metabolism of APP and its polarized localization and secretion from the RPE.

In hypoxia, iron and APP levels are both depleted. Additionally, APP is not processed fully when iron levels are lowered. Therefore, hypoxia will first be utilized to look at the changes in APP levels within the RPE. The polarized localization of APP will also be measured. APP secretion will also be measured from polarized RPE to understand how RPE cells alter APP processing in a diseased state such as hypoxia. These studies will allow for a better understanding of the temporal and spatial control of APP processing and the ultimate disposition of APP from the RPE. Changes in APP levels due to altered oxygen or iron levels will be evaluated at the mechanistic level. Specifically, hypoxia is able to alter the synthesis of proteins. Therefore, hypoxia will be investigated as a means of changing the ability of APP to be correctly synthesized within the RPE. Since hypoxia is known to alter iron levels, APP will be examined in the presence of iron chelation to better understand how iron affects APP metabolism. The main focus of this investigation will be whether iron chelation is able to alter the glycosylation of APP. Lastly, preliminary studies will be undertaken to gain a better understanding of the physiological role of APP within the retina. Since APP is expressed on the apical surface of RPE cells and may function in cell adhesion or as a receptor, APP will be examined for its ability to aid in the phagocytosis of photoreceptors to further understand the functionality of APP. Overall, results of this work will provide information critical to the development of new treatments for diseases in which iron and APP play key roles.

REFERENCES

1. Cunha-Vaz J, Bernardes R, Lobo C. Blood-retinal barrier. Eur J Ophthalmol 2011; 21 Suppl 6:S3-9.

2. Xu HZ, Le YZ. Significance of outer blood-retina barrier breakdown in diabetes and ischemia. Invest Ophthalmol Vis Sci 2011; 52(5):2160-4.

3. Gonzalez A, Rodriguez-Boulan E. Clathrin and AP1B: key roles in basolateral trafficking through trans-endosomal routes. FEBS Lett 2009; 583(23):3784-95.

4. Lehmann GL, Benedicto I, Philp NJ, Rodriguez-Boulan E. Plasma membrane protein polarity and trafficking in RPE cells: past, present and future. Exp Eye Res 2014; 126:5-15.

5. Strauss O. The retinal pigment epithelium in visual function. Physiol Rev 2005; 85(3):845-81.

6. Gundersen D, Orlowski J, Rodriguez-Boulan E. Apical polarity of Na,K-ATPase in retinal pigment epithelium is linked to a reversal of the ankyrin-fodrin submembrane cytoskeleton. J Cell Biol 1991; 112(5):863-72.

7. Ames A, 3rd, Li YY, Heher EC, Kimble CR. Energy metabolism of rabbit retina as related to function: high cost of Na+ transport. J Neurosci 1992; 12(3):840-53.

8. Lall MM, Ferrell J, Nagar S, Fleisher LN, McGahan MC. Iron regulates L-cystine uptake and glutathione levels in lens epithelial and retinal pigment epithelial cells by its effect on cytosolic aconitase. Invest Ophthalmol Vis Sci 2008; 49(1):310-9.

9. Ban Y, Rizzolo LJ. Regulation of glucose transporters during development of the retinal pigment epithelium. Brain Res Dev Brain Res 2000; 121(1):89-95.

10. Adler AJ, Southwick RE. Distribution of glucose and lactate in the interphotoreceptor matrix. Ophthalmic Res 1992; 24(4):243-52.

11. Guymer R, Luthert P, Bird A. Changes in Bruch's membrane and related structures with age. Prog Retin Eye Res 1999; 18(1):59-90.

12. Takei Y, Ozanics V. Origin and development of Bruch's membrane in monkey fetuses: an electron microscopic study. Invest Ophthalmol 1975; 14(12):903-16.

13. van Lookeren Campagne M, LeCouter J, Yaspan BL, Ye W. Mechanisms of age-related macular degeneration and therapeutic opportunities. J Pathol 2014; 232(2):151-64.

14. Cerman E, Eraslan M, Cekic O. Age-related macular degeneration and Alzheimer disease. Turk J Med Sci 2015; 45(5):1004-9.

15. Ratnayaka JA, Serpell LC, Lotery AJ. Dementia of the eye: the role of amyloid beta in retinal degeneration. Eye (Lond) 2015.

16. Geirsdottir A, Hardarson SH, Olafsdottir OB, Stefansson E. Retinal oxygen metabolism in exudative age-related macular degeneration. Acta Ophthalmol 2014; 92(1):27-33.

17. He X, Hahn P, Iacovelli J, Wong R, King C, Bhisitkul R, Massaro-Giordano M, Dunaief JL. Iron homeostasis and toxicity in retinal degeneration. Prog Retin Eye Res 2007; 26(6):649-73.

18. Inoue Y, Yanagi Y, Matsuura K, Takahashi H, Tamaki Y, Araie M. Expression of hypoxia-inducible factor 1alpha and 2alpha in choroidal neovascular membranes associated with age-related macular degeneration. Br J Ophthalmol 2007; 91(12):1720-1.

19. Molday RS, Moritz OL. Photoreceptors at a glance. J Cell Sci 2015; 128(22):4039-45.

20. Mazzoni F, Safa H, Finnemann SC. Understanding photoreceptor outer segment phagocytosis: use and utility of RPE cells in culture. Exp Eye Res 2014; 126:51-60.

21. Kusakabe TG, Takimoto N, Jin M, Tsuda M. Evolution and the origin of the visual retinoid cycle in vertebrates. Philos Trans R Soc Lond B Biol Sci 2009; 364(1531):2897-910.

22. Kiser PD, Golczak M, Palczewski K. Chemistry of the retinoid (visual) cycle. Chem Rev 2014; 114(1):194-232.

23. Kiser PD, Golczak M, Maeda A, Palczewski K. Key enzymes of the retinoid (visual) cycle in vertebrate retina. Biochim Biophys Acta 2012; 1821(1):137-51.

24. Saari JC. Vitamin A metabolism in rod and cone visual cycles. Annu Rev Nutr 2012; 32:125-45.

25. Nandrot EF, Chang Y, Finnemann SC. Alphavbeta5 integrin receptors at the apical surface of the RPE: one receptor, two functions. Adv Exp Med Biol 2008; 613:369-75.

26. Beatty S, Koh H, Phil M, Henson D, Boulton M. The role of oxidative stress in the pathogenesis of age-related macular degeneration. Surv Ophthalmol 2000; 45(2):115-34.

27. Conrad ME, Umbreit JN, Moore EG. Iron absorption and transport. Am J Med Sci 1999; 318(4):213-29.

28. Chepelev NL, Willmore WG. Regulation of iron pathways in response to hypoxia. Free Radic Biol Med 2011; 50(6):645-66.

29. Garcia-Castineiras S. Iron, the retina and the lens: a focused review. Exp Eye Res 2010; 90(6):664-78.

30. McGahan MC, Harned J, Mukunnemkeril M, Goralska M, Fleisher L, Ferrell JB. Iron alters glutamate secretion by regulating cytosolic aconitase activity. Am J Physiol Cell Physiol 2005; 288(5):C1117-24.

31. Moiseyev G, Takahashi Y, Chen Y, Gentleman S, Redmond TM, Crouch RK, Ma JX. RPE65 is an iron(II)-dependent isomerohydrolase in the retinoid visual cycle. J Biol Chem 2006; 281(5):2835-40.

32. Gutteridge JM, Rowley DA, Halliwell B. Superoxide-dependent formation of hydroxyl radicals in the presence of iron salts. Detection of 'free' iron in biological systems by using bleomycin-dependent degradation of DNA. Biochem J 1981; 199(1):263-5.

33. Truscott RJ. Age-related nuclear cataract-oxidation is the key. Exp Eye Res 2005; 80(5):709-25.

34. Shoham A, Hadziahmetovic M, Dunaief JL, Mydlarski MB, Schipper HM. Oxidative stress in diseases of the human cornea. Free Radic Biol Med 2008; 45(8):1047-55.

35. Feng Y, vom Hagen F, Lin J, Hammes HP. Incipient diabetic retinopathy--insights from an experimental model. Ophthalmologica 2007; 221(4):269-74.

36. Aslan M, Cort A, Yucel I. Oxidative and nitrative stress markers in glaucoma. Free Radic Biol Med 2008; 45(4):367-76.

37. Song D, Dunaief JL. Retinal iron homeostasis in health and disease. Front Aging Neurosci 2013; 5:24.

38. Saraswathy S, Rao NA. Photoreceptor mitochondrial oxidative stress in experimental autoimmune uveitis. Ophthalmic Res 2008; 40(3-4):160-4.

39. McGahan MC, Fleisher LN. A micromethod for the determination of iron and total iron-binding capacity in intraocular fluids and plasma using electrothermal atomic absorption spectroscopy. Anal Biochem 1986; 156(2):397-402.

40. Chowers I, Wong R, Dentchev T, Farkas RH, Iacovelli J, Gunatilaka TL, Medeiros NE, Presley JB, Campochiaro PA, Curcio CA, Dunaief JL, Zack DJ. The iron carrier transferrin is upregulated in retinas from patients with age-related macular degeneration. Invest Ophthalmol Vis Sci 2006; 47(5):2135-40.

41. Picard E, Jonet L, Sergeant C, Vesvres MH, Behar-Cohen F, Courtois Y, Jeanny JC. Overexpressed or intraperitoneally injected human transferrin prevents photoreceptor degeneration in rd10 mice. Mol Vis 2010; 16:2612-25.

42. Goralska M, Ferrell J, Harned J, Lall M, Nagar S, Fleisher LN, McGahan MC. Iron metabolism in the eye: a review. Exp Eye Res 2009; 88(2):204-15.

43. McGahan MC, Fleisher LN. Antioxidant activity of aqueous and vitreous humor from the inflamed rabbit eye. Curr Eye Res 1986; 5(9):641-5.

44. McGahan MC, Fleisher LN. Inflammation-induced changes in the iron concentration and total iron-binding capacity of the intraocular fluids of rabbits. Graefes Arch Clin Exp Ophthalmol 1988; 226(1):27-30.

45. Goralska M, Nagar S, Fleisher LN, Mzyk P, McGahan MC. Source-dependent intracellular distribution of iron in lens epithelial cells cultured under normoxic and hypoxic conditions. Invest Ophthalmol Vis Sci 2013; 54(12):7666-73.

46. Hunt RC, Dewey A, Davis AA. Transferrin receptors on the surfaces of retinal pigment epithelial cells are associated with the cytoskeleton. J Cell Sci 1989; 92 (Pt 4):655-66.

47. McCarthy RC, Kosman DJ. Mechanisms and regulation of iron trafficking across the capillary endothelial cells of the blood-brain barrier. Front Mol Neurosci 2015; 8:31.

48. Hahn P, Dentchev T, Qian Y, Rouault T, Harris ZL, Dunaief JL. Immunolocalization and regulation of iron handling proteins ferritin and ferroportin in the retina. Mol Vis 2004; 10:598-607.

49. Dunaief JL, Richa C, Franks EP, Schultze RL, Aleman TS, Schenck JF, Zimmerman EA, Brooks DG. Macular degeneration in a patient with aceruloplasminemia, a disease associated with retinal iron overload. Ophthalmology 2005; 112(6):1062-5.

50. Hahn P, Qian Y, Dentchev T, Chen L, Beard J, Harris ZL, Dunaief JL. Disruption of ceruloplasmin and hephaestin in mice causes retinal iron overload and retinal degeneration with features of age-related macular degeneration. Proc Natl Acad Sci U S A 2004; 101(38):13850-5.

51. Cabantchik ZI. Labile iron in cells and body fluids: physiology, pathology, and pharmacology. Front Pharmacol 2014; 5:45.

52. Goralska M, Harned J, Fleisher LN, McGahan MC. The effect of ascorbic acid and ferric ammonium citrate on iron uptake and storage in lens epithelial cells. Exp Eye Res 1998; 66(6):687-97.

53. Rouault TA. The role of iron regulatory proteins in mammalian iron homeostasis and disease. Nat Chem Biol 2006; 2(8):406-14.

54. Goralska M, Holley BL, McGahan MC. Identification of a mechanism by which lens epithelial cells limit accumulation of overexpressed ferritin H-chain. J Biol Chem 2003; 278(44):42920-6.

55. Goralska M, Nagar S, Fleisher LN, McGahan MC. Differential degradation of ferritin H- and L-chains: accumulation of L-chain-rich ferritin in lens epithelial cells. Invest Ophthalmol Vis Sci 2005; 46(10):3521-9.

56. Cabantchik ZI, Munnich A, Youdim MB, Devos D. Regional siderosis: a new challenge for iron chelation therapy. Front Pharmacol 2013; 4:167.

57. Fleming RE, Ponka P. Iron overload in human disease. N Engl J Med 2012; 366(4):348-59.

58. Rouault TA. Iron metabolism in the CNS: implications for neurodegenerative diseases. Nat Rev Neurosci 2013; 14(8):551-64.

59. Song D, Zhao L, Li Y, Hadziahmetovic M, Song Y, Connelly J, Spino M, Dunaief JL. The oral iron chelator deferiprone protects against systemic iron overload-induced retinal degeneration in hepcidin knockout mice. Invest Ophthalmol Vis Sci 2014; 55(7):4525-32.

60. Carmeliet P, Dor Y, Herbert JM, Fukumura D, Brusselmans K, Dewerchin M, Neeman M, Bono F, Abramovitch R, Maxwell P, Koch CJ, Ratcliffe P, Moons L, Jain RK, Collen D, Keshert E. Role of HIF-1alpha in hypoxia-mediated apoptosis, cell proliferation and tumour angiogenesis. Nature 1998; 394(6692):485-90.

61. Lopez-Barneo J, Pardal R, Ortega-Saenz P. Cellular mechanism of oxygen sensing. Annu Rev Physiol 2001; 63:259-87.

62. Semenza GL. HIF-1 and mechanisms of hypoxia sensing. Curr Opin Cell Biol 2001; 13(2):167-71.

63. Banasiak KJ, Xia Y, Haddad GG. Mechanisms underlying hypoxia-induced neuronal apoptosis. Prog Neurobiol 2000; 62(3):215-49.

64. Kimble EA, Svoboda RA, Ostroy SE. Oxygen consumption and ATP changes of the vertebrate photoreceptor. Exp Eye Res 1980; 31(3):271-88.

65. Weiter JJ, Zuckerman R. The influence of the photoreceptor-RPE complex on the inner retina. An explanation for the beneficial effects of photocoagulation. Ophthalmology 1980; 87(11):1133-9.

66. Yu DY, Cringle SJ. Retinal degeneration and local oxygen metabolism. Exp Eye Res 2005; 80(6):745-51.

67. Wangsa-Wirawan ND, Linsenmeier RA. Retinal oxygen: fundamental and clinical aspects. Arch Ophthalmol 2003; 121(4):547-57.

68. Caprara C, Grimm C. From oxygen to erythropoietin: relevance of hypoxia for retinal development, health and disease. Prog Retin Eye Res 2012; 31(1):89-119.

69. Semenza GL. Hypoxia-inducible factors in physiology and medicine. Cell Death Differ 2012; 148:399-408.

70. Li SY, Fu ZJ, Lo AC. Hypoxia-induced oxidative stress in ischemic retinopathy. Oxid Med Cell Longev 2012; 2012:426769.

71. Ivan M, Kondo K, Yang H, Kim W, Valiando J, Ohh M, Salic A, Asara JM, Lane WS, Kaelin WG, Jr. HIFalpha targeted for VHL-mediated destruction by proline hydroxylation: implications for O2 sensing. Science 2001; 292(5516):464-8.

72. Jaakkola P, Mole DR, Tian YM, Wilson MI, Gielbert J, Gaskell SJ, von Kriegsheim A, Hebestreit HF, Mukherji M, Schofield CJ, Maxwell PH, Pugh CW, Ratcliffe PJ. Targeting of HIF-alpha to the von Hippel-Lindau ubiquitylation complex by O2-regulated prolyl hydroxylation. Science 2001; 292(5516):468-72.

73. Lee DW, Rajagopalan S, Siddiq A, Gwiazda R, Yang L, Beal MF, Ratan RR, Andersen JK. Inhibition of prolyl hydroxylase protects against 1-methyl-4-phenyl-1,2,3,6-tetrahydropyridine-induced neurotoxicity: model for the potential involvement of the hypoxia-inducible factor pathway in Parkinson disease. J Biol Chem 2009; 284(42):29065-76.

74. Lakhal S, Schodel J, Townsend AR, Pugh CW, Ratcliffe PJ, Mole DR. Regulation of type II transmembrane serine proteinase TMPRSS6 by hypoxia-inducible factors: new link between hypoxia signaling and iron homeostasis. J Biol Chem 2011; 286(6):4090-7.

75. Klimova T, Chandel NS. Mitochondrial complex III regulates hypoxic activation of HIF. Cell Death Differ 2008; 15(4):660-6.

76. Olney JW. The toxic effects of glutamate and related compounds in the retina and the brain. Retina 1982; 2(4):341-59.

77. Kitajima H, Shiomoto H, Osada K, Yokogoshi H. Co-administration of proline and inorganic iron enhance the improvement of behavioral and hematological function of iron-deficient anemic rats. J Nutr Sci Vitaminol (Tokyo) 2003; 49(1):7-12.

78. Harned J, Nagar S, McGahan MC. Hypoxia controls iron metabolism and glutamate secretion in retinal pigmented epithelial cells. Biochim Biophys Acta 2014; 1840(10):3138-44.

79. Dawson DW, Volpert OV, Gillis P, Crawford SE, Xu H, Benedict W, Bouck NP. Pigment epithelium-derived factor: a potent inhibitor of angiogenesis. Science 1999; 285(5425):245-8.

80. Cayouette M, Smith SB, Becerra SP, Gravel C. Pigment epithelium-derived factor delays the death of photoreceptors in mouse models of inherited retinal degenerations. Neurobiol Dis 1999; 6(6):523-32.

81. Sonoda S, Sreekumar PG, Kase S, Spee C, Ryan SJ, Kannan R, Hinton DR. Attainment of polarity promotes growth factor secretion by retinal pigment epithelial cells: relevance to age-related macular degeneration. Aging (Albany NY) 2009; 2(1):28-42.

82. Sonoda S, Spee C, Barron E, Ryan SJ, Kannan R, Hinton DR. A protocol for the culture and differentiation of highly polarized human retinal pigment epithelial cells. Nat Protoc 2009; 4(5):662-73.

83. Becerra SP, Fariss RN, Wu YQ, Montuenga LM, Wong P, Pfeffer BA. Pigment epithelium-derived factor in the monkey retinal pigment epithelium and interphotoreceptor matrix: apical secretion and distribution. Exp Eye Res 2004; 78(2):223-34.

84. Ohno-Matsui K. Parallel findings in age-related macular degeneration and Alzheimer's disease. Prog Retin Eye Res 2011; 30(4):217-38.

85. Crabb JW. The proteomics of drusen. Cold Spring Harb Perspect Med 2014; 4(7):a017194.

86. Zheng H, Koo EH. Biology and pathophysiology of the amyloid precursor protein. Mol Neurodegener 2011; 6(1):27.

87. Nalivaeva NN, Turner AJ. The amyloid precursor protein: a biochemical enigma in brain development, function and disease. FEBS Lett 2013; 587(13):2046-54.

88. O'Brien RJ, Wong PC. Amyloid precursor protein processing and Alzheimer's disease. Annu Rev Neurosci 2011; 34:185-204.

89. Yoshida T, Ohno-Matsui K, Ichinose S, Sato T, Iwata N, Saido TC, Hisatomi T, Mochizuki M, Morita I. The potential role of amyloid beta in the pathogenesis of age-related macular degeneration. J Clin Invest 2005; 115(10):2793-800.

90. Bruban J, Glotin AL, Dinet V, Chalour N, Sennlaub F, Jonet L, An N, Faussat AM, Mascarelli F. Amyloid-beta(1-42) alters structure and function of retinal pigmented epithelial cells. Aging Cell 2009; 8(2):162-77.

91. Johnson LV, Leitner WP, Rivest AJ, Staples MK, Radeke MJ, Anderson DH. The Alzheimer's A beta -peptide is deposited at sites of complement activation in pathologic deposits associated with aging and age-related macular degeneration. Proc Natl Acad Sci U S A 2002; 99(18):11830-5.

92. Ding JD, Johnson LV, Herrmann R, Farsiu S, Smith SG, Groelle M, Mace BE, Sullivan P, Jamison JA, Kelly U, Harrabi O, Bollini SS, Dilley J, Kobayashi D, Kuang B, Li W, Pons J, Lin JC, Bowes Rickman C. Anti-amyloid therapy protects against retinal pigmented epithelium damage and vision loss in a model of age-related macular degeneration. Proc Natl Acad Sci U S A 2011; 108(28):E279-87.

93. Dawkins E, Small DH. Insights into the physiological function of the beta-amyloid precursor protein: beyond Alzheimer's disease. J Neurochem 2014; 129(5):756-69.

94. Wong BX, Tsatsanis A, Lim LQ, Adlard PA, Bush AI, Duce JA. beta-Amyloid precursor protein does not possess ferroxidase activity but does stabilize the cell surface ferrous iron exporter ferroportin. PLoS One 2014; 9(12):e114174.

95. McCarthy RC, Park YH, Kosman DJ. sAPP modulates iron efflux from brain microvascular endothelial cells by stabilizing the ferrous iron exporter ferroportin. EMBO Rep 2014; 15(7):809-15.

96. Duce JA, Tsatsanis A, Cater MA, James SA, Robb E, Wikhe K, Leong SL, Perez K, Johanssen T, Greenough MA, Cho HH, Galatis D, Moir RD, Masters CL, McLean C, Tanzi RE, Cappai R, Barnham KJ, Ciccotosto GD, Rogers JT, Bush AI. Iron-export ferroxidase activity of beta-amyloid precursor protein is inhibited by zinc in Alzheimer's disease. Cell 2010; 142(6):857-67.

97. Ebrahimi KH, Hagedoorn PL, Hagen WR. A synthetic peptide with the putative iron binding motif of amyloid precursor protein (APP) does not catalytically oxidize iron. PLoS One 2012; 7(8):e40287.

98. Honarmand Ebrahimi K, Dienemann C, Hoefgen S, Than ME, Hagedoorn PL, Hagen WR. The amyloid precursor protein (APP) does not have a ferroxidase site in its E2 domain. PLoS One 2013; 8(8):e72177.

99. Rogers JT, Randall JD, Cahill CM, Eder PS, Huang X, Gunshin H, Leiter L, McPhee J, Sarang SS, Utsuki T, Greig NH, Lahiri DK, Tanzi RE, Bush AI, Giordano T, Gullans SR. An iron-responsive element type II in the 5'-untranslated region of the Alzheimer's amyloid precursor protein transcript. J Biol Chem 2002; 277(47):45518-28.

100. Guo LY, Alekseev O, Li Y, Song Y, Dunaief JL. Iron increases APP translation and amyloid-beta production in the retina. Exp Eye Res 2014; 129:31-7.

101. Zheng W, Xin N, Chi ZH, Zhao BL, Zhang J, Li JY, Wang ZY. Divalent metal transporter 1 is involved in amyloid precursor protein processing and Abeta generation. FASEB J 2009; 23(12):4207-17.

102. Ho T, Vessey KA, Cappai R, Dinet V, Mascarelli F, Ciccotosto GD, Fletcher EL. Amyloid precursor protein is required for normal function of the rod and cone pathways in the mouse retina. PLoS One 2012; 7(1):e29892.

103. Hahn P, Milam AH, Dunaief JL. Maculas affected by age-related macular degeneration contain increased chelatable iron in the retinal pigment epithelium and Bruch's membrane. Arch Ophthalmol 2003; 121(8):1099-105.

104. Burd C, Cullen PJ. Retromer: a master conductor of endosome sorting. Cold Spring Harb Perspect Biol 2014; 6(2).

105. McGough IJ, Steinberg F, Gallon M, Yatsu A, Ohbayashi N, Heesom KJ, Fukuda M, Cullen PJ. Identification of molecular heterogeneity in SNX27-retromer-mediated endosome-to-plasma membrane recycling. J Cell Sci 2014.

106. Pocha SM, Wassmer T, Niehage C, Hoflack B, Knust E. Retromer controls epithelial cell polarity by trafficking the apical determinant Crumbs. Curr Biol 2011; 21(13):1111-7.

107. Lu L, Hong W. From endosomes to the trans-Golgi network. Semin Cell Dev Biol 2014; 31:30-9.

108. Tabuchi M, Yanatori I, Kawai Y, Kishi F. Retromer-mediated direct sorting is required for proper endosomal recycling of the mammalian iron transporter DMT1. J Cell Sci 2010; 123:756-66.

109. Chen C, Garcia-Santos D, Ishikawa Y, Seguin A, Li L, Fegan KH, Hildick-Smith GJ, Shah DI, Cooney JD, Chen W, King MJ, Yien YY, Schultz IJ, Anderson H, Dalton AJ, Freedman ML, Kingsley PD, Palis J, Hattangadi SM, Lodish HF, Ward DM, Kaplan J, Maeda T, Ponka P, Paw BH. Snx3 Regulates Recycling of the Transferrin Receptor and Iron Assimilation. Cell Metab 2013.

110. Choy RW, Cheng Z, Schekman R. Amyloid precursor protein (APP) traffics from the cell surface via endosomes for amyloid beta (Abeta) production in the trans-Golgi network. Proc Natl Acad Sci U S A 2012; 109(30):E2077-82.

111. Wang S, Tan KL, MAgosto MA, Xiong G, Yamamoto S, Sandoval H, Jaiswal M, Bayat V, Zhang E, Charng WL, David G, Duraine L, Venkatachalam, Wensel TG, Bellen HJ. The retromer complex is required for rhodopsin recycling and its loss leads to photoreceptor degeneration. PLOS Biology 2014; 12(4):e1001847.

112. Seaman MN. The retromer complex - endosomal protein recycling and beyond. J Cell Sci 2012; 125(Pt 20):4693-702.

113. Fjorback AW, Andersen OM. SorLA is a molecular link for retromer-dependent sorting of the Amyloid precursor protein. Commun Integr Biol 2012; 5(6):616-9.

114. Strochlic TI, Setty TG, Sitaram A, Burd CG. Grd19/Snx3p functions as a cargo-specific adapter for retromer-dependent endocytic recycling. J Cell Biol 2007; 177(1):115-25.

115. Reitz C. The role of intracellular trafficking and the VPS10d receptors in Alzheimer's disease. Future Neurol 2012; 7(4):423-31.

116. Vieira SI, Rebelo S, Esselmann H, Wiltfang J, Lah J, Lane R, Small SA, Gandy S, da Cruz ESEF, da Cruz ESOA. Retrieval of the Alzheimer's amyloid precursor protein from the endosome to the TGN is S655 phosphorylation state-dependent and retromer-mediated. Mol Neurodegener 2010; 5:40.

117. Scherzer CR, Offe K, Gearing M, Rees HD, Fang G, Heilman CJ, Schaller C, Bujo H, Levey AI, Lah JJ. Loss of apolipoprotein E receptor LR11 in Alzheimer disease. Arch Neurol 2004; 61(8):1200-5.

118. Li C, Shah SZ, Zhao D, Yang L. Role of the Retromer Complex in Neurodegenerative Diseases. Front Aging Neurosci 2016; 8:42.

119. Muhammad A, Flores I, Zhang H, Yu R, Staniszewski A, Planel E, Herman M, Ho L, Kreber R, Honig LS, Ganetzky B, Duff K, Arancio O, Small SA. Retromer deficiency observed in Alzheimer's disease causes hippocampal dysfunction, neurodegeneration, and Abeta accumulation. Proc Natl Acad Sci U S A 2008; 105(20):7327-32.

120. Schedin-Weiss S, Winblad B, Tjernberg LO. The role of protein glycosylation in Alzheimer disease. FEBS J 2014; 281(1):46-62.

121. Taniguchi M, Okayama Y, Hashimoto Y, Kitaura M, Jimbo D, Wakutani Y, Wada-Isoe K, Nakashima K, Akatsu H, Furukawa K, Arai H, Urakami K. Sugar chains of cerebrospinal fluid transferrin as a new biological marker of Alzheimer's disease. Dement Geriatr Cogn Disord 2008; 26(2):117-22.

122. Dick G, Akslen-Hoel LK, Grondahl F, Kjos I, Prydz K. Proteoglycan synthesis and golgi organization in polarized epithelial cells. J Histochem Cytochem 2012; 60:926-935.

123. Markowska AI, Cao Z, Panjwani N. Glycobiology of ocular angiogensis. Glycobiology 2014.

124. Shirato K, Nakajima K, Korekane H, Takamatsu S, Gao C, Angata T, Ohtsubo K, Taniguchi N. Hypoxic regulation of glycosylation via the N-acetylgulcosamine cycle. J Clin Biochem Nutr 2011; 48:20-5.

125. Shirato K, Nakajima K, Korekane H, Takamatsu S, Gao C, Angata T, Ohtsubo K, Taniguchi N. Hypoxic regulation of glycosylation via the N-acetylgulcosamine cycle. J Clin Biochem Nutr 2011; 48:20-5.

126. Hunt RC, Riegler R, Davis AA. Changes in glycosylation alter the affinity of the human transferrin receptor for its ligand. J Biol Chem 1989; 264:9643-8.

127. Williams AM, Enns CA. A region of the C-terminal portion of the human transferrin receptor contains an asparagine-linked glycosylation site critical for receptor structure and function. J Biol Chem 1993; 268(17):12780-6.

128. Apweiler R, Hermjakob H, Sharon N. On the frequency of protein glycosylation, as deduced from analysis of the SWISS-PROT database. Biochim Biophys Acta 1999; 1473(1):4-8.

129. Ullrich S, Munch A, Neumann S, Kremmer E, Tatzelt J, Lichtenthaler SF. the novelmembrane protein TMEM59 modulates complex glycosylation, cell surface expression and secretion of the amyloid precursor protein. J Biol Chem 2010; 185:20664-74.

130. Chun YS, Park Y, Oh HG, Kim TW, Yang HO, Park MK, Chung S. O-GlcNAcylation promotes non-amyloidogenic processing of amyloid-beta protein precursor via inhibition of endocytosis from the plasma membrane. J Alzheimers Dis 2015; 44(1):261-75.

131. Nakagawa K, Kitazume S, Oka R, Maruyama K, Saido T, Sato Y, Endo T, Hashimoto Y. Sialylation enhances the secretion of neurotoxic amyloid-B peptides. J Neurochemistry 2006; 96:9242-933.

132. McFarlane I, Georgopoulou N, Coughlan CM, Gillian AM, Breen KC. The role of the protein glycosylation state in the control of cellular transport of the amyloid beta precursor protein. Neuroscience 1999; 90(1):15-25.

133. Deyts C, Thinakaran G, Parent AT. APP Receptor? To Be or Not To Be. Trends Pharmacol Sci 2016; 37(5):390-411.

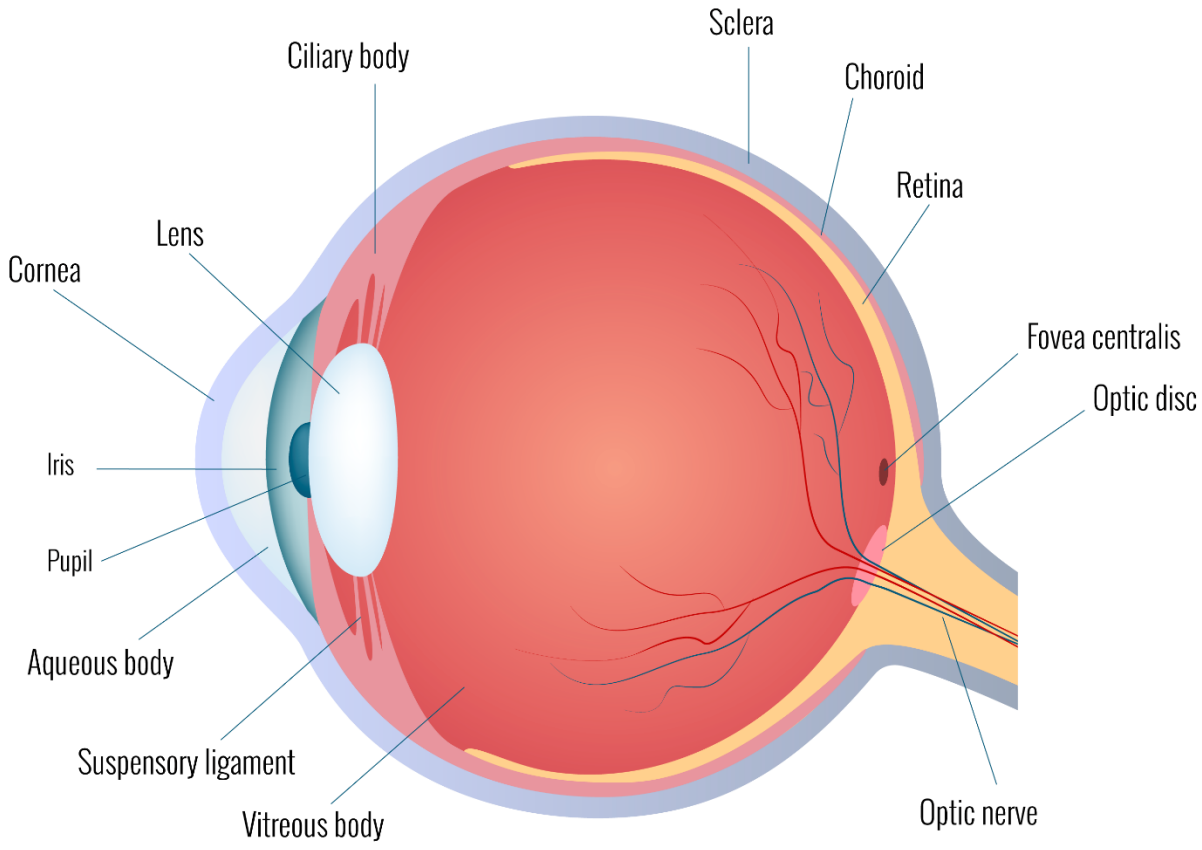

Figure 1.1 Cross section of the vertebrate eye Schematic cross section of the vertebrate eye with relevant anatomical structures labeled.

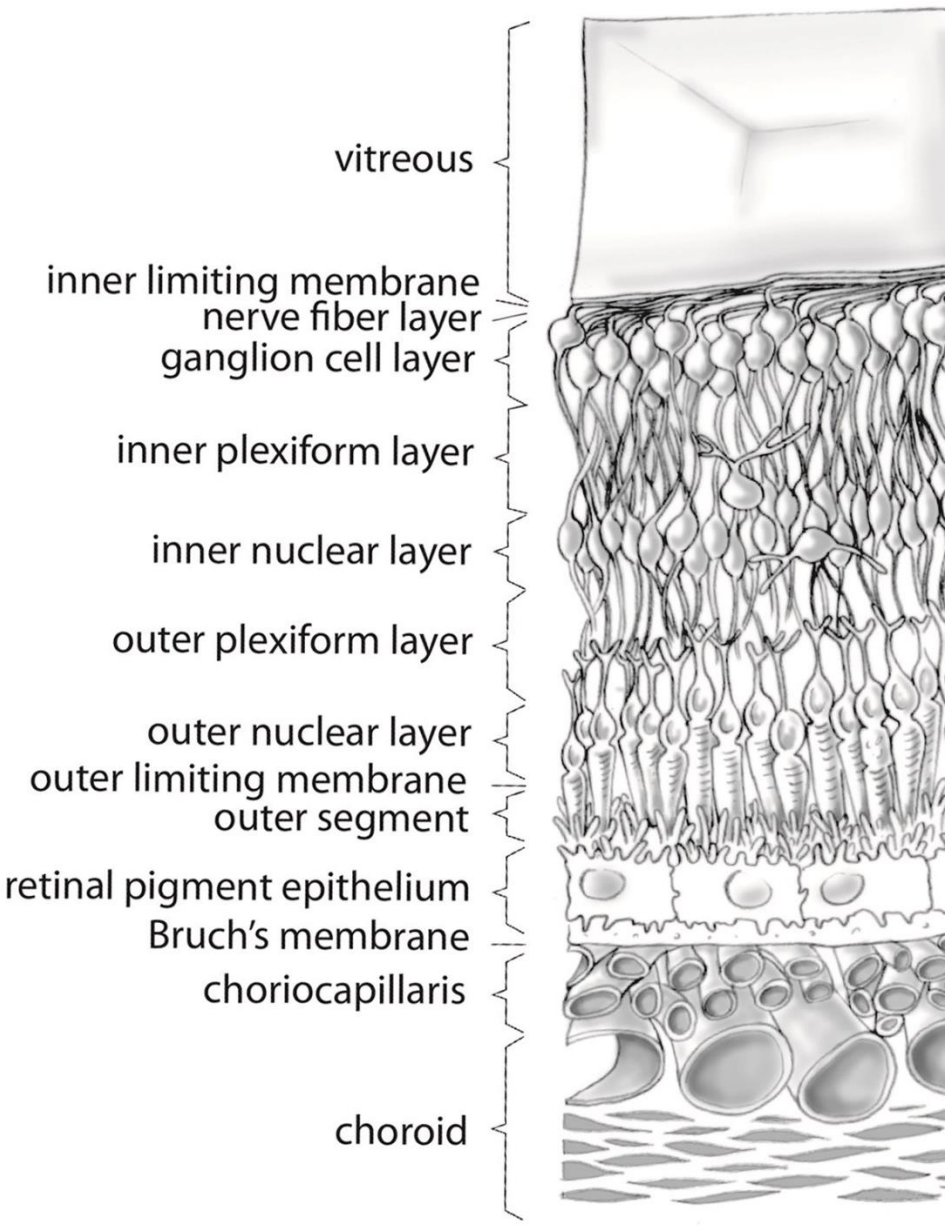

Figure 1.2 Cross section of the vertebrate retina This drawing of the retina depicts the major cell types in the retina. The ganglion cells (the output neurons of the retina) are located on the inner surface of the retina, and the photoreceptors (the rods and cones) are interdigitating with the retinal pigmented epithelium, which lies above the choroid. Light must travel through the thickness of the retina before striking and activating the rods and cones. (Birmingham, 2016).

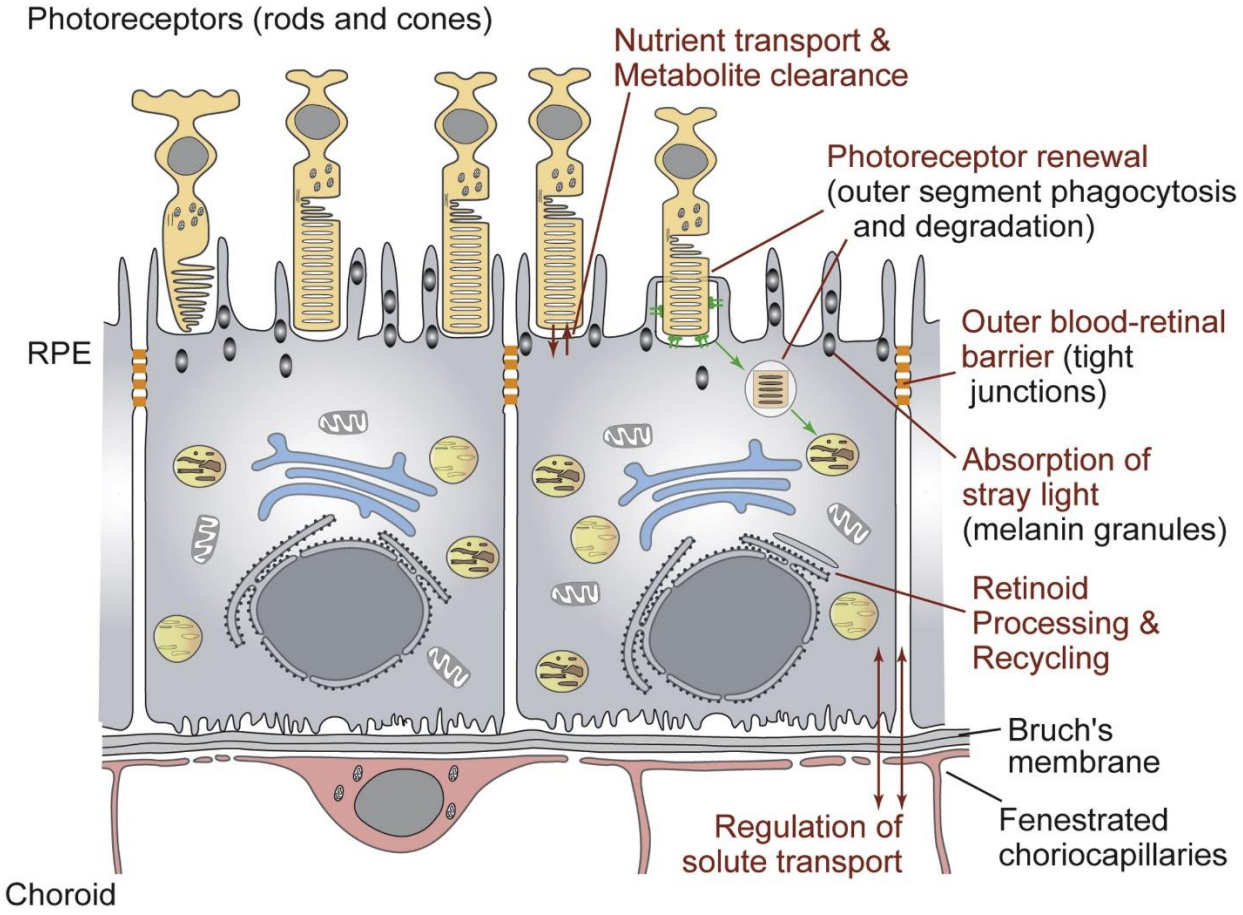

Figure 1.3 Functions of the Retinal Pigmented Epithelium Schematic diagram of the retinal pigmented epithelium, with key functions highlighted. The photoreceptors are directly above the retinal pigmented epithelium and interdigitate with their apical processes. Bruch's membrane and the choroid are below the retinal pigmented epithelium's basolateral surface. (Lehmann et al., 2014).

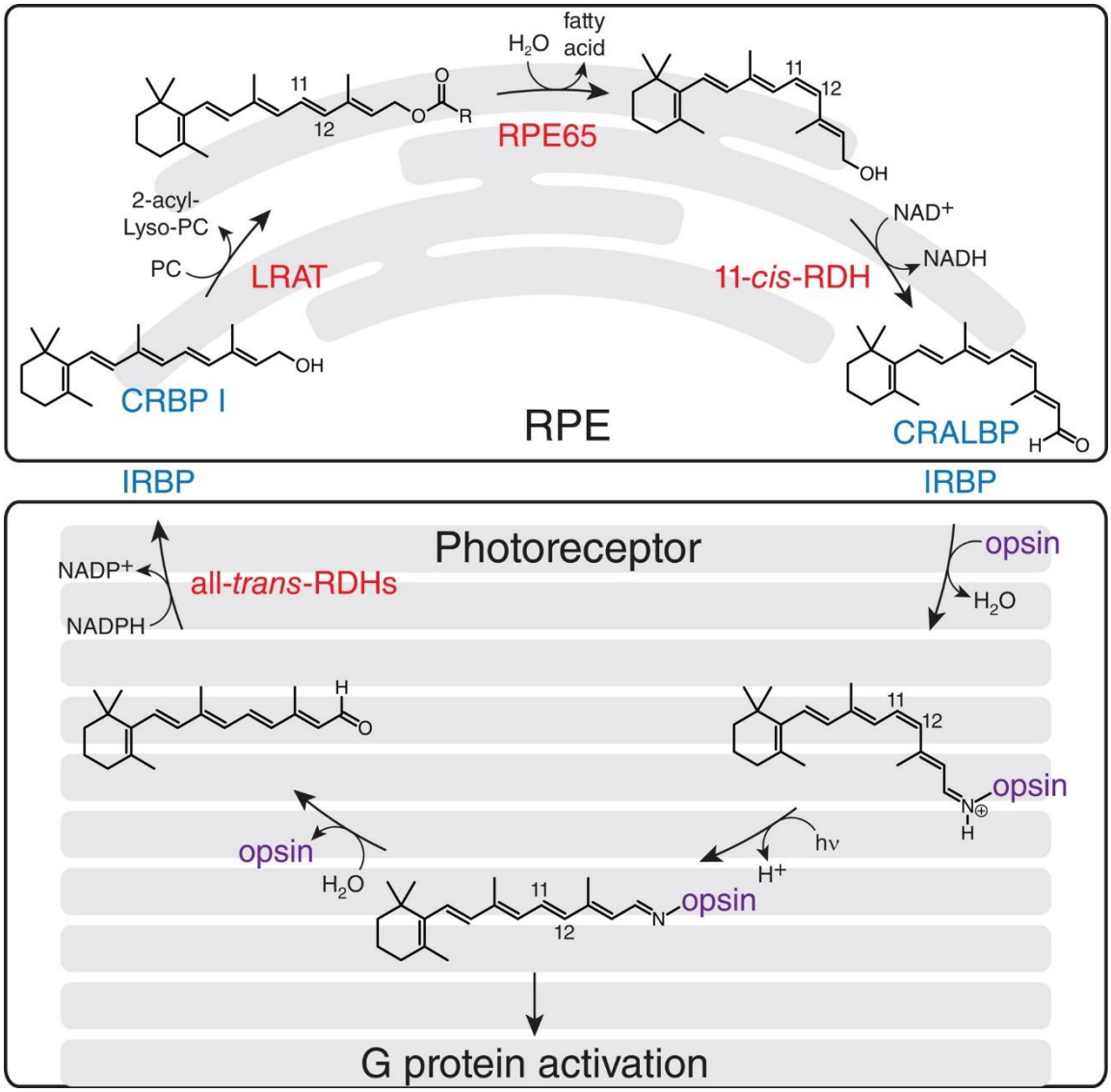

Figure 1.4 RPE participation in the visual cycle Enzymes (red) and binding proteins (blue) involved in 11-*cis*-retinal regeneration are found in both photoreceptor and RPE cells. Metabolic transformations occurring in the RPE take place in the smooth ER, where key enzymes of the visual cycle are located. (Kiser, 2014).

Figure 1.5 Regulation of Intracellular Iron Content Transferrin has two iron-binding sites which have high affinity for Fe^{3+}. Diferric transferrin binds to transferrin receptor (TfR) which is then endocytosed. The endocytic vesicle is acidified by the actions of a vesicular ATPase (V-ATPase) which is a proton pump, actively moving H+ into the vesicle. At low pH, transferrin releases its cargo of iron which can leave the endocytic vesicle either through ferroportin or by co-transport with H+ through the divalent metal transporter-1 (DMT1). Iron may then transit through what is called the labile iron pool (LIP) to sites of storage or utilization, or may leave the cell through ferroportin present in the plasma membrane. Iron can also enter the LIP from heme which is broken down by heme oxygenase. Iron brought into the cells can regulate the activities of the iron regulatory proteins-1 and 2, which in turn regulate proteins involved in iron metabolism. It can also be stored in ferritin. The protein hepcidin regulates ferroportin levels by triggering its degradation. In turn, hepcidin is regulated by HFE which triggers an increase in hepcidin synthesis. HFE is normally bound to transferrin receptor, but the binding site is also recognized by diferric transferrin which competes with HFE for binding. The HFE is released and binds to transferrin receptor-2 (TfR-2) which triggers a signaling pathway up-regulating hepcidin. The movement of iron out of the cell by ferroportin is enhanced by the ferroxidase activities of ceruloplasmin (Cp) and/or hephaestin. In this figure, dotted lines indicate movement and solid lines indicate descriptors. The labile iron pool (LIP) is surrounded by a dotted line indicating that the LIP is not a discrete entity located within an organelle, but likely exists throughout the cytoplasm. (Goralska et al., 2009).

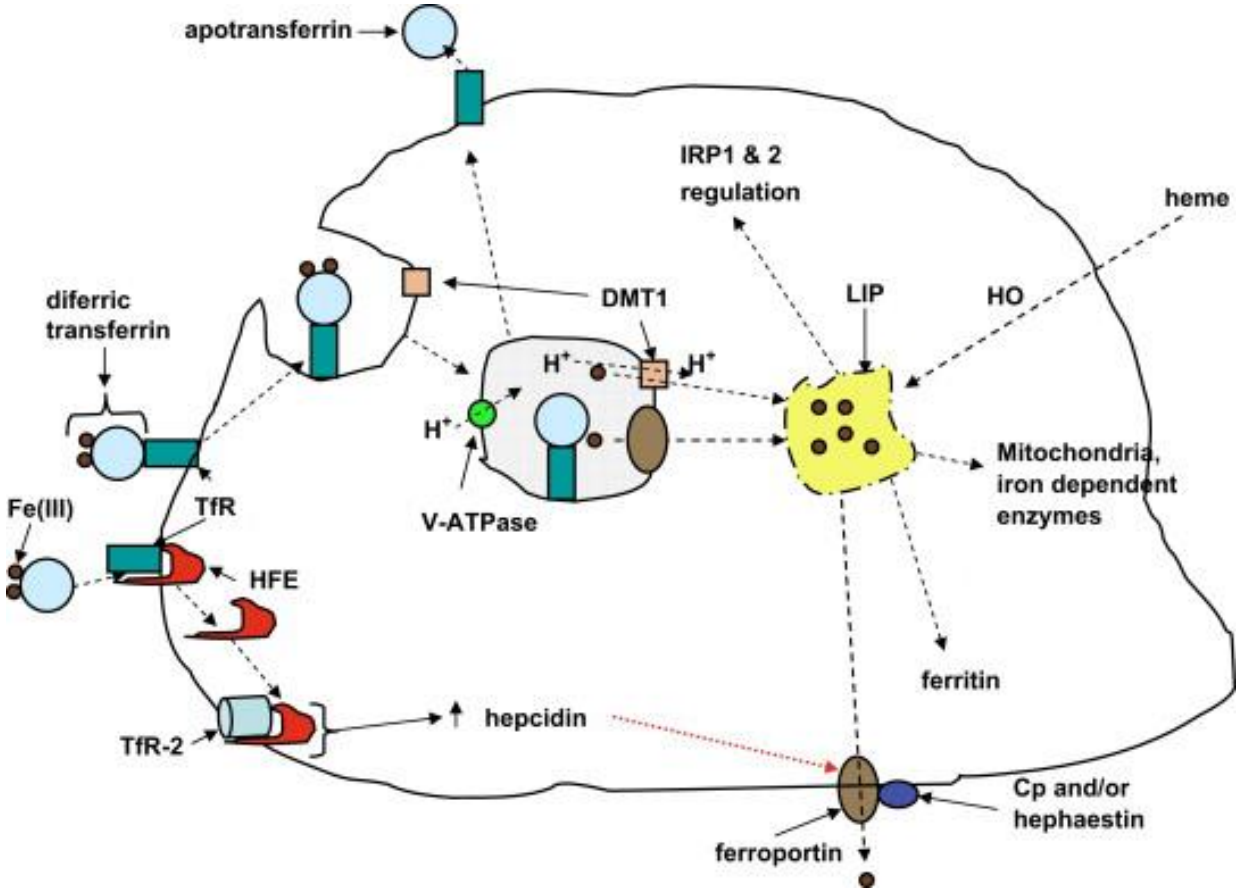
apotransferrin
IRP1 & 2
regulation
heme
diferric
transferrin
DMT1
LIP
HO
H+
H+
H+
Mitochondria,
iron dependent
enzymes
V-ATPase
Fe(III)
TfR
HFE
ferritin
hepcidin
TfR-2
Cp and/or
hephaestin
ferroportin

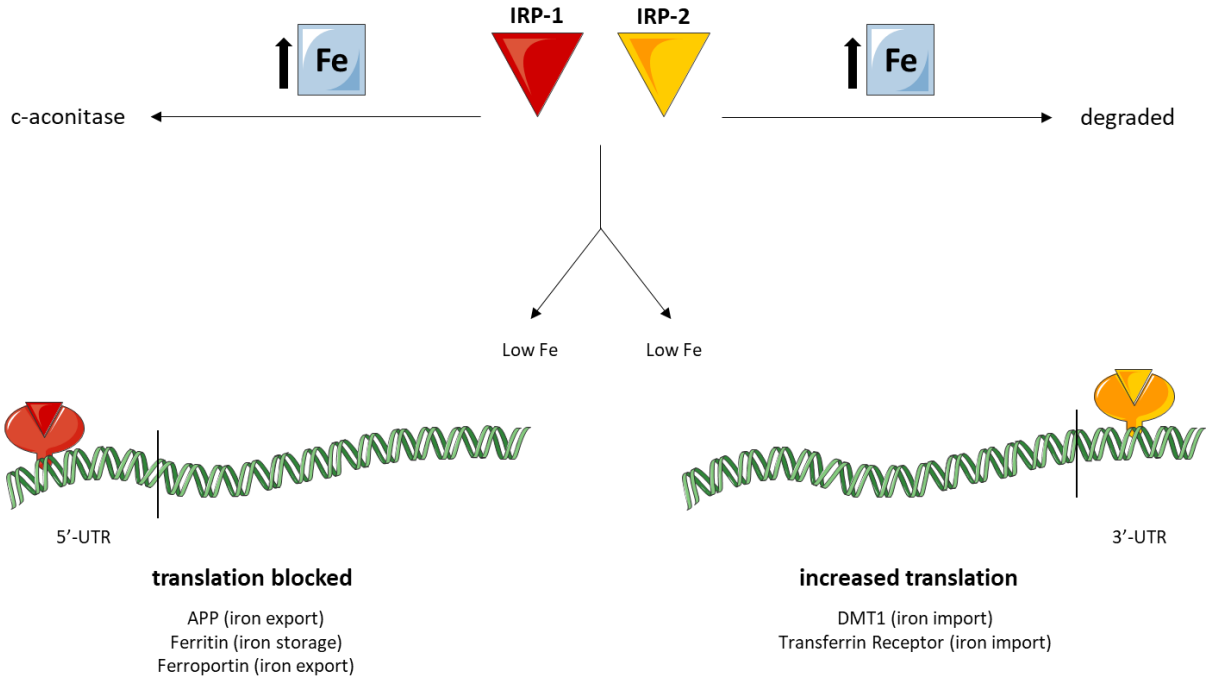

Figure 1.6 Functions and regulation of iron regulatory protein-1 and 2 Iron regulatory protein 1 (IRP-1) exists in two conformations depending upon the availability of iron. When high iron levels are present IRP-1 attains aconitase activity and does not bind the iron response element (IRE) in either the 3'- or 5'-untranslated regions (UTRs) of the mRNAs of numerous proteins including ferritin, ferroportin, or the amyloid precursor protein. In low iron conditions, IRP-1 is responsible for blocking translation of iron storage and export proteins, allowing the cell to utilize its intracellular iron. The presence of iron causes the degradation of iron regulatory protein 2 (IRP-2), decreasing IRP binding to IREs. In low iron conditions, IRP-2 is responsible for IRE binding and regulation of the translation of multiple iron import proteins, allowing the cell to increase its intracellular iron levels.

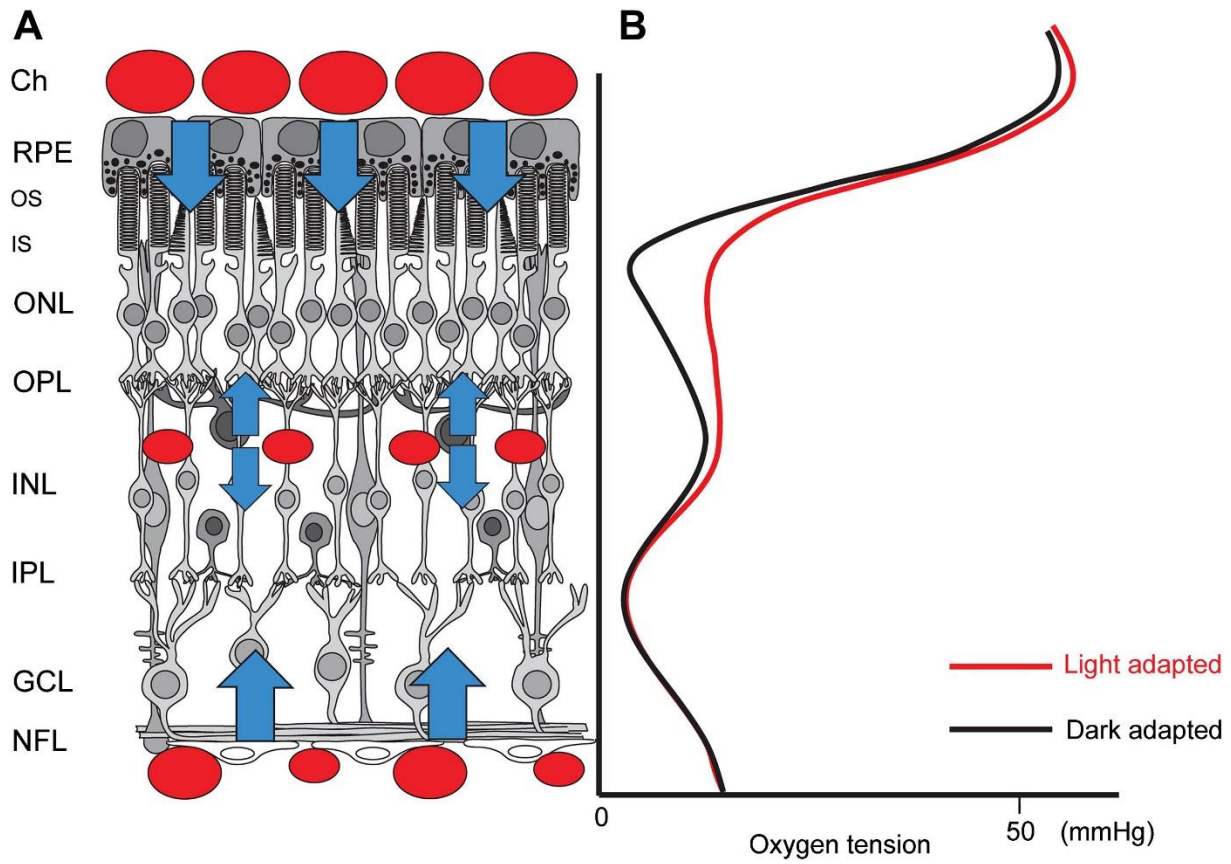

Figure 1.7 Oxygen Levels in the Vertebrate Retina A: Schematic representation of the vertebrate retina. Red circles represent vessels; blue arrows show the directions of oxygen diffusion from the corresponding vessels. **B:** Oxygen distribution profile of the vertebrate retina. The oxygen distribution profiles of a light adapted (red line) and a dark-adapted (black line) retina are shown. The y-axis follows the section through the retina shown in A. Oxygen tension is highest near the choroidal vasculature and falls dramatically towards the inner segments of the photoreceptors. In the inner retina, oxygen tension is lower in the avascular plexiform layers, whereas higher oxygen tension is measured in the region where the retinal vasculature is found. (Caprara et al., 2012).

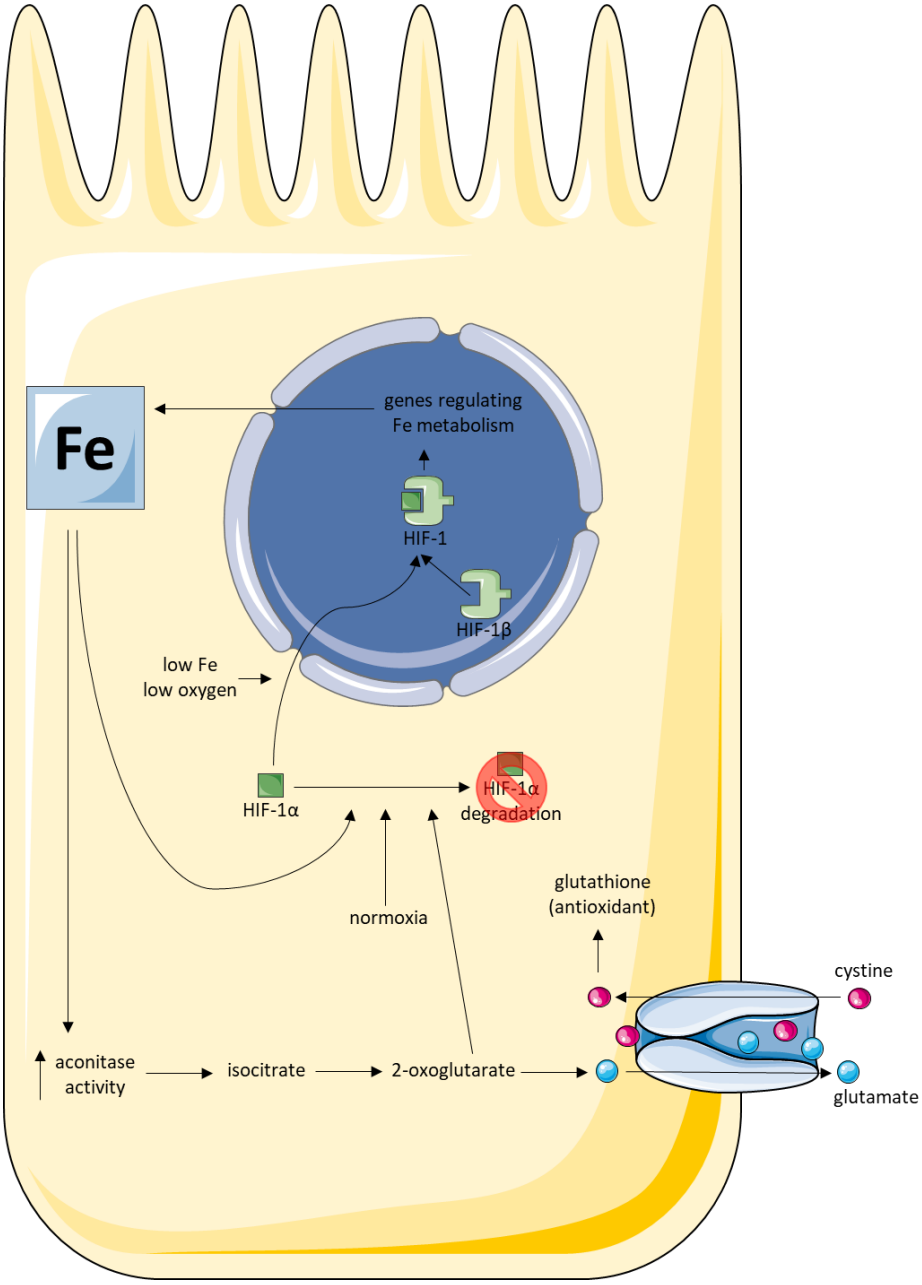

Figure 1.8 Hypoxia Inducible Factor Metabolism In the presence of normoxia, iron, and 2-oxoglutarate, HIF-1α is targeted for degradation by the proteasome. However, in hypoxic conditions and when iron is limited in availability, HIF-1α moves into the nucleus where it dimerizes with HIF-1β to form the transcription factor HIF-1 which controls genes regulating iron metabolism. Iron also regulates aconitase activity resulting in control of glutamate, cystine uptake, and production of glutathione levels in the RPE.

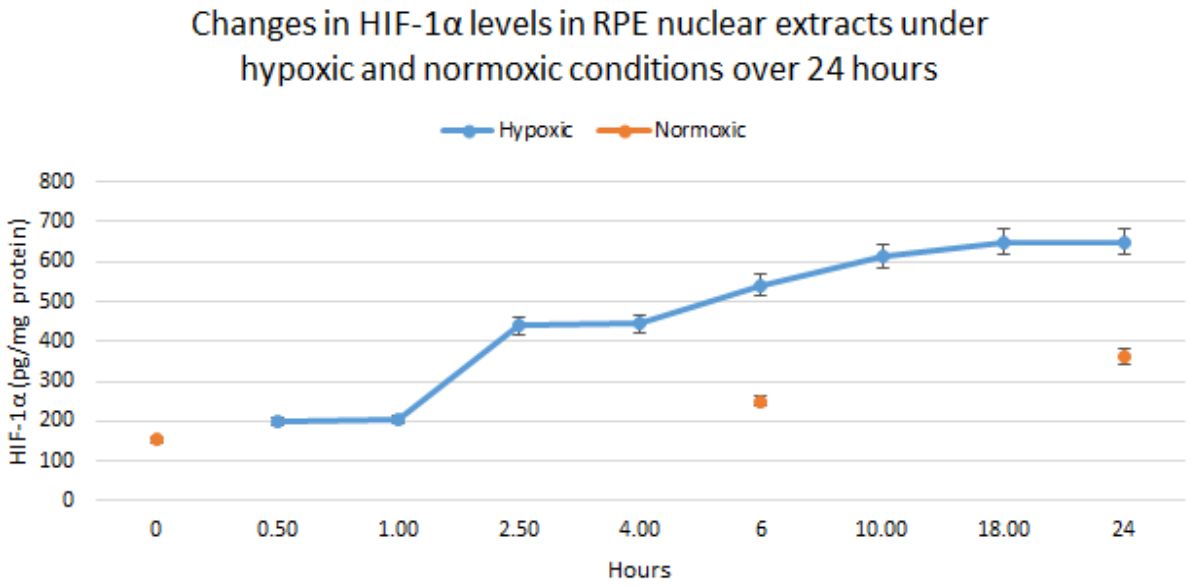

Figure 1.9 Hypoxia Alters HIF-1α Levels in RPE Lysates RPE cells were placed in 0.5% or 21% oxygen for 24 hours and HIF-1α expression was measured. HIF-1α levels in hypoxia rose at a faster rate than those in normoxic conditions.

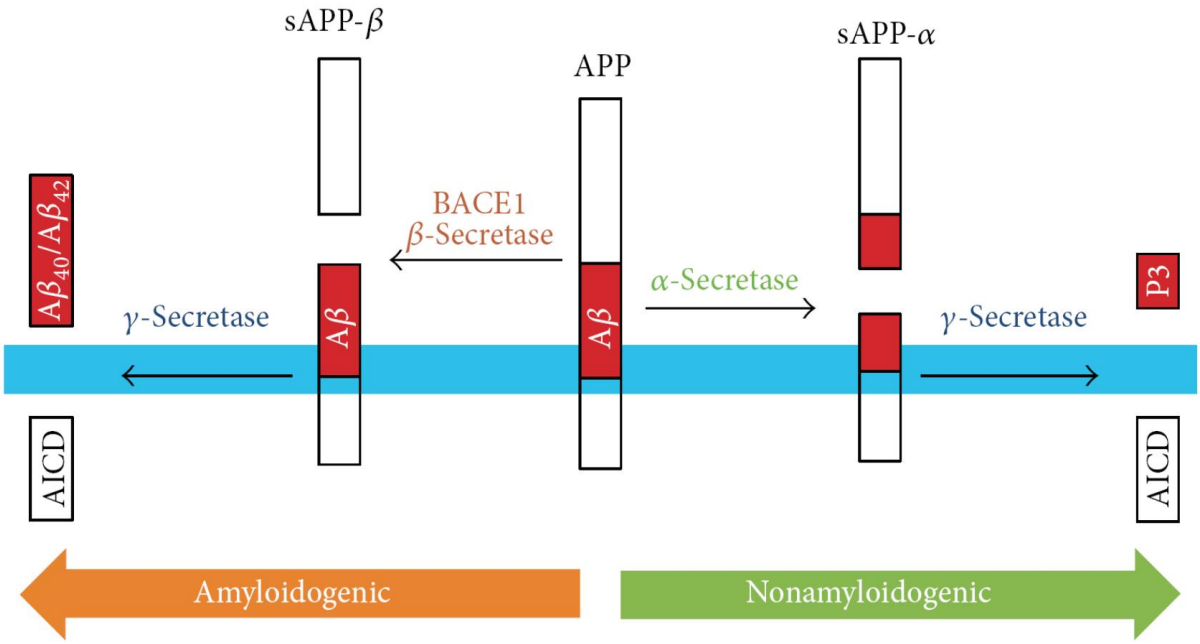

Figure 1.10 Amyloid Precursor Protein Cleavage Pathway Diagram showing the two main cleavage pathways for the amyloid precursor protein. The amyloidogenic pathway creates a functional Aβ fragment, while the non-amyloidogenic pathway renders Aβ non-functional. (Pająk et al., 2015).

CHAPTER 2

Regulation of Polarized Amyloid Precursor Protein Expression and Secretion in Retinal Pigmented Epithelial cells by Hypoxia and Retromer

Abstract

Purpose

Amyloid precursor protein is ubiquitously expressed and produces amyloid-beta (Aβ) and soluble APP (sAPP). Aβ is a key component of plaques found in Alzheimer's disease and in drusen present in age-related macular degeneration (AMD). sAPP plays important roles in cell differentiation and iron metabolism. Retromer is an intracellular retrograde protein transport complex, which regulates the polarized movement of APP from endosomes to the trans Golgi network and then to apical or basolateral surfaces for secretion. The retinal pigmented epithelium (RPE) underlies the retina and is an integral component of the blood ocular barrier. Because RPE can be exposed to hypoxic conditions in pathologic situations, such as AMD, we studied the effects of hypoxia on APP levels in RPE and its polarized secretion.

Methods

RPE were isolated from canine eyes and grown to confluence. Cells were then dispersed on 6 well tissue culture plates or on cell culture inserts and grown to confluent polarized monolayers. Cells were placed under hypoxic (0.5% O_2) or normoxic (21% O_2) conditions for 24 or 48 hours and siRNA was used to knockdown APP. Lysates and cell-conditioned media (CCM) were collected and analyzed by immunoblotting and immunofluorescence for APP.

Results

Oxygen levels significantly altered polarized secretion of APP in RPE cells. After 48 hours of hypoxia, APP secretion was significantly decreased in the apical direction by 92%. Hypoxia decreased retromer levels in lysates of polarized RPE cells by 84% at 48 hours. Furthermore, when retromer was knocked down with siRNA in RPE cells, APP secretion was reduced by an average of 38% in both normoxic and hypoxic conditions.

Conclusions

Hypoxia alters intracellular APP levels in RPE, and therefore the amount available for secretion. Importantly, while the hypoxia-induced reduction in APP matches the amount secreted in the basolateral direction, the amount secreted in the apical direction is reduced more significantly. This indicates the possibility that there are dynamic changes in polarized movement of APP in RPE caused by hypoxia. Other data indicate that this could be due to changes in the level or function of the intracellular protein transporter, retromer. Significantly, a reduction in APP levels in cells could cause a deleterious increase in iron levels because of APP's role in regulation of iron efflux from cells. As hypoxia is a common pathology of the retina, understanding how it affects the processing, polarized localization, and secretion of proteins is vital to understanding the pathophysiology of RPE. This is the first study demonstrating that hypoxia affects both polarized APP secretion and retromer levels in any cell type.

Introduction

The retinal pigmented epithelial (RPE) cells underlie photoreceptor cells and sit atop the choroid, ultimately supporting retinal function. They comprise the outer blood-retinal barrier (oBRB), which is analogous to the blood-brain barrier in that the oBRB restricts the movement of large molecules into the eye [1]. These large molecules are restricted because tight junctions between RPE cells provide a barrier to movement of molecules and ions and separate the RPE apical and basolateral surfaces, allowing for appropriate directional movement of nutrients and wastes into and out of the retina. These functions are dependent upon tightly controlled polarized protein localization in the RPE. Furthermore, the apical surface of the RPE is in direct contact with and regulates the turnover of the photoreceptor outer segments and the

interphotoreceptor matrix, which are essential for vision. If RPE function is compromised, ocular health is severely impaired [2, 3].

Amyloid precursor protein (APP) is ubiquitously expressed and produces amyloid beta (Aβ), which is a key component of the plaques present in Alzheimer's disease; it is also found in the drusen (an extracellular conglomerate of proteins, lipids, carbohydrates, and other cellular components that lies beneath the RPE [4]) and is associated with age-related macular degeneration (AMD) [5]. APP has various isoforms, three of which are shown in Figure 2.1. APP_{695} is found only in the brain, whereas APP_{751} and APP_{770} are found throughout the body [6]. The various isoforms may be identified using antibodies to their specific domains; APP_{751} has a Kunitz-type protease inhibitor (KPI) domain and APP_{770} has both a KPI and an OX-2 homology (OX-2) domain [7]. Regardless of the isoform, APP is cleaved in either one of two pathways: the amyloidogenic pathway, which produces Aβ, or the non-amyloidogenic pathway. The amyloidogenic pathway begins with β-secretase cleavage. This cleavage occurs primarily within the *trans*-Golgi network, though some does occur at the cell membrane and within endosomes. In either case, the soluble APPβ (sAPPβ) ectodomain is produced. γ-secretase then cleaves off functional Aβ [8]. The non-amyloidogenic pathway, which is found primarily at the cell membrane, is initiated when APP is first cleaved by α-secretase. This cleaves off part of the Aβ domain of APP, preventing formation of functional Aβ, and produces the large ectodomain soluble APP alpha (sAPPα), which can be secreted. In both pathways, the small C-terminal fragment, APP Intracellular Domain (AICD) is produced when γ–secretase cleavage occurs [7].

Recent studies have elucidated the metabolism of APP and accumulation of its byproducts in the eye as it relates to the pathology of AMD. Our current understanding of APP

regulation in the eye is reviewed by Ratnayaka, et al [9]. Importantly, there is an iron regulatory component to APP metabolism and function. In the presence of iron, one of the byproducts of APP cleavage, sAPPα, stabilizes ferroportin (FPN), the only known mammalian iron exporter, in HEK293T cells [10], primary neuronal cultures [10], and brain endothelial cells [11, 12]. By stabilizing FPN, sAPPα may regulate iron levels within the RPE and prevent the harmful effects of iron overload. Additionally APP mRNA also has an iron-regulatory element (IRE) [13]. IREs are RNA stem loops that control the translation of iron regulatory proteins, including APP, and thus balance cellular iron storage and transport. Addition of exogenous iron increases APP translation in RPE cells [14]. Thus, more sAPPα can be produced which can stabilize FPN and increase removal of excess iron from the cell. It is important to note that increased iron is found in the RPE of eyes with AMD [15] and that an iron-induced increase in APP alone may not be sufficient to clear the excess iron from retinal cells in this pathological situation.

Hypoxia is a causative factor in AMD [16], although how this occurs is incompletely understood. Hypoxia alters polarized protein localization, specifically the localization of the vascular endothelial growth factor (VEGF) [17]. During hypoxia, RPE cells were shown to secrete higher amounts of VEGF in the basolateral direction. Disruption of this polarized localization of proteins may play a role in AMD [18]. One regulator of polarized protein movement is the cytosolic protein complex, retromer [19]. Importantly, retromer transports APP from endosomes to the trans-Golgi network for recycling and shuttles APP to the apical membrane [20-23].

Exposure of RPE to hypoxic conditions, which may disrupt protein polarization and thus polarized function, is not uncommon. Yet, polarized secretion of APP from RPE and the role of retromer in this process have not been previously studied. The objective of this study was to

determine if there is polarized secretion of APP from RPE, if retromer has a role in this process, and if hypoxia alters this secretion.

Materials and Methods

Tissue culture

Dogs were obtained from the Johnston County, NC animal shelter immediately after being euthanized. Eyes were removed within 3 hours of death and RPE were isolated by trypsinization and transferred to 60 mm tissue culture dishes where they were grown to confluence in Ham's F-12/DMEM (1:1) medium (cat# 31765-035 and #10566-016, Invitrogen, Rockville, MD) with 10% fetal bovine serum (FBS) (Hyclone, Logan, Utah) and 1% antibiotic/antimycotic solution (Mediatech,Manassas, VA). Cultures were incubated at 37 °C, 5% CO_2, 95% humidity until confluence was reached in 7 to 10 days. For subsequent experiments, the cells were then dispersed by trypsinization either onto 6 well tissue culture plates for non-polarized cultures, or onto 6-well Millicell hanging cell culture inserts to establish polarized RPE cultures (polyethylene terephthalate membrane; 1.0 μm pore size) (EMD Millipore, Ballerica, MA) with the apical and basolateral sides bathed separately. Apical medium was comprised of Ham's F-12/DMEM (1:1) medium with 20% 10X B27 Supplement (cat# 17504-044 Invitrogen, Rockville, MD) and 1% antibiotic/antimycotic solution (Mediatech, Manassas, VA). Basal medium was the same as the 10% FBS culture medium described above. For all experiments, primary RPE were plated at 200,000 cells per well or insert. RPE cells plated onto Millicell inserts were determined to be tight junctional by measuring transepithelial electrical resistance (TEER) once a week after plating. Cultures were used for experiments once they exhibited TEER readings over 300 Ω x cm^2 and directional secretion of glutamate to the basal compartment (at least 5 times more to basal than apical compartments indicating a

polarized epithelium). Cultures typically achieved these parameters in 4–8 weeks. For further description of this polarized RPE model see [24]. At the end of the experiments RPE cell lysates and conditioned cell media (CCM) from non-polarized and from apical and basolateral compartments of polarized RPE cells were collected.

Hypoxic treatment

For all experiments involving hypoxia, cells were placed under hypoxic (0.5% O_2) conditions for 24 or 48 hours in a hypoxia chamber (Ruskinn INVIVO2 300 workstation), with corresponding cells placed under normoxic conditions (21% O_2) in a standard cell culture incubator as a control. It is known that hypoxic conditions activate both hypoxia inducible factor 1 and VEGF production (both known hypoxia indicators) within the RPE [25]. Studies were carried out to 48 hours to determine the effects of sustained hypoxic insult to RPE cells. Prior to treatment, cells were washed two times with serum-free, glutamine-free Minimal Essential Medium (MEM) (cat# 51200-038, Invitrogen, Rockville, MD) and then placed in MEM under conditions described above. Additionally, cell metabolic activity was tested using the MTT assay (Trevigen Inc., Gaithersburg, MD) to ensure that hypoxic conditions were not altering RPE cell viability over the course of the experiments.

siRNA Transfection

siRNA for retromer subunit VPS35 (ON-TARGETplus Human VPS35 (55737) siRNA-SMARTpool #L-010894-00-0005) was obtained from GE Dharmacon (Lafayette, CO) as well as a control nontargeting siRNA pool (ON-TARGETplus Non-targeting Pool #D-001810-10-05, Dharmacon). Cells were plated at a density of 125,000 cells/well on six-well plates in 1.5 ml/well of DMEM/F12+10% FBS without antibiotics and incubated overnight at 37°C, typically reaching 30% to 40% confluence. Media were replaced with 900 µl of DMEM/F12+10% FBS

without antibiotics. Lipophilic transfection reagent (0.9 µL/mL, Lipofectamine® RNAiMAX; Invitrogen, Grand Island, NY) siRNA complexes were formed, according to the manufacturer's protocol, in serum-free, glutamine-free MEM without antibiotics and added to each well at a final concentration of 20 nM siRNA/well. Retromer siRNA was added to one set of cells and the control nontargeting siRNA pool was added to cells in a parallel well on each plate as a control for non–sequence-specific cell responses, with each well having a final media volume of 1 ml. After overnight incubation, transfection medium was replaced with 2 ml/well of DMEM/F12+10% FBS with antibiotics. After 72h medium was switched to 2 ml/well serum-free, glutamine-free MEM and cells were exposed to either normoxic (21% O_2) or hypoxic (5% O_2) conditions for 24 or 48 hours and then CCM and lysates were collected for analysis.

Immunoblotting for identification of APP and retromer

After treatment, CCM were collected and cells were lysed using sodium dodecyl sulfate (SDS) lysis buffer. The resulting homogenate was centrifuged for 15 min at 14,000 x g at 11°C, after which the lysate supernatant was collected. CCM were concentrated using an Amicon Ultra 4mL 30kDa filter (EMD Millipore, Ballerica, MA; cat. # UFC803024). Protein concentrations were measured by the BCA assay. Canine cerebral cortex tissue lysate (Zyagen, San Diego, CA) was used as a positive control for APP and retromer. 100 µg total protein from dog cerebral cortex and 15 - 40 µg total protein from primary cultured canine RPE were subjected to 8% SDS-PAGE and the proteins were transferred to a nitrocellulose membrane. The membrane was then blocked in a 10% milk solution in tris-buffered saline (50mM Tris, 150mM NaCl, 1% tween 20). The transferred proteins were probed with primary antibodies to APP clone 3E9 (1 µg/ml; GeneTex, Irvine, CA; cat. # GTX12338) for CCM samples and APP KPI domain (2 µg/ml; EMD Millipore; cat. # AB5302), APP OX2 domain (1 µg/ml; EMD Millipore;

cat. # AB5988P), retromer VPS35 (1:10,000; Abcam, Cambridge, MA; cat. # 157220), or actin (0.7 µg/ml; Santa Cruz, Dallas, TX; cat. # sc-1615) for lysate samples. Different APP antibodies were used for CCM and lysate immunoblots to obtain the lowest background. Specifically, both the KPI and 3E9 antibodies are located on the N terminal of APP. The 3E9 antibody is able to detect all isoforms of APP as it is a synthetic peptide with the sequence LEVPTDGNAGLLAEPQIAMFC, corresponding to amino acids 18-38 of APP. Within the CCM, it was found that 3E9 gave lower background levels than KPI, resulting in better quantitation of the mature and immature bands on the immunoblot. After washing with TBST, the membrane was incubated with horseradish-peroxidase (HRP) conjugated anti-rabbit IgG antibody (4 µg/ml; eBioscience, Inc., San Diego, CA; cat. # 18-8816-33) or HRP conjugated anti-mouse IgG (0.5 µg/ml; EMD Millipore; cat. # 12-349). Proteins were visualized using an enhanced chemiluminescence detection system (GE Healthcare Life Sciences, Pittsburgh, PA) according to manufacturer's protocol and the blot was imaged using a ChemiDoc™ MP System (BioRad, Hercules, CA). Immunoblots were normalized using the total protein normalization method, which removes the need to use housekeeping proteins for loading controls. Total protein normalization allows for greater quantitative accuracy in measuring target proteins [26-28]. Additionally, total protein normalization has recently become the preferred method for the Journal of Biological Chemistry for immunoblot normalization.

Immunofluorescence

Polarized RPE cells grown on Millicell inserts were fixed in 2.0% formaldehyde in PBS, permeabilized with PBS+0.1% Triton X-100, blocked in PBS+5.0% normal donkey serum, and then incubated overnight at 4°C with mouse anti-APP antibodies (clone 3E9) (GeneTex GTX12338, 5.0 µg/ml) and rabbit anti-ZO-1 antibodies (Invitrogen 40-2200, 2.5 µg/ml) in

PBS+0.1% bovine serum albumin (PBS/BSA). After PBS washes, APP was detected with donkey anti-mouse AlexaFluor® 568 IgG (Invitrogen) and ZO-1 was detected with donkey anti-rabbit Alexa Fluor® 488 IgG (Invitrogen), both at 2.0 µg/ml in PBS/BSA for 2 hours at room temperature. After PBS washes, filters with labeled RPE cells were cut from the inserts with a scalpel blade and mounted on slides in Prolong®Gold anti-fade mounting medium containing DAPI (Invitrogen). Cells were viewed on a Leica AF7000 widefield fluorescence microscope. Image stacks were captured with an Andor Clara interline CCD using the same exposures for all samples, deconvolved using the Leica LAS AF software 3D deconvolution tool, rendered as 3D volume projections, and then arranged using Adobe® Photoshop® CS4.

Statistics

The data were analyzed by ANOVA with Tukey's HSD test for multiple comparisons in SYSTAT 13 (San Jose, California). Results were considered significant when $p < 0.05$.

Results

Canine RPE cells express amyloid precursor protein (APP_{770})

Non-polarized RPE cell lysates were collected and immunoblotted using the APP primary antibody, OX2. The OX2 domain is only present in the APP_{770} isoform, therefore this isoform is present in RPE cells (Figure 2.2). APP is found in both an immature, non-glycosylated form and a mature, highly glycosylated form in RPE lysates. Both forms of APP_{770} were visible on the immunoblot for APP. The lower band is the immature form, and the upper band is the mature glycosylated form.

Effects of hypoxia on APP expression and secretion from non-polarized RPE cells

Preliminary studies were first conducted in non-polarized RPE. Non-polarized RPE were exposed to normoxic (21% O_2) or hypoxic (0.5% O_2) conditions for 24 or 48 hours. MTT

viability testing showed no significant differences between RPE cells placed in normoxic or hypoxic conditions (data not shown). Lysates from these cells had a significant reduction ($p<0.05$) in APP levels after both 24 and 48 hours in hypoxia (Figure 2.3A). CCM from the same cells also showed a significant reduction ($p<0.05$) in APP at 48 hours in hypoxia (Figure 2.3B).

Effects of hypoxia on APP expression, accumulation, and secretion in polarized RPE cells

Building upon the intriguing results seen in the non-polarized model, RPE cells were plated on Millicell tissue culture inserts and grown to confluence as tight junctional, polarized monolayers. This culture system allows separate analysis of metabolites secreted from the apical and basolateral membrane domains as well as analysis of cell culture lysates within a more in-vivo like model. These polarized RPE were then exposed to normoxic (21% O_2) or hypoxic (0.5% O_2) conditions for 24 or 48 hours and both the cell lysates and CCM from the apical and basolateral compartments were analyzed by immunoblotting. APP expression was significantly reduced ($p<0.05$) in the lysates after 48 hours in hypoxia (Figure 2.4A).

Apical APP secretion was unchanged in normoxic samples between 24 and 48 hours (Figure 2.4B). Hypoxia caused a 47% decrease ($p<0.05$) in apical APP secretion at 24 hours and an even further decrease of 92% ($p<0.05$) at 48 hours when compared to normoxic samples. Basolateral media samples had a 30% increase in APP accumulation under normoxic conditions from 24 to 48 hours ($p<0.05$). APP accumulation in basolateral media was decreased by 31% ($p<0.05$) at 24 hours in hypoxia but was not significantly different at 48 hours in hypoxia compared to normoxia (Figure 2.4B). Additionally, apical and basolateral secretions of APP were significantly different ($p<0.05$) from one another at 48 hours in hypoxia, the only time

point at which this occurred, indicating a more pronounced effect of hypoxia on apical APP secretion. This suggested that hypoxia may affect polarized secretion of APP after 48 hours.

Fluorescent immunolocalization of APP showed polarized accumulation of APP in RPE cells at 48 hours (Figure 2.5). We observed abundant APP-specific fluorescence on the apical side of polarized RPE cells grown in normoxic conditions (Figure 2.5A). RPE exposed to hypoxic conditions for 48 hours showed a dramatic decrease in apical APP-specific fluorescence (Figure 2.5B).

Retromer is expressed in RPE cells and hypoxia decreased its expression

Retromer sorts proteins, including APP [20, 22], from the endosome to the *trans*-Golgi network. Defective retromer pathways incorrectly sort the divalent metal transporter to lysosomal domains instead of properly recycling it to the plasma membrane [29]. When the retromer pathway is disrupted, APP processing favors amyloidogenic processing over the non-amyloidogenic pathway [30]. Therefore, we investigated a possible role for retromer in hypoxia-induced reduction of APP secretion. First, the effect of hypoxia on retromer expression was determined. One major subunit of retromer (VPS35) was detected in RPE lysates by immunoblotting. In non-polarized RPE, hypoxia did not change retromer levels at any time point (Figure 2.6A). In polarized RPE, there were no significant changes in retromer levels after 24 hours of hypoxia, but after 48 hours of hypoxia, retromer levels significantly ($p<0.05$) decreased by 83% (Figure 2.6A). This retromer decrease was similar to the hypoxia-induced decrease in apical APP secretion seen at 48 hours in hypoxia (Figure 2.4B). Figure 2.6B is a representative immunoblot of retromer expression in non-polarized and polarized RPE lysates obtained under normoxic and hypoxic conditions at 24 and 48 hours.

Retromer knockdown with siRNA decreased APP secretion from RPE cells

To determine if retromer expression is linked with APP secretion, retromer expression was knocked down with siRNA and APP secretion was measured in the CCM after 24 and 48 hours under normoxic and hypoxic conditions. Non-polarized cells were used as it was not possible to transfect polarized RPE cells. All time points were paired with a negative control siRNA treatment. Retromer knock-down significantly ($p<0.05$) reduced APP secretion under both normoxic and hypoxic conditions at all time points except the 48 hour normoxic time point (Figure 2.7A).

Discussion

Amyloid precursor protein (APP) is a ubiquitous protein with important roles in the pathology of Alzheimer's disease and AMD. APP also functions as a proliferative factor for epithelial cells [31, 32] and is involved in iron metabolism [14]. First, we determined which variant of APP was present within RPE cells. Immunoblotting for the OX2 domain, which is only present in APP_{770}, showed that RPE cells predominantly express this variant. This was not surprising since this splice variant is found in most cells, while APP_{695} is the predominant form in neurons. We detected both the mature (glycosylated) and the immature (non-glycosylated) form of APP_{770} when RPE lysates were probed for APP by immunoblotting. Most of the secreted APP_{770} found in the CCM was in the mature form.

Hypoxia is a key pathological factor in disease states leading to cellular degradation, death, and loss of retinal function. Thus, it may play a role in AMD [16]. In the current study we determined the effects of hypoxia on APP expression and secretion by RPE. Under 24 and 48 hours of hypoxia, APP within the lysates of non-polarized RPE was significantly reduced (80% and 60% respectively). In the CCM of non-polarized RPE, APP was significantly reduced

by almost 60% at 48 hours, which very closely mirrors the decrease seen in the lysates. That there was a reduction in APP in cell lysates at 24 hours but not an accumulation in the CCM may be due to a slow decrease in APP secretion that reflects a gradually decreasing cellular pool of APP.

Using our polarized, tight junctional RPE cell model, we determined that hypoxia affects directional secretion of APP. APP accumulation in the basolateral compartment was reduced under hypoxia at 24 hours when compared to normoxia. However, there was no further decrease in basolateral APP accumulation from 24 and 48 hours. Apical APP accumulation was reduced at 24 hours and continued to decline with time becoming almost undetectable at 48 hours. These findings demonstrate that hypoxia alters APP polarized secretion more significantly in the apical direction than in the basolateral. Under normoxia, apical and basolateral APP secretion remained relatively constant in the CCM. It should be noted that APP could be degraded by proteolytic enzymes within the CCM. However, this is likely not the case as the fluorescent immunolocalization in figure 2.5 shows that APP within the cell is also significantly decreased after 48 hours in hypoxia. APP levels in lysates from polarized RPE decreased after 48 hours in hypoxia, likely contributing to the decreased amounts of APP seen in the CCM. These results were again supported by those using fluorescent immunolocalization, i.e., polarized RPE cells exposed to hypoxia for 48 hours showed dramatically reduced accumulation of APP at the apical membrane compared to cells grown under normoxic conditions.

This demonstration of a hypoxic effect leading to alterations in directional APP secretion led to studies to identify which intracellular transporter of APP was affected by hypoxia. Retromer is a multimeric protein which regulates the polarized movement of proteins including APP from endosomes to the *trans*-Golgi network for recycling, and then to apical or basolateral

surfaces [22, 33, 34]. Because hypoxia affected polarized secretion of APP in RPE, its effects on retromer expression were determined. Hypoxia decreased retromer levels in polarized RPE cell lysates an average of 83% after 48 hours, which is similar to the 92% decrease in apical APP secretion at the same time point. Significantly, when retromer in RPE cells was knocked down with siRNA, APP secretion was reduced under both normoxic and hypoxic conditions. The consistent reduction of APP accumulation in the CCM implies that retromer may control its secretion. Our results suggest that in polarized RPE cells, retromer may be responsible for the movement of APP to the apical surface and this activity is disrupted by hypoxia.

Reducing retromer levels within the cell disrupts the APP pathway and production of its byproducts [30, 35]. Specifically when retromer activity is disrupted, it cannot recycle APP from endosomes back to the *trans*-Golgi network, leading to increased amyloidogenic processing of APP in the enzymatically favorable endosomal environment [35]. Therefore, hypoxia, by decreasing retromer levels could contribute to Aβ production and accumulation in age-related macular degeneration and Alzheimer's disease.

In non-polarized cells, the retromer pathway may be utilized less since polarized localization of proteins may not be a priority for non-polarized cells. Non-polarized cells may preferentially use the recycling pathway of retromer and not its ability to facilitate polarized protein transport. The finding that hypoxia decreases APP in lysates and accumulation in CCM of non-polarized cells at 48 hours, while retromer levels are unaffected, suggests that hypoxia affects more than one pathway controlling APP movement and secretion, and that hypoxia has differential effects on non-polarized and polarized RPE cells. The following examples illustrate how experimental conditions can affect non-polarized and polarized RPE cells differently. TNF-α has been shown to upregulate vascular endothelial growth factor (VEGF) secretion in non-

polarized RPE cells. However, in polarized RPE cells it downregulates VEGF secretion [36]. Additionally, thrombin disrupts ZO-1 and F-actin in non-polarized RPE cells, but does not affect them in polarized RPE cells [37].

APP has recently been reported to regulate iron efflux [12]. Specifically, one of APP's byproducts, sAPPα, can stabilize FPN in the cell membrane [10], allowing excess iron to exit the cell. In mice fed an iron rich diet, the retina was spared from iron overload [38]; an interaction between APP and FPN may be an important factor in this effect [10]. Therefore, a decrease in intracellular APP, and/or APP secretion caused by hypoxia, could decrease iron efflux, which could contribute to the increased iron seen within the RPE of those with AMD [15]. Our lab has shown that hypoxia caused polarized RPE cells to preferentially secrete iron in the basolateral direction [24]. A decrease in availability of APP for stabilizing FPN within the RPE apical membrane, as indicated by the results of the current study, could be a contributing factor.

This is the first demonstration that hypoxia decreased APP secretion and retromer levels in any cell type. The hypoxia-induced decrease in retromer levels may be responsible for the dramatic changes seen in apical APP secretion in polarized RPE. Understanding how hypoxia affects protein processing, polarized localization, and secretion is vital to a comprehensive understanding of RPE pathophysiology and in all cells with retromer-regulated polarized protein movement that are exposed to hypoxic conditions

REFERENCES

1. Campbell M, Humphries P. The blood-retina barrier: tight junctions and barrier modulation. Adv Exp Med Biol 2012; 763:70-84.

2. Kaur C, Foulds WS, Ling EA. Blood-retinal barrier in hypoxic ischaemic conditions: basic concepts, clinical features and management. Prog Retin Eye Res 2008; 27(6):622-47.

3. Klaassen I, Van Noorden CJ, Schlingemann RO. Molecular basis of the inner blood-retinal barrier and its breakdown in diabetic macular edema and other pathological conditions. Prog Retin Eye Res 2013; 34:19-48.

4. Crabb JW. The proteomics of drusen. Cold Spring Harb Perspect Med 2014; 4(7):a017194.

5. Ohno-Matsui K. Parallel findings in age-related macular degeneration and Alzheimer's disease. Prog Retin Eye Res 2011; 30(4):217-38.

6. Zheng H, Koo EH. Biology and pathophysiology of the amyloid precursor protein. Mol Neurodegener 2011; 6(1):27.

7. Nalivaeva NN, Turner AJ. The amyloid precursor protein: a biochemical enigma in brain development, function and disease. FEBS Lett 2013; 587(13):2046-54.

8. O'Brien RJ, Wong PC. Amyloid precursor protein processing and Alzheimer's disease. Annu Rev Neurosci 2011; 34:185-204.

9. Ratnayaka JA, Serpell LC, Lotery AJ. Dementia of the eye: the role of amyloid beta in retinal degeneration. Eye (Lond) 2015.

10. Wong BX, Tsatsanis A, Lim LQ, Adlard PA, Bush AI, Duce JA. beta-Amyloid precursor protein does not possess ferroxidase activity but does stabilize the cell surface ferrous iron exporter ferroportin. PLoS One 2014; 9(12):e114174.

11. McCarthy RC, Kosman DJ. Mechanisms and regulation of iron trafficking across the capillary endothelial cells of the blood-brain barrier. Front Mol Neurosci 2015; 8:31.

12. McCarthy RC, Park YH, Kosman DJ. sAPP modulates iron efflux from brain microvascular endothelial cells by stabilizing the ferrous iron exporter ferroportin. EMBO Rep 2014; 15(7):809-15.

13. Rogers JT, Randall JD, Cahill CM, Eder PS, Huang X, Gunshin H, Leiter L, McPhee J, Sarang SS, Utsuki T, Greig NH, Lahiri DK, Tanzi RE, Bush AI, Giordano T, Gullans SR. An iron-responsive element type II in the 5'-untranslated region of the Alzheimer's amyloid precursor protein transcript. J Biol Chem 2002; 277(47):45518-28.

14. Guo LY, Alekseev O, Li Y, Song Y, Dunaief JL. Iron increases APP translation and amyloid-beta production in the retina. Exp Eye Res 2014; 129:31-7.

15. Hahn P, Milam AH, Dunaief JL. Maculas affected by age-related macular degeneration contain increased chelatable iron in the retinal pigment epithelium and Bruch's membrane. Arch Ophthalmol 2003; 121(8):1099-105.

16. Blasiak J, Petrovski G, Vereb Z, Facsko A, Kaarniranta K. Oxidative stress, hypoxia, and autophagy in the neovascular processes of age-related macular degeneration. Biomed Res Int 2014; 2014:768026.

17. Blaauwgeers HG, Holtkamp GM, Rutten H, Witmer AN, Koolwijk P, Partanen TA, Alitalo K, Kroon ME, Kijlstra A, van Hinsbergh VW, Schlingemann RO. Polarized vascular endothelial growth factor secretion by human retinal pigment epithelium and localization of vascular endothelial growth factor receptors on the inner choriocapillaris. Evidence for a trophic paracrine relation. Am J Pathol 1999; 155(2):421-8.

18. Kay P, Yang YC, Hiscott P, Gray D, Maminishkis A, Paraoan L. Age-related changes of cystatin C expression and polarized secretion by retinal pigment epithelium: potential age-related macular degeneration links. Invest Ophthalmol Vis Sci 2014; 55(2):926-34.

19. Burd C, Cullen PJ. Retromer: a master conductor of endosome sorting. Cold Spring Harb Perspect Biol 2014; 6(2).

20. Choy RW, Cheng Z, Schekman R. Amyloid precursor protein (APP) traffics from the cell surface via endosomes for amyloid beta (Abeta) production in the trans-Golgi network. Proc Natl Acad Sci U S A 2012; 109(30):E2077-82.

21. Reitz C. The role of intracellular trafficking and the VPS10d receptors in Alzheimer's disease. Future Neurol 2012; 7(4):423-31.

22. Vieira SI, Rebelo S, Esselmann H, Wiltfang J, Lah J, Lane R, Small SA, Gandy S, da Cruz ESEF, da Cruz ESOA. Retrieval of the Alzheimer's amyloid precursor protein from the endosome to the TGN is S655 phosphorylation state-dependent and retromer-mediated. Mol Neurodegener 2010; 5:40.

23. Lu L, Hong W. From endosomes to the trans-Golgi network. Semin Cell Dev Biol 2014; 31:30-9.

24. Harned J, Nagar S, McGahan MC. Hypoxia controls iron metabolism and glutamate secretion in retinal pigmented epithelial cells. Biochim Biophys Acta 2014; 1840(10):3138-44.

25. Goralska M, Ferrell J, Harned J, Lall M, Nagar S, Fleisher LN, McGahan MC. Iron metabolism in the eye: a review. Exp Eye Res 2009; 88(2):204-15.

26. Taylor SC, Berkelman T, Yadav G, Hammond M. A defined methodology for reliable quantification of Western blot data. Mol Biotechnol 2013; 55(3):217-26.

27. Gilda JE, Gomes AV. Stain-Free total protein staining is a superior loading control to beta-actin for Western blots. Anal Biochem 2013; 440(2):186-8.

28. Gurtler A, Kunz N, Gomolka M, Hornhardt S, Friedl AA, McDonald K, Kohn JE, Posch A. Stain-Free technology as a normalization tool in Western blot analysis. Anal Biochem 2013; 433(2):105-11.

29. Tabuchi M, Yanatori I, Kawai Y, Kishi F. Retromer-mediated direct sorting is required for proper endosomal recycling of the mammalian iron transporter DMT1. J Cell Sci 2010; 123(Pt 5):756-66.

30. Sullivan CP, Jay AG, Stack EC, Pakaluk M, Wadlinger E, Fine RE, Wells JM, Morin PJ. Retromer disruption promotes amyloidogenic APP processing. Neurobiol Dis 2011; 43(2):338-45.

31. Pietrzik CU, Hoffmann J, Stober K, Chen CY, Bauer C, Otero DA, Roch JM, Herzog V. From differentiation to proliferation: the secretory amyloid precursor protein as a local mediator of growth in thyroid epithelial cells. Proc Natl Acad Sci U S A 1998; 95(4):1770-5.

32. Hoffmann J, Twiesselmann C, Kummer MP, Romagnoli P, Herzog V. A possible role for the Alzheimer amyloid precursor protein in the regulation of epidermal basal cell proliferation. Eur J Cell Biol 2000; 79(12):905-14.

33. Zhou B, Wu Y, Lin X. Retromer regulates apical-basal polarity through recycling Crumbs. Dev Biol 2011; 360(1):87-95.

34. Coudreuse DY, Roel G, Betist MC, Destree O, Korswagen HC. Wnt gradient formation requires retromer function in Wnt-producing cells. Science 2006; 312(5775):921-4.

35. Cuartero Y, Mellado M, Capell A, Alvarez-Dolado M, Verges M. Retromer regulates postendocytic sorting of beta-secretase in polarized Madin-Darby canine kidney cells. Traffic 2012; 13(10):1393-410.

36. Terasaki H, Kase S, Shirasawa M, Otsuka H, Hisatomi T, Sonoda S, Ishida S, Ishibashi T, Sakamoto T. TNF-alpha decreases VEGF secretion in highly polarized RPE cells but increases it in non-polarized RPE cells related to crosstalk between JNK and NF-kappaB pathways. PLoS One 2013; 8(7):e69994.

37. Terasaki H, Shirasawa M, Otsuka H, Yamashita T, Uchino E, Hisatomi T, Sonoda S, Sakamoto T. Different Effects of Thrombin on VEGF Secretion, Proliferation, and Permeability in Polarized and Non-polarized Retinal Pigment Epithelial Cells. Curr Eye Res 2015; 40(9):936-45.

38. Bhoiwala DL, Song Y, Cwanger A, Clark E, Zhao LL, Wang C, Li Y, Song D, Dunaief JL. CD1 Mouse Retina Is Shielded From Iron Overload Caused by a High Iron Diet. Invest Ophthalmol Vis Sci 2015; 56(9):5344-52.

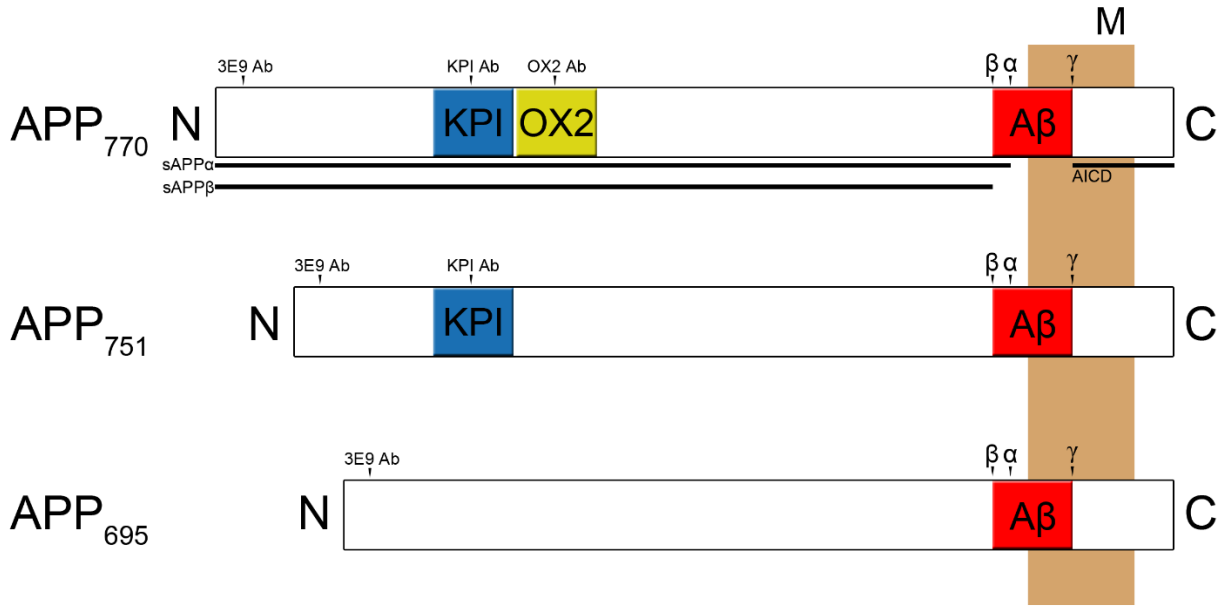

Figure 2.1 APP Isoforms Schematic representation of the proteins from the APP family and their major domains. They are all type I transmembrane glycoproteins. APP_{695} lacks the KPI and OX2 domains, contained in APP_{770}, while APP_{751} has only the KPI domain. All three isoforms contain the Aβ domain. β, α, and γ secretase cleavage sites are marked by their Greek letters on each APP isoform. The soluble APP α and β fragments (sAPPα and sAPPβ respectively) and the APP Intracellular Domain (AICD) fragment are denoted by black lines on the APP_{770} isoform. Antibody recognition sites are marked on each isoform. M = membrane.

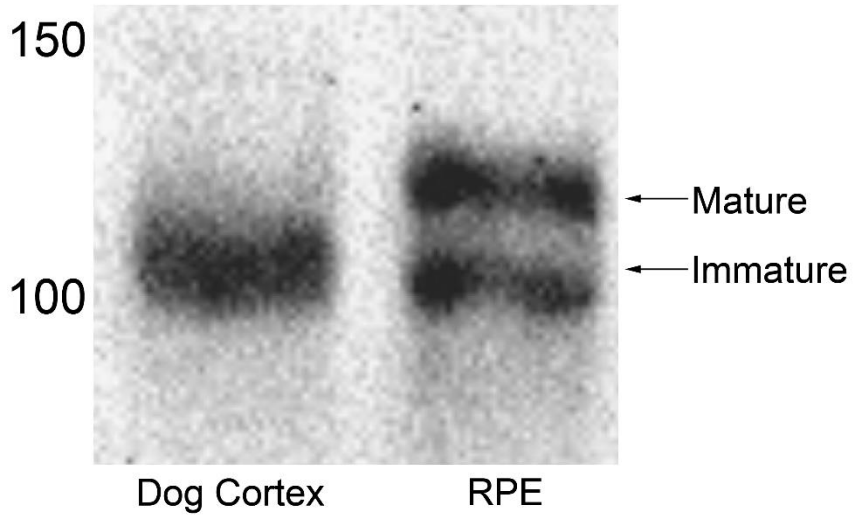

Figure 2.2 Canine RPE Cells Contain APP 770 RPE cells were exposed to normoxic conditions for 24 hrs. Canine cerebral cortex lysate (100µg total protein), labeled as dog cortex, and RPE lysates (40 µg total protein) were run on an 8% gel and probed with an antibody against the OX2 APP extracellular domain, which is only present on the 770 isoform of APP. The two bands in the RPE lysates represent immature APP (bottom band) and its mature glycosylated form (top band).

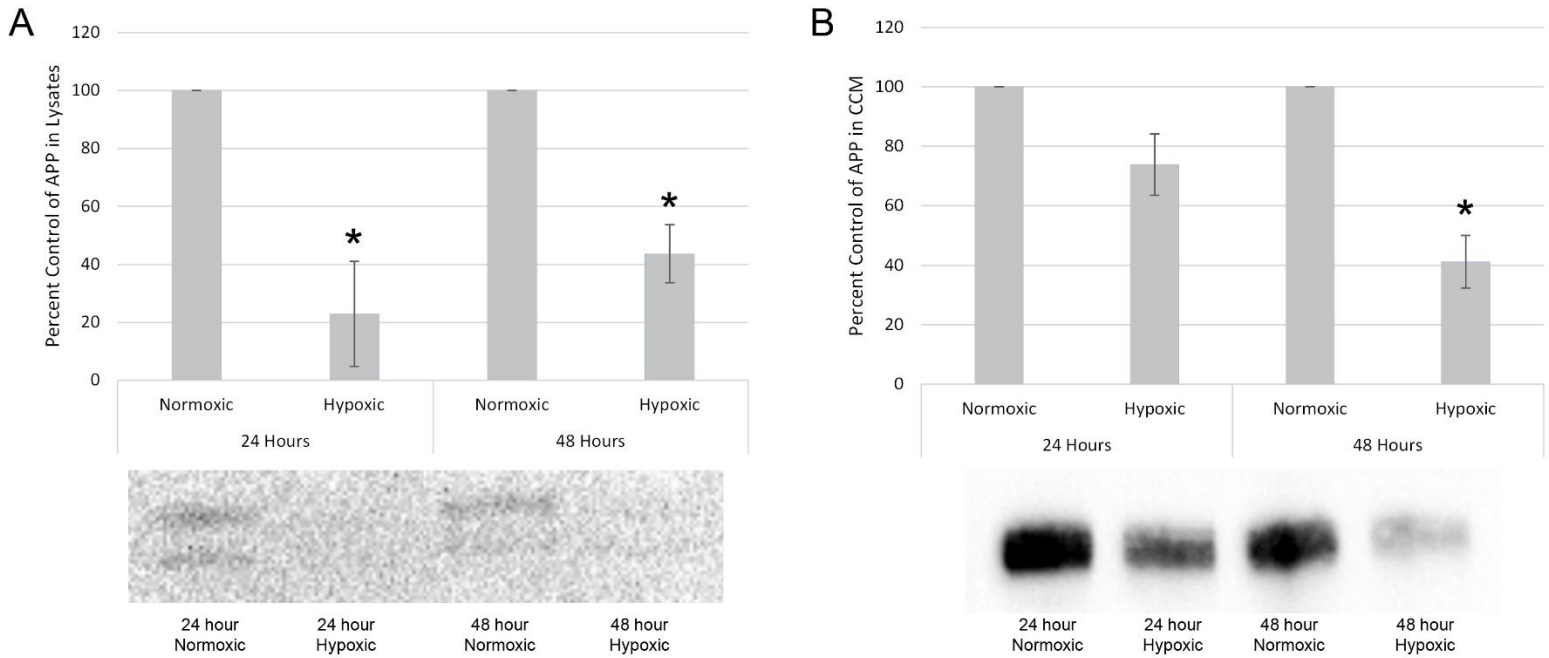

Figure 2.3 APP Expression and Secretion Decrease in Hypoxia in Non-Polarized RPE Cells Lysates (20 µg total protein) and CCM (15 µg total protein) from non-polarized RPE cells exposed to normoxia and hypoxia for 24 or 48 hours were probed for APP with the 3E9 antibody for CCM and the KPI antibody for lysates. **A:** Percent control of APP expression in non-polarized RPE lysates, with representative immunoblot below the graph. **B:** Percent control of APP secreted into the non-polarized RPE CCM, with representative immunoblot below the graph. * = Significantly different ($p < 0.05$) from the paired normoxic condition as determined from percent control data previously normalized to total protein loaded from 4 experiments (A) and 3 experiments (B) and analyzed statistically in Systat 13 by ANOVA, with post-hoc Tukey's HSD and SEM

Figure 2.4 Hypoxia Decreases Expression of APP in Polarized RPE Lysates and Changes Polarized APP Secretion RPE cells were grown on Millicell™ inserts until polarized, tight junctional monolayers were formed. Cells were then incubated in either normoxic or hypoxic conditions for 24 or 48 hours. CCM was collected and concentrated from both the apical and basolateral compartments of the Millicell™ inserts. Lysates were also collected. The CCM (15 µg total protein) was probed with the APP antibody for 3E9 and lysates (20 µg total protein) were probed with the APP antibody for KPI. **A:** Percent control data of APP expression in polarized RPE lysates, with representative immunoblot below the graph. * = Significantly different ($p < 0.05$) from paired normoxic condition as determined from percent control data previously normalized to total protein loaded from 4 experiments and analyzed statistically in Systat 13 by ANOVA, with post-hoc Tukey's HSD and SEM. Δ = Basal secretion significantly different ($p < 0.05$) as determined from percent control data previously normalized to total protein loaded from 4 experiments and analyzed statistically in Systat 13 by ANOVA, with post-hoc Tukey's HSD and SEM. **B:** Secreted APP content of CCM from polarized RPE cells. The RPE monolayer is represented on the graph at value 0 on the Y axis, with apical secretion above and basolateral secretion below. * = Significantly different ($p < 0.05$) from indicated condition as determined from percent control data from 4 experiments and analyzed statistically in Systat 13 by ANOVA, with post-hoc Tukey's HSD and SEM. **C:** Representative immunoblot showing secreted APP in concentrated CCM from polarized RPE cells.

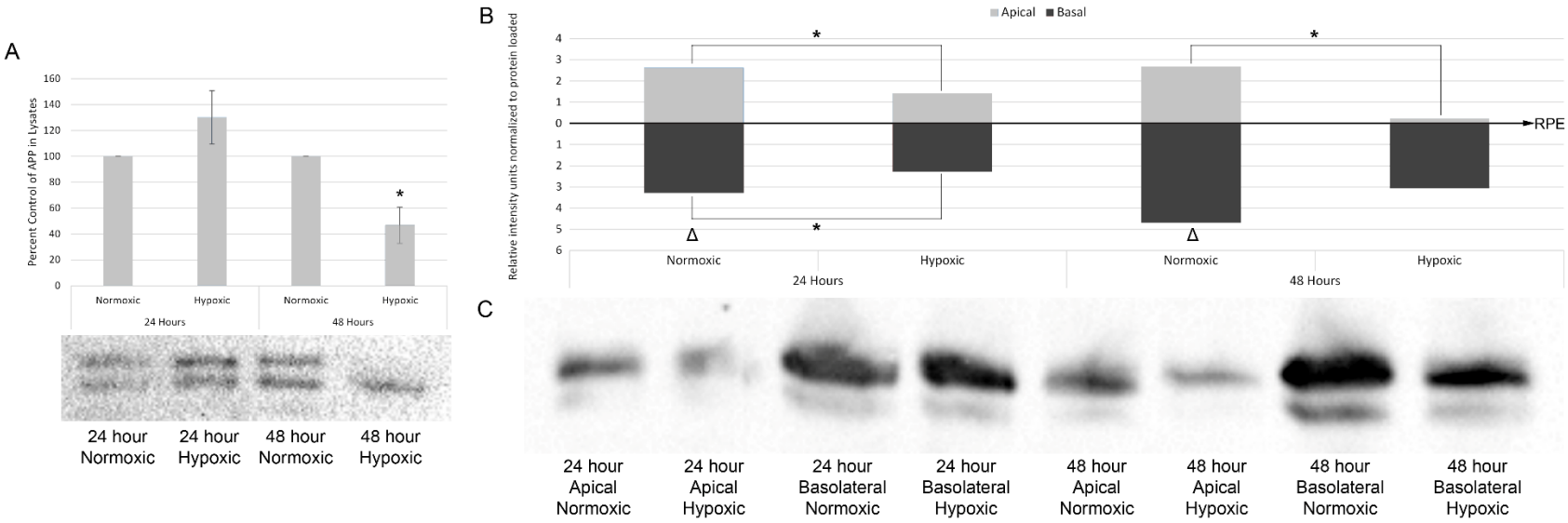
A
Percent Control of APP in Lysates
160
140
120
100
80
60
40
20
0
Normoxic
Hypoxic
Normoxic
Hypoxic
24 Hours
48 Hours
*
24 hour Normoxic
24 hour Hypoxic
48 hour Normoxic
48 hour Hypoxic
B
Apical
Basal
Relative intensity units normalized to protein loaded
4
3
2
1
0
1
2
3
4
5
6
*
*
*
Δ
Δ
RPE
Normoxic
Hypoxic
Normoxic
Hypoxic
24 Hours
48 Hours
C
24 hour Apical Normoxic
24 hour Apical Hypoxic
24 hour Basolateral Normoxic
24 hour Basolateral Hypoxic
48 hour Apical Normoxic
48 hour Apical Hypoxic
48 hour Basolateral Normoxic
48 hour Basolateral Hypoxic

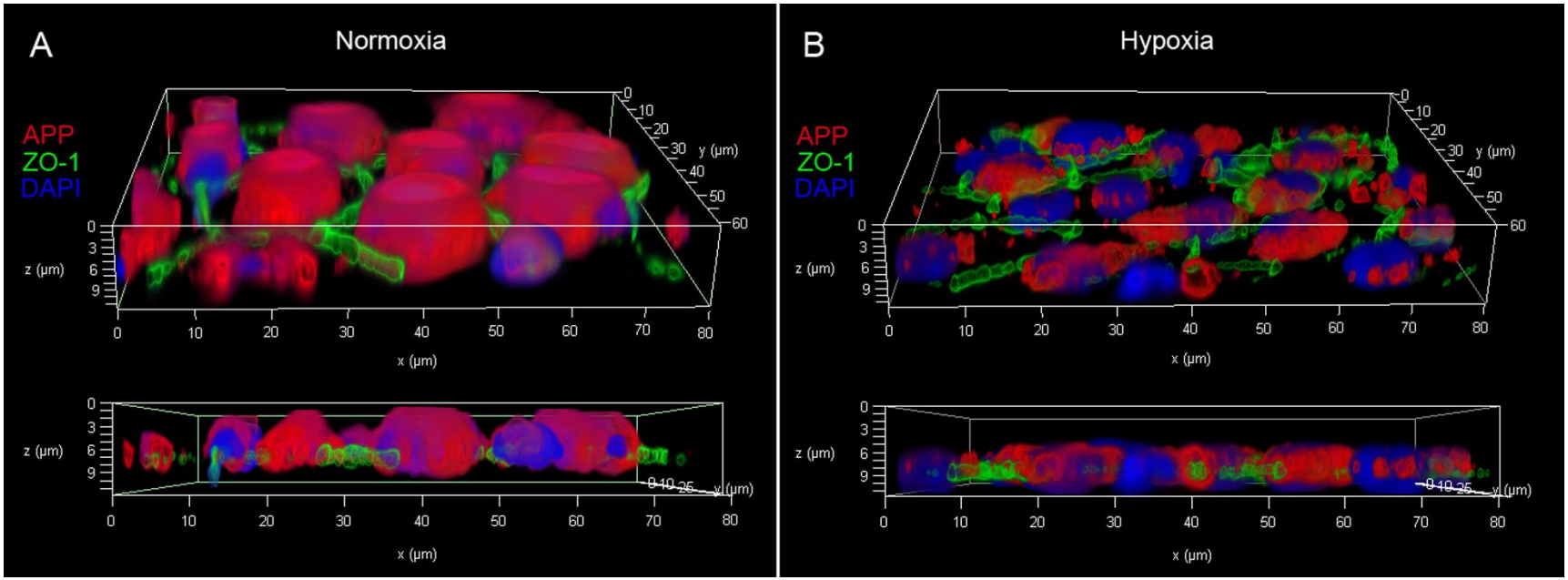

Figure 2.5 Apical Localization of APP Decreases Under Hypoxic Conditions Polarized RPE cells grown on cell culture inserts were exposed to (**A**) normoxic (20% O_2) or (**B**) hypoxic (0.5% O_2) conditions for 48 hours, fixed and labeled for APP (red), ZO-1 (green), and DAPI for nuclei (blue). A and B show 3D deconvolved reconstructions of z-stacks through the monolayers projected as 3D volumes. Upper images are tilted XY views. Lower images are XZ projections showing representative cross-sectional views at the edges of the fields of cells. ZO-1 labels tight junctions and demarks the boundary between the apical and basolateral cell compartments of these polarized cells. Red APP-specific fluorescence is much lower in the apical regions (above the green ZO-1 tight junctions) of RPE cells grown under hypoxia for 48 hours.

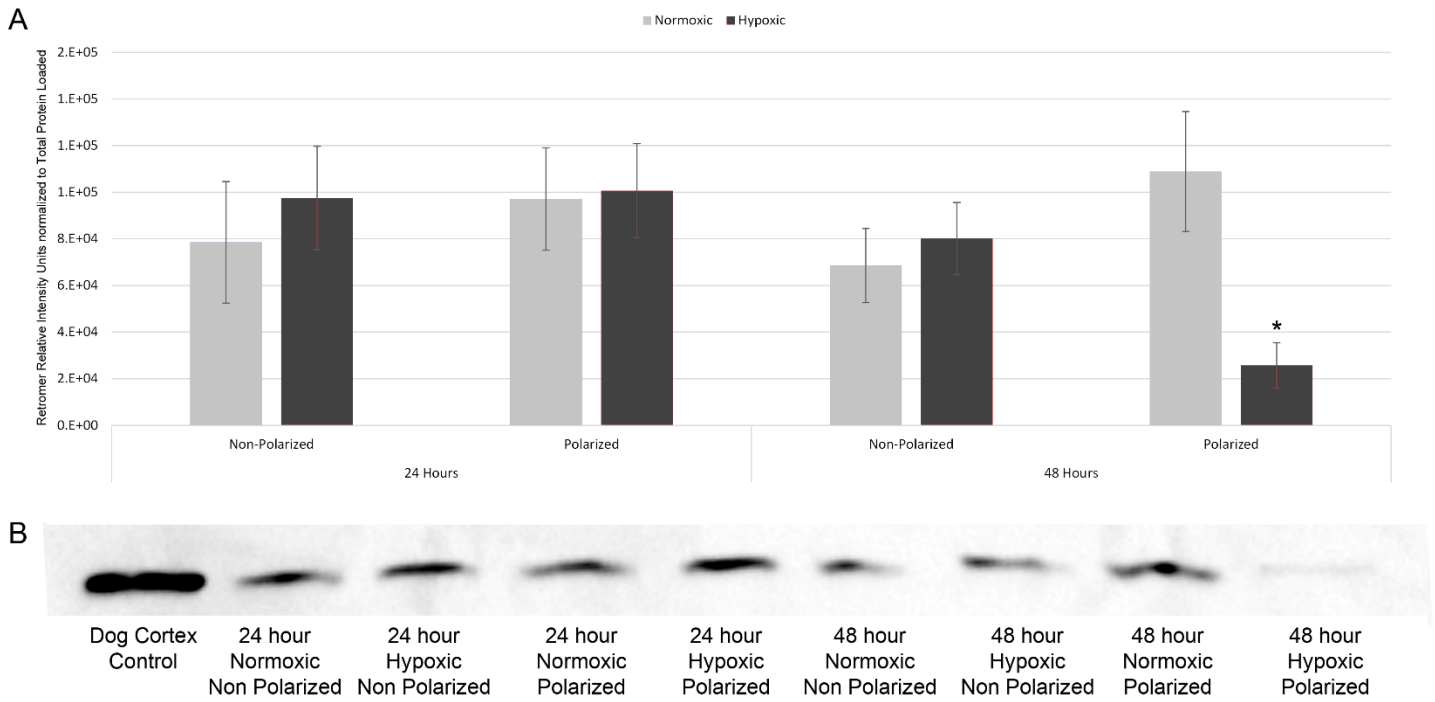

Figure 2.6 Hypoxia Decreases Retromer Expression in Polarized RPE Cells A: Non-polarized and polarized RPE cells were incubated in either normoxic or hypoxic conditions for 24 or 48 hours, after which lysates were collected. Lysates (20 µg total protein) were probed with VPS35 (retromer) antibody. * = Significantly different ($p < 0.05$) from paired normoxic condition as determined from percent control data previously normalized to total protein loaded from 4 experiments and analyzed statistically in Systat 13 by ANOVA, with post-hoc Tukey's HSD and SEM. **B:** Representative immunoblot of retromer expression in non-polarized and polarized RPE cells after 24 and 48 hours in normoxic and hypoxic conditions. Dog cortex was used as a positive control for retromer expression.

Figure 2.7 Retromer Knockdown Decreases APP Secretion into the CCM in Non-Polarized RPE Cells in Normoxic and Hypoxic conditions CCM was collected and concentrated from RPE cells that had been treated with VPS35 (retromer) siRNA overnight, grown to confluence for 72 hours, and then placed in normoxic or hypoxic conditions for 24 or 48 hours. Lysates were also collected. Lysates (20 µg total protein) were probed with VPS35 (retromer) antibody to confirm knockdown of retromer in the RPE cells. CCM (20 µg total protein), secreted from the same RPE lysates that were probed for retromer, was probed with the 3E9 APP antibody. **A:** Percent control data of APP secretion into the CCM of siRNA treated RPE cells. * = Significantly different ($p < 0.05$) from paired negative siRNA control as determined from percent control data previously normalized to total protein loaded from 5 experiments and analyzed statistically in Systat 13 by ANOVA, with post-hoc Tukey's HSD and SEM. **B:** Representative immunoblot of CCM probed for APP after cells had been treated with retromer siRNA for 24 hours and subsequently placed in normoxic or hypoxic conditions for 24 or 48 hours. **C:** Representative immunoblot of RPE lysates from same cells as in (B) probed for retromer, confirming effective knockdown of retromer.

A

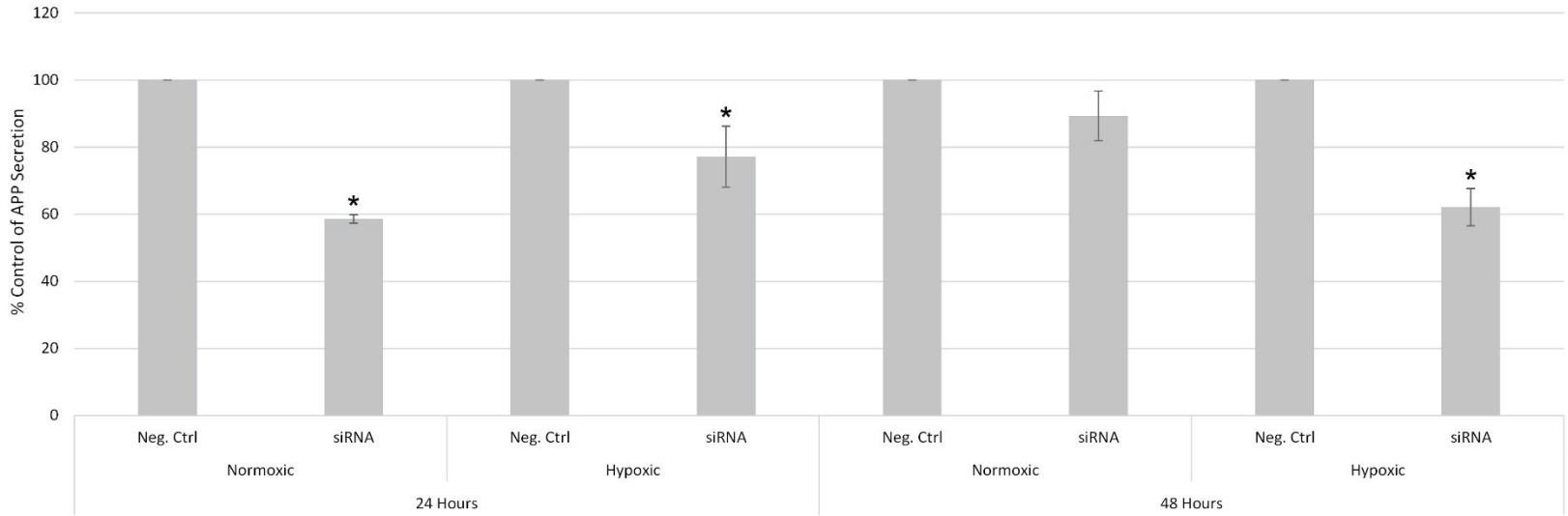
120
100
80
60
40
20
0
% Control of APP Secretion
*
*
*
Neg. Ctrl
siRNA
Neg. Ctrl
siRNA
Neg. Ctrl
siRNA
Neg. Ctrl
siRNA
Normoxic
Hypoxic
Normoxic
Hypoxic
24 Hours
48 Hours

B

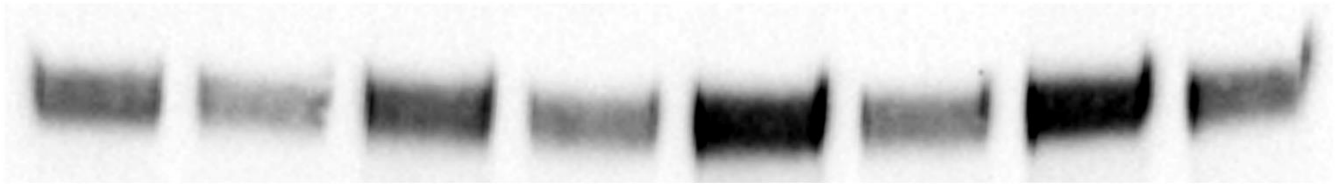
Neg. Ctrl siRNA Normoxic 24 hr.
Retromer siRNA Normoxic 24 hr.
Neg. Ctrl siRNA Hypoxic 24 hr.
Retromer siRNA Hypoxic 24 hr.
Neg. Ctrl siRNA Normoxic 48 hr.
Retromer siRNA Normoxic 48 hr.
Neg. Ctrl siRNA Hypoxic 48 hr.
Retromer siRNA Hypoxic 48 hr.

C

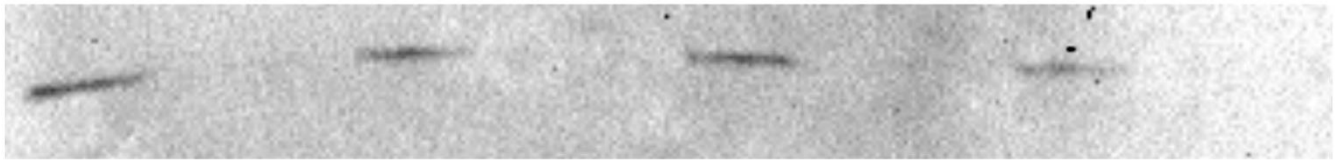

CHAPTER 3

Nascent Synthesis of the Amyloid Precursor Protein in Retinal Pigmented Epithelial Cells is Reduced in Hypoxia

Abstract

Purpose

Amyloid precursor protein (APP) is a ubiquitously expressed protein that is metabolized to amyloid beta (present in drusen in AMD and in plaques in Alzheimer disease brains) and soluble APP alpha and beta (sAPPα and β). We previously found that hypoxia dramatically decreased APP levels in and secretion from retinal pigmented epithelial (RPE) cells. In the current study we examined the mechanisms by which hypoxia affects APP levels and secretion by inhibiting the degradation pathways within the RPE, inducing endoplasmic reticulum (ER) stress, and by studying the nascent synthesis of APP. Additionally, since APP is expressed on the apical surface of RPE cells and may function in cell adhesion or as a receptor, we examined the ability of APP to aid in the phagocytosis of photoreceptors to further understand the functionality of APP.

Methods

RPE were isolated from canine eyes. Cells were placed under hypoxic (0.5% O_2) or normoxic (21% O_2) conditions for 16 or 48 hours. For degradation studies, cells were treated with either the lysosomal inhibitor chloroquine or the proteasomal inhibitor MG-132. For ER stress studies, cells were treated with either the ER stress inducer tunicamycin or the ER stress inhibitor 4-PBA. Lysates were collected and immunoblotted for APP. For photoreceptor phagocytosis studies, APP was knocked down with siRNA and RPE cells were then fed FITC labeled photoreceptor outer segments. Outer segment binding and internalization was quantified.

Results

Lysosomal inhibition did not rescue APP levels in hypoxic conditions. Surprisingly, proteasomal inhibition vastly lowed APP levels in RPE lysates. Inducing ER stress with

tunicamycin caused a decrease in APP in RPE lysates. However, the ER stress inhibitor 4-PBA did not reverse the hypoxia induced decrease in APP levels. Hypoxia reduced APP's nascent synthesis by 32% in RPE cells. Significantly, siRNA knockdown of APP caused a decrease in the binding and internalization of photoreceptor outer segments.

Conclusions

As hypoxia is a common pathology of the retina, understanding how it affects the processing and secretion of proteins is vital to understanding the pathophysiology of the RPE. Hypoxia's effects on APP are not likely due to increased degradation or ER stress. This is the first study demonstrating that hypoxia affects the nascent synthesis of APP in RPE cells and that APP has a role in photoreceptor phagocytosis.

Introduction

The retinal pigmented epithelium (RPE) is a monolayer of tight junctional, polarized, and pigmented cells that underlies and support the photoreceptors and comprise part of the outer blood retina barrier [1]. A key function of the RPE is the regulation of the polarized movement of multiple molecules both towards and away from the sub retinal space. If RPE function is compromised, ocular health is severely impaired [2, 3].

Oxidative damage and immunological insult to the RPE monolayer are thought to be early events in AMD; with advanced dry AMD leading to geographic atrophy and photoreceptor cell death. One cause of oxidative stress is from hypoxia, and hypoxia is a causative factor in AMD and alters polarized protein localization and may play a role in AMD [4-6]. Disruption of polarized localization of proteins may play a role in AMD.

The amyloid precursor protein (APP) is ubiquitously expressed and produces amyloid beta (Aβ), which is a component of the plaques present in Alzheimer's disease and is associated

with age-related macular degeneration (AMD) [7]. Recent studies have examined the metabolism of APP and accumulation of its byproducts in the eye as it relates to the pathology of AMD [8].

After synthesis, APP transits from the Golgi, where it undergoes significant glycosylation, to the cell surface. At the cell surface, APP is inserted into the membrane, where it can be secreted, or it may bind to extracellular proteins. From the membrane, APP can also be recycled back to the Golgi or degraded. APP has been shown to be primarily degraded within the lysosome [9]. Under diseased states, this normal degradative process can be accelerated or altered, causing a large increase in the degradation of APP and the production of harmful amyloidogenic fragments [10]. Since hypoxia induces stress in RPE cells, both the lysosomal and proteasomal pathways (the main pathways for protein degradation) were investigated as possibly being altered under hypoxic conditions [11]. During the course of this investigation, it was found that inhibiting the proteasomal degradation pathway caused a vast reduction in APP levels within the RPE. This was an unexpected finding, but it has also been shown that proteasomal inhibition can lead to ER stress, and ultimately initiate the unfolded protein response within cells, causing autophagy [12]. Importantly, this induction of the ER stress/unfolded protein response has been shown to reduce the amount of mature APP within cells [12].

APP may be a cell adhesion molecule or a membrane receptor that can interact with various binding protein partners, activating signaling pathways and eliciting physiological responses. [13, 14]. Photoreceptors lie in close contact with the apical surface of the neighboring RPE cells. The RPE regularly eliminates and recycles spent photoreceptor outer segments (POS) [15]. If this process is interrupted due to disease or other factors, POS build up within the RPE and photoreceptor degeneration occurs, ultimately leading to vision loss [15]. Since our previous

work had shown that APP does not properly localize to the apical surface under hypoxia, we examined whether APP may have a function in the proper phagocytosis of photoreceptors. If APP does function in the photoreceptor phagocytosis pathway, its disruption could contribute to the progression of AMD.

Our previous work showed that hypoxia decreased APP levels in RPE lysates and substantially reduced apical localization and secretion of APP in the basolateral direction towards the choroid. This suggested that there are dynamic changes in polarized movement of APP in the RPE caused by hypoxia. The current study was designed to determine hypoxia alters APP expression and secretion within the RPE. To do so, we examined the primary degradation pathways within the RPE, the possible involvement of stress and the nascent synthesis of APP. Lastly, we examined if the loss of APP on the apical surface of the RPE would affect photoreceptor phagocytosis.

Materials and Methods

Tissue culture

Dogs were obtained from the Johnston County, NC animal shelter immediately after being euthanized. Eyes were removed within 2 hours of death and RPE were isolated by trypsinization and transferred to 60 mm tissue culture dishes where they were grown to confluence in Ham's F-12/DMEM (1:1) medium (cat# 31765-035 and #10566-016, Invitrogen, Rockville, MD) with 10% fetal bovine serum (FBS) (Hyclone, Logan, Utah) and 1% antibiotic/antimycotic solution (Mediatech, Manassas, VA). Cultures were incubated at 37°C, 5% CO_2, 95% humidity until confluence was reached in 7 to 10 days. For subsequent experiments, the cells were dispersed by trypsinization either onto 6 well tissue culture plates for non-polarized cultures, or onto 6-well Greiner hanging cell culture inserts to establish polarized

RPE cultures (polyethylene terephthalate membrane; 1.0 μm pore size; cat # 657610) (Greiner Bio-One North America Inc., Monroe, NC) with the apical and basolateral sides bathed separately. Apical medium was comprised of Ham's F-12/DMEM (1:1) medium with 20% 10X B27 Supplement (cat# 17504-044 Invitrogen, Rockville, MD) and 1% antibiotic/antimycotic solution (Mediatech, Manassas, VA). Basal medium was the same as the 10% FBS culture medium described above. For all experiments, primary RPE were plated at 200,000 cells per well for non-polarized cultures or 300,000 cells per insert for polarized cultures. RPE cells plated onto Greiner inserts were determined to be tight junctional by measuring transepithelial electrical resistance (TEER) once a week after plating. Cultures were used for experiments once they exhibited TEER readings over 300 Ω x cm^2 and directional secretion of glutamate to the basal compartment (at least 5 times more to basal than apical compartments indicating a polarized epithelium). Cultures typically achieved these parameters in 4–8 weeks. For further description of this polarized RPE model see [11]

Hypoxic treatment

For all experiments involving hypoxia, cells were placed under hypoxic (0.5% O_2) conditions for 24 or 48 hours in a hypoxia chamber (Ruskinn INVIVO2 300 workstation), with corresponding cells placed under normoxic conditions (21% O_2) in a standard cell culture incubator as a control. It is known that hypoxic conditions activate both hypoxia inducible factor 1 and VEGF production (both known hypoxia indicators) within the RPE [16]. All studies except the nascent protein synthesis studies were carried out to 48 hours to determine the effects of sustained hypoxic insult to RPE cells. Nascent protein synthesis studies were carried out for 16 hours in hypoxia to account for the short half-life of APP [17-19].

Lysosomal and proteasomal inhibition

RPE cells were grown on Greiner ThinCert™ inserts until polarized, tight junctional monolayers were formed as described above. Prior to treatment cells were washed two times with serum-free, glutamine-free Minimal Essential Medium (MEM) (cat# 51200-038, Invitrogen, Rockville, MD) and then placed in MEM in the presence of the lysosomal inhibitor chloroquine (75µM) (Tocris, Minneapolis, MN; cat. # 4109), the proteasomal inhibitor MG-132 (10µM) (EMD Millipore, Ballerica, MA; cat. # 474790-5mg), or left untreated as a control. Cells were then incubated in normoxic (21% O_2) or hypoxic (0.5% O_2) conditions for 48 hours. Lysates were collected and immunoblotted for APP as described below.

Endoplasmic reticulum stress inhibition and induction

Non-polarized RPE cells were grown to confluence as described above. Prior to treatment cells were washed two times with MEM and then placed in MEM in the presence of the ER stress inhibitor 4-PBA (2.5mM) (EMD Millipore; cat. # 567616-100mg), the ER stress inducer tunicamycin (1µM) (Tocris; cat. # 3516), or left untreated as a control. Cells were then incubated in normoxic (21% O_2) or hypoxic (0.5% O_2) conditions for 48 hours. Lysates were collected and immunoblotted for APP as described below.

Nascent APP synthesis

Non-polarized RPE cells were grown to 90% confluence. Prior to treatment cells were washed two times with MEM. Cells were then starved of methionine for 30 minutes in methionine free media with 5% dialyzed FBS, after which 35µM L-azidohomoalaine (AHA) (Thermo Fisher, Waltham, MA; cat. # C10102) was added. Cells were incubated in normoxic (21% O_2) or hypoxic (0.5% O_2) conditions for 16 hours. Cells were then washed twice in ice-cold PBS (Corning, Tewksbury, MA) and incubated on ice for 10 minutes in 200ul RIPA buffer (Thermo Fisher, Waltham, MA) with protease inhibitors added, with periodic mixing. The

resulting homogenate was centrifuged for 10 min at 13,000 x g at 4°C, after which the lysate supernatant was collected. Protein concentrations were measured by BCA assay. 250µg of cell lysate was combined with the Y188 antibody for APP (Abcam, Cambridge, MA; cat. # ab32136) at a 1:30 dilution of antibody to cell lysate, after which the antibody/lysate solution was diluted to 500µl with RIPA buffer. The solutions were incubated at 4°C overnight with mixing to form the immune complex. The next day, 25µl of protein A/G magnetic beads (Thermo Fisher, Waltham, MA) were placed into low protein binding microcentrifuge tubes, to which 175µl of RIPA buffer was added and the beads were vortexed to mix. The tubes were placed into a magnetic stand to collect the beads and the supernatant was removed. This was repeated twice. The antibody/lysate solutions from the day before were added to the pre-washed beads and incubated at room temperature for one hour with mixing. After one hour, the beads were collected with a magnetic stand and the unbound sample was removed. The beads were then washed five times in 500µl RIPA buffer. The washed beads were then used in the Click-IT™ biotin protein analysis detection kit (Thermo Fisher, Waltham, MA; cat. # C33372) to label the azide modified proteins with the alkyne-biotin complex according to the manufactures instructions (steps 1.1 through 2.7 only). After labeling, the beads were collected on a magnetic stand and the excess labeling solution was removed. The beads were then washed twice in 500µl RIPA buffer. 50µl of 2x SDS-PAGE loading buffer (1M Tris/HCl pH 6.5, 10% glycerol, 200mM SDS, 150µM bromophenol blue, 70mM DTT) was added to the beads, after which they were heated at 75°C for 15 minutes to elute and denature the labeled APP from the beads. The eluate was placed on a magnetic stand to capture the beads after which equal volume (25 µl) of eluate was subjected to 8% SDS-PAGE and the proteins were transferred to a nitrocellulose membrane. APP immunoblotting was carried out as described below using the KPI antibody for

APP. For detection of the biotin tag, membranes were blocked with 1X Carbo-Free blocking solution (Vector Labs, Burlingame, CA; cat. # SP-5040). The transferred proteins were probed with horseradish peroxidase (HRP) conjugated streptavidin (2µg/ml; Pierce, Rockford, IL; cat. # 21126), washed three times with tris-buffered saline with tween (TBST) (50mM Tris, 150mM NaCl, 1% tween 20, pH 7.4) and once with tris-buffered saline (TBS) (50mM Tris, 150mM NaCl, pH 7.4). Proteins were visualized using an enhanced chemiluminescence detection system (GE Healthcare Life Sciences, Pittsburgh, PA) according to manufacturer's protocol and the blot was imaged using a ChemiDoc^{TM} MP System (BioRad, Hercules, CA) and normalized using the total protein detection method described below.

Immunoblotting for identification of APP

After treatment, cells were lysed using sodium dodecyl sulfate (SDS) lysis buffer with protease inhibitors added. The resulting homogenate was centrifuged for 15 min at 14,000 x g at 11°C, after which the lysate supernatant was collected. Protein concentrations were measured by the BCA assay. Canine cerebral cortex tissue lysate (Zyagen, San Diego, CA) was used as a positive control for APP. 100 µg total protein from canine cerebral cortex and 20 µg total protein from primary cultured canine RPE were subjected to 8% SDS-PAGE and the proteins were transferred to a nitrocellulose membrane. The membrane was then blocked in a 10% milk solution in tris-buffered saline (TBST) (50mM Tris, 150mM NaCl, 1% tween 20, pH 7.4). The transferred proteins were probed with the primary antibody to APP KPI domain (2 µg/ml; EMD Millipore; cat. # AB5302). After washing with TBST, the membrane was incubated with horseradish-peroxidase (HRP) conjugated anti-rabbit IgG antibody (4 µg/ml; eBioscience, Inc., San Diego, CA; cat. # 18-8816-33). Proteins were visualized using an enhanced chemiluminescence detection system (GE Healthcare Life Sciences, Pittsburgh, PA) according to

manufacturer's protocol and the blot was imaged using a ChemiDoc™ MP System (BioRad, Hercules, CA). Immunoblots were normalized using the total protein normalization method, which removes the need to use housekeeping proteins for loading controls. Total protein normalization allows for greater quantitative accuracy in measuring target proteins [20-22]. Additionally, total protein normalization has recently become the preferred method for the Journal of Biological Chemistry for immunoblot normalization.

Photoreceptor binding and internalization assay

To test if APP may be involved in photoreceptor phagocytosis, APP was knocked down in RPE cells using APP siRNA, after which RPE cells were fed fluorescently labeled photoreceptor outer segments for 30 minutes, 1 hour, 2 hours, 3 hours, 4 hours, and 5 hours.

Photoreceptor rod outer segments (POS) were purchased from InVision BioResources (Seattle, WA). POS were labeled with fluorescein-5-isothiocyanate (FITC) (Thermo Fisher, Waltham, MA) as described by Parinot, et al. [23]. siRNA for APP (ON-TARGETplus Human APP (351) siRNA-SMARTpool #L-003731-00-0005) was obtained from GE Dharmacon (Lafayette, CO) as well as a control nontargeting siRNA pool (ON-TARGETplus Non-targeting Pool #D-001810-10-05, Dharmacon). Cells were plated at a density of 7,500 cells/well on 96-well black walled plates in 0.2 ml/well of DMEM/F12+10% FBS without antibiotics and incubated overnight at 37°C, typically reaching 50% to 60% confluence. Media was replaced with 100 µl of DMEM/F12+10% FBS without antibiotics. Lipophilic transfection reagent (0.9 µL/mL, Lipofectamine® RNAiMAX; Invitrogen, Grand Island, NY) siRNA complexes were formed, according to the manufacturer's protocol, in serum-free, glutamine-free MEM without antibiotics and added to each well at a final concentration of 45 nM siRNA/well. APP siRNA was added to one set of cells and the control nontargeting siRNA pool was added to cells in a

parallel well on each plate as a control for non–sequence-specific cell responses, with each well having a final media volume of 0.2 ml. In addition, a third set of cells had 100 µl of serum-free, glutamine-free MEM without antibiotics added to ensure that the siRNA and transfection reagent were not adversely affecting the RPE cells. After overnight incubation, transfection medium was replaced with 0.2 ml/well of DMEM/F12+10% FBS with antibiotics. After 72h medium was switched to 180 µl/well serum-free, phenol red DMD and the photoreceptor phagocytosis assay was carried out as described in sections 3.2 through 3.4 of the protocol by Mao, et al., with 40 FITC labeled POS applied per plated RPE cell (20 µl total) [24]. Plates were read on a fluorescent plate reader (Fluoroskan Ascent FL; Thermo Fisher, Waltham, MA) to determine the total, bound, and internalized photoreceptor amounts after APP knockdown.

Statistics

The data were analyzed by ANOVA with Tukey's HSD test for multiple comparisons and SEM for all experiments except the nascent protein synthesis studies and photoreceptor phagocytosis studies. Nascent protein synthesis and photoreceptor phagocytosis data were analyzed by paired t-test and SEM. All data were analyzed in SYSTAT 13 (San Jose, California). Results were considered significant when $p < 0.05$.

Results

Effects of lysosomal and proteasomal inhibition on APP levels in RPE cells

In order to determine if hypoxia altered the degradation pathway of APP, polarized RPE were treated with either the lysosomal inhibitor chloroquine, the proteasomal inhibitor MG-132, or left untreated as a control. We determined the concentration of inhibitors to use by reviewing the literature for the lowest effective concentration used within RPE cells to block degradation. Cells were then incubated in normoxic (21% O_2) or hypoxic (0.5% O_2) conditions for 48 hours

and lysates were analyzed by immunoblot for APP. APP was found in both an immature, non-glycosylated form (lower band) and the mature, highly glycosylated form (upper band) in RPE lysates. APP expression was significantly reduced ($p<0.05$) in the control lysates after 48 hours in hypoxia (Figure 3.1). Lysosomal inhibition caused the levels of APP in the lysates to increase in normoxic conditions. The decrease in APP levels induced by hypoxia was not rescued by lysosomal inhibition. Surprisingly, proteasomal inhibition caused a substantial reduction (80%) in APP levels in both normoxic and hypoxic conditions (Figure 3.1).

Effects of endoplasmic reticulum stress induction and inhibition on APP levels in RPE cells

ER stress is known to initiate the unfolded protein response within cells, ultimately leading to autophagy [12]. This induction of the ER stress/unfolded protein response has been shown to reduce the amount of mature APP within cells [12]. Importantly, hypoxia induces the ER stress pathway [25, 26]. Because lysosomal and proteasomal inhibition did not rescue APP in hypoxic conditions, we next investigated if ER stress was causing APP expression to decrease in hypoxia. RPE were treated with either the ER stress inhibitor 4-PBA, the ER stress inducer tunicamycin, or left untreated as a control. Effective concentrations of 4-PBA and tunicamycin were determined by reviewing the literature for their use within RPE cells. Cells were then incubated in normoxic (21% O_2) or hypoxic (0.5% O_2) conditions for 48 hours. APP levels were significantly reduced ($p<0.05$) in the lysates after 48 hours in hypoxia. Inhibition of ER stress with 4-PBA had no effect on APP expression in normoxic or hypoxic conditions (Figure 3.2). Inducing ER stress caused a significant reduction in APP expression in normoxic and hypoxic conditions when compared to the normoxic control (Figure 3.2).

Effect of hypoxia on the nascent synthesis of APP in RPE cells

Since inhibition of the lysosomal, proteasomal, and ER stress pathway were not found to rescue APP expression in hypoxia, we next investigated if hypoxia altered the nascent synthesis of APP. Hypoxia caused a significant 32% reduction ($p<0.05$) in the nascent synthesis of APP after 16 hours, as measured by AHA incorporation, when compared to normoxic APP nascent synthesis (Figure 3.3).

Effect of APP knockdown on photoreceptor phagocytosis

Transmembrane APP may have a role in cellular adhesion and may have a function as a cellular receptor. We have previously shown that hypoxia substantially reduces the amount of APP on the apical surface of the RPE. RPE are crucial to the processing of photoreceptors because of their ability to bind and phagocytose photoreceptor outer segments. We tested whether APP may play a role in photoreceptor phagocytosis by the RPE. APP was knocked down with siRNA in RPE cells for 72 hours, and cells were then fed FITC labeled photoreceptor outer segments for 30 minutes, 1 hour, 2 hours, 3 hours, 4 hours or 5 hours. These time points were chosen based off of previous work by Finnemann, et al. which states that this time frame simulates all phases of photoreceptor activity from active POS binding (early phase of uptake), ongoing binding and internalization, and active internalization of bound photoreceptors (late phase of uptake) [24]. Additionally, Finnemann has shown that primary RPE, which are the only types of RPE used in this current study, phagocytose RPE faster than cells lines (30 minutes to 2 hours for primary RPE, versus 2 to 5 hours for RPE cell lines) [15]. However, since APP has never been studied in the context of photoreceptor phagocytosis, the current study used time points past those suggested by Finnemann for primary cells to ensure no other observable effects were occurring after the 2 hour time point. Fluorescent readings for each time point indicated that APP knockdown did lower the total amount of photoreceptors detected, as well as the

amount bound and internalized by the RPE cells (Figure 3.4). This was significantly pronounced at the 1 hour time point, though photoreceptor levels were still down for all conditions after 1 hour.

Discussion

The amyloid precursor protein is ubiquitous, and has important roles in the pathology of age related macular degeneration (AMD) as well as Alzheimer's disease. APP is known to have functions involving cell growth and cell maintenance and may have roles as a cellular receptor. Hypoxia is a key pathological factor in disease states leading to cellular degradation, death, and loss of retinal function. In Chapter 2, we showed that hypoxia decreases intracellular and apical levels of APP in the RPE. In the current study, we examined the mechanism by which hypoxia decreases APP levels by examining lysosomal degradation, endoplasmic reticulum stress, and the nascent synthesis of APP. We also examined how such a loss of APP may alter the ability of the RPE to properly phagocytose photoreceptors.

APP is known to be primarily degraded within the lysosome [17]. For RPE cells placed in hypoxic conditions, APP was significantly decreased when compared to the normoxic control (Figure 3.1). Inhibiting lysosomal degradation with chloroquine did not rescue APP levels in hypoxia, though it did raise APP levels in normoxia as expected. We next investigated whether hypoxia was causing APP to be degraded by the proteasomal pathway instead of the primary lysosomal pathway. Inhibiting the proteasome with MG-132 significantly lowered APP levels in both normoxic and hypoxic conditions when compared to the normoxic control. This was an unexpected result since the proteasomal degradation pathway is not the main pathway of APP degradation.

Due to the unexpected finding that proteasomal inhibition lowered APP levels intracellularly, we investigated the mechanism by which this may be occurring. It has been shown that proteasome inhibitors can activate the endoplasmic reticulum (ER) stress pathway, ultimately leading to autophagy and a reduction of APP levels [12]. Therefore, ER stress was investigated as a potential method by which proteasomal inhibition and hypoxia were lowering APP levels. While chemically inducing ER stress with tunicamycin did lower APP levels in the RPE similarly to those seen in hypoxia, the ER stress inhibitor 4-PBA did not rescue APP levels (Figure 3.2). Because of the inability of 4-PBA to rescue APP in hypoxia, it is unlikely that ER stress lowers APP levels in hypoxia.

Hypoxia has been shown to decrease the nascent synthesis of proteins [27-29]. The retina is part of the brain, and it has been shown in the brain that hypoxia affects the synthesis of proteins by causing a 32% to 34% decrease in overall protein synthesis [29]. Therefore, the effect of hypoxia on nascent synthesis was next investigated as a cause of the decrease in APP levels. We found that the nascent synthesis of APP is decreased by 32% in hypoxia after 16 hours in hypoxia (Figure 3.3). This short hypoxic incubation was chosen because APP is known to have a short half-life [17-19]. We believe that hypoxia's ability to decrease the synthesis of APP is a likely pathway by which hypoxia decreases the levels of APP in the RPE and, as we previously reported in Chapter 2, the amounts that are localized to the apical surface.

The apical membrane of the RPE abuts the photoreceptors, where photoreceptor outer segments (POS) are engulfed and recycled. Two ligand-receptor pairs, MFG-E8-αvβ5 integrin and Gas6/Protein S-MerTK, are located on the apical membrane of the RPE and are essential for POS phagocytosis [15]. MFG-E8 and Gas6/Protein S both recognize the POS, with MFG-E8-αvβ5 integrin acting upstream of Gas6/Protein S-MerTK. Activation of MerTK initiates a

negative feedback mechanism to limit αvβ5 activity. As Chapter 2 showed, under hypoxic conditions APP localization to the apical membrane is drastically reduced. Therefore, because the apical surface shows a decrease in APP localization under hypoxia and it is the site of photoreceptor phagocytosis, we wanted to examine if APP may play a role in photoreceptor phagocytosis. Instead of exposing the RPE cells to hypoxia, which would cause additional effects beyond affecting just APP apical localization, we utilized siRNA to knockdown APP within RPE cells. When APP is knocked down, we have now shown that photoreceptor phagocytosis is inhibited within the RPE (Figure 3.4). As improper photoreceptor phagocytosis is one hallmark of AMD, the finding that APP plays a role in photoreceptor binding and internalization could be crucial to determining if APP's restoration may be a therapeutic target to restore proper photoreceptor function in AMD.

This study furthers our understanding of hypoxia's regulation of the amyloid precursor protein. Understanding how hypoxia affects protein synthesis is vital to a comprehensive understanding of RPE pathophysiology and in all cells that are exposed to hypoxic conditions. Additionally, this study shows for the first time that APP may have a role in photoreceptor phagocytosis. This novel functional role for APP helps to further elucidate its role beyond the amyloidogenic properties that its byproduct Aβ is often associated with and may help lead to potential therapeutic targets to combat AMD.

REFERENCES

1. Campbell M, Humphries P. The blood-retina barrier: tight junctions and barrier modulation. Adv Exp Med Biol 2012; 763:70-84.

2. Kaur C, Foulds WS, Ling EA. Blood-retinal barrier in hypoxic ischaemic conditions: basic concepts, clinical features and management. Prog Retin Eye Res 2008; 27(6):622-47.

3. Klaassen I, Van Noorden CJ, Schlingemann RO. Molecular basis of the inner blood-retinal barrier and its breakdown in diabetic macular edema and other pathological conditions. Prog Retin Eye Res 2013; 34:19-48.

4. Blasiak J, Petrovski G, Vereb Z, Facsko A, Kaarniranta K. Oxidative stress, hypoxia, and autophagy in the neovascular processes of age-related macular degeneration. Biomed Res Int 2014; 2014:768026.

5. Blaauwgeers HG, Holtkamp GM, Rutten H, Witmer AN, Koolwijk P, Partanen TA, Alitalo K, Kroon ME, Kijlstra A, van Hinsbergh VW, Schlingemann RO. Polarized vascular endothelial growth factor secretion by human retinal pigment epithelium and localization of vascular endothelial growth factor receptors on the inner choriocapillaris. Evidence for a trophic paracrine relation. Am J Pathol 1999; 155(2):421-8.

6. Kay P, Yang YC, Hiscott P, Gray D, Maminishkis A, Paraoan L. Age-related changes of cystatin C expression and polarized secretion by retinal pigment epithelium: potential age-related macular degeneration links. Invest Ophthalmol Vis Sci 2014; 55(2):926-34.

7. Ohno-Matsui K. Parallel findings in age-related macular degeneration and Alzheimer's disease. Prog Retin Eye Res 2011; 30(4):217-38.

8. Ratnayaka JA, Serpell LC, Lotery AJ. Dementia of the eye: the role of amyloid beta in retinal degeneration. Eye (Lond) 2015.

9. Haass C, Koo EH, Mellon A, Hung AY, Selkoe DJ. Targeting of cell-surface beta-amyloid precursor protein to lysosomes: alternative processing into amyloid-bearing fragments. Nature 1992; 357(6378):500-3.

10. Otero MG, Bessone IF, Hallberg AE, Cromberg LE, De Rossi MC, Saez TM, Levi V, Almenar-Queralt A, Falzone TL. Proteasome stress leads to APP axonal transport defects by promoting its amyloidogenic processing in lysosomes. J Cell Sci 2018.

11. Harned J, Nagar S, McGahan MC. Hypoxia controls iron metabolism and glutamate secretion in retinal pigmented epithelial cells. Biochim Biophys Acta 2014; 1840(10):3138-44.

12. Zhou F, van Laar T, Huang H, Zhang L. APP and APLP1 are degraded through autophagy in response to proteasome inhibition in neuronal cells. Protein Cell 2011; 2(5):377-83.

13. Deyts C, Thinakaran G, Parent AT. APP Receptor? To Be or Not To Be. Trends Pharmacol Sci 2016; 37(5):390-411.

14. Dawkins E, Small DH. Insights into the physiological function of the beta-amyloid precursor protein: beyond Alzheimer's disease. J Neurochem 2014; 129(5):756-69.

15. Mazzoni F, Safa H, Finnemann SC. Understanding photoreceptor outer segment phagocytosis: use and utility of RPE cells in culture. Exp Eye Res 2014; 126:51-60.

16. Goralska M, Ferrell J, Harned J, Lall M, Nagar S, Fleisher LN, McGahan MC. Iron metabolism in the eye: a review. Exp Eye Res 2009; 88(2):204-15.

17. Caporaso GL, Gandy SE, Buxbaum JD, Greengard P. Chloroquine inhibits intracellular degradation but not secretion of Alzheimer beta/A4 amyloid precursor protein. Proc Natl Acad Sci U S A 1992; 89(6):2252-6.

18. Lyckman AW, Confaloni AM, Thinakaran G, Sisodia SS, Moya KL. Post-translational processing and turnover kinetics of presynaptically targeted amyloid precursor superfamily proteins in the central nervous system. J Biol Chem 1998; 273(18):11100-6.

19. Gersbacher MT, Goodger ZV, Trutzel A, Bundschuh D, Nitsch RM, Konietzko U. Turnover of amyloid precursor protein family members determines their nuclear signaling capability. PLoS One 2013; 8(7):e69363.

20. Taylor SC, Berkelman T, Yadav G, Hammond M. A defined methodology for reliable quantification of Western blot data. Mol Biotechnol 2013; 55(3):217-26.

21. Gilda JE, Gomes AV. Stain-Free total protein staining is a superior loading control to beta-actin for Western blots. Anal Biochem 2013; 440(2):186-8.

22. Gurtler A, Kunz N, Gomolka M, Hornhardt S, Friedl AA, McDonald K, Kohn JE, Posch A. Stain-Free technology as a normalization tool in Western blot analysis. Anal Biochem 2013; 433(2):105-11.

23. Parinot C, Rieu Q, Chatagnon J, Finnemann SC, Nandrot EF. Large-scale purification of porcine or bovine photoreceptor outer segments for phagocytosis assays on retinal pigment epithelial cells. J Vis Exp 2014(94).

24. Mao Y, Finnemann SC. Analysis of photoreceptor outer segment phagocytosis by RPE cells in culture. Methods Mol Biol 2013; 935:285-95.

25. Lopez-Hernandez B, Cena V, Posadas I. The endoplasmic reticulum stress and the HIF-1 signalling pathways are involved in the neuronal damage caused by chemical hypoxia. Br J Pharmacol 2015; 172(11):2838-51.

26. Yang D, Gao L, Wang T, Qiao Z, Liang Y, Zhang P. Hypoxia triggers endothelial endoplasmic reticulum stress and apoptosis via induction of VLDL receptor. FEBS Lett 2014; 588(23):4448-56.

27. Connolly E, Braunstein S, Formenti S, Schneider RJ. Hypoxia inhibits protein synthesis through a 4E-BP1 and elongation factor 2 kinase pathway controlled by mTOR and uncoupled in breast cancer cells. Mol Cell Biol 2006; 26(10):3955-65.

28. Tinton S, Calderon PB. Role of protein phosphorylation in the inhibition of protein synthesis caused by hypoxia in rat hepatocytes. Int J Toxicol 2001; 20(1):21-7.

29. Preedy VR, Smith DM, Sugden PH. The effects of 6 hours of hypoxia on protein synthesis in rat tissues in vivo and in vitro. Biochem J 1985; 228(1):179-85.

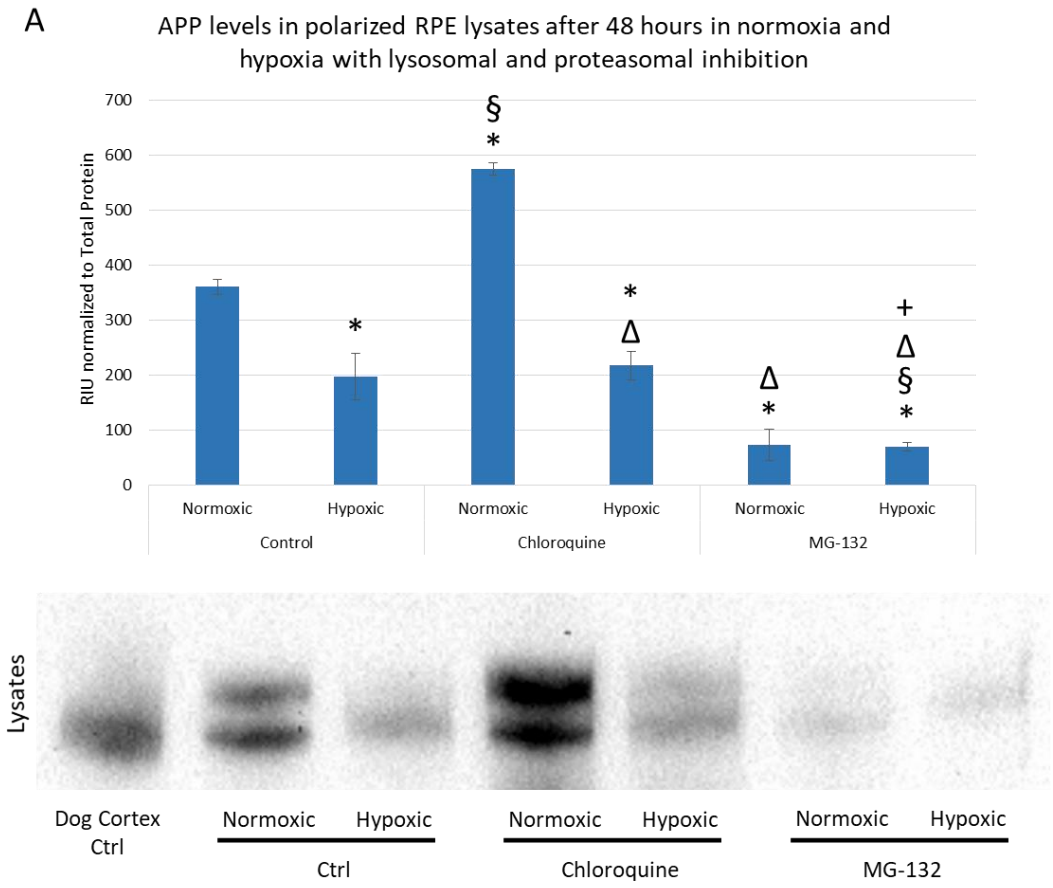

Figure 3.1 APP levels decrease with proteasomal inhibition RPE cells were grown on Greiner ThinCert™ inserts until polarized, tight junctional monolayers were formed. Cells were then incubated in normoxic (21% O_2) or hypoxic (0.5% O_2) conditions for 48 hours in the presence of the lysosomal inhibitor chloroquine (75µM) or the proteasomal inhibitor MG-132 (10µM). Lysates (20 µg total protein) were probed with the KPI antibody for APP. A: APP levels in polarized RPE cells after lysosomal and proteasomal inhibition in normoxic or hypoxic conditions, with representative immunoblot below the graph. Three experiments analyzed statistically in Systat 13 by ANOVA, with post-hoc Tukey's HSD and SEM.* = significantly different from normoxic control. § = significantly different from hypoxic control. Δ = significantly different from normoxic chloroquine. + = significantly different from hypoxic chloroquine.

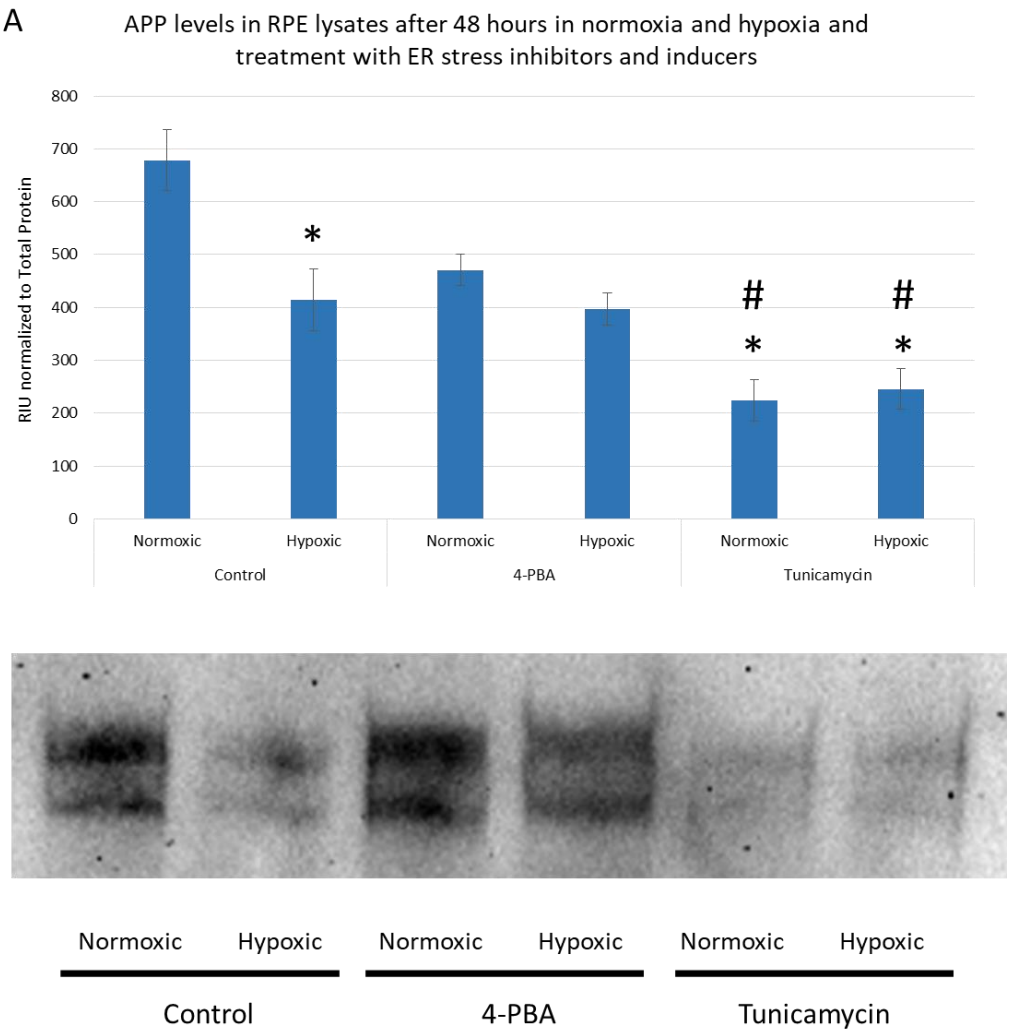

Figure 3.2 ER stress decreases APP levels Non-polarized RPE cells were grown to confluence. Cells were treated with either the ER stress inhibitor 4-PBA (2.5mM) , the ER stress inducer tunicamycin (1µM), or left untreated as a control. Cells were then incubated in normoxic (21% O_2) or hypoxic (0.5% O_2) conditions for 48 hours. Lysates were collected. Lysates (20 µg total protein) were probed with the KPI antibody for APP. A: APP levels in RPE lysates after ER stress inhibition or induction in normoxic and hypoxic conditions, with representative immunoblot below the graph. Three experiments analyzed statistically in Systat 13 by ANOVA, with post-hoc Tukey's HSD and SEM. * = significantly different than normoxic control # = significantly different than normoxic 4-PBA.

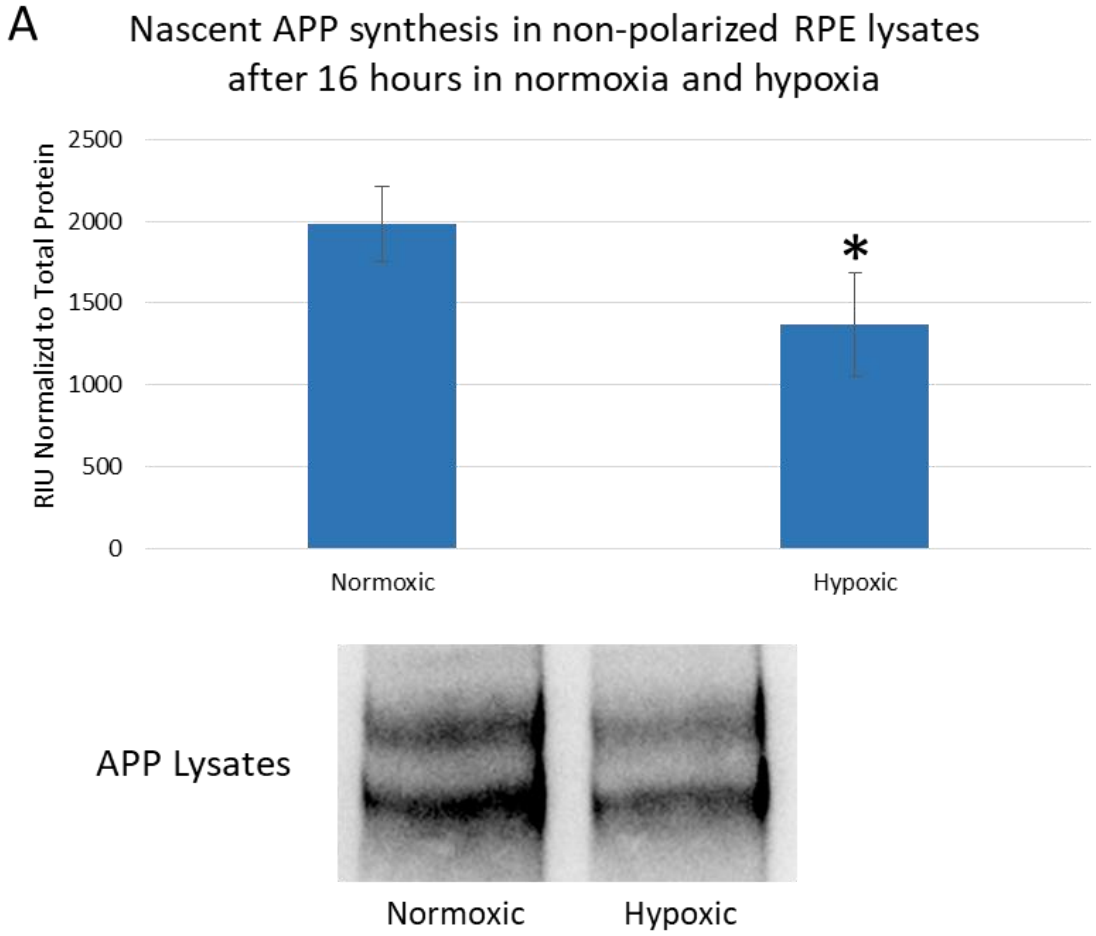

Figure 3.3 Hypoxia decreases nascent APP synthesis Non-polarized RPE cells were grown to 90% confluence. Cells were then starved of methionine for 30 minutes in methionine free media with 5% FBS, after which L-azidohomoalaine (AHA) was added. Cells were then incubated in normoxic (21% O_2) or hypoxic (0.5% O_2) conditions for 16 hours. Lysates were then collected and immunoprecipitated for APP. After immunoprecipitation, cells underwent chemoselective ligation with the alkene labeled biotin and were then eluted into loading buffer. Equal volume (25 µl) of eluate was probed with the KPI antibody for APP for the immunoblot and streptavidin-HRP for the biotin blot. A: Nascent APP synthesis, with representative biotin blot below the graph. Three experiments analyzed statistically in Systat 13 by paired t-test and SEM. * = significantly different from normoxic control.

Figure 3.4 Photoreceptor binding and internalization decrease with APP knockdown RPE cells were treated with APP siRNA overnight, grown to confluence for 72 hours, and then fed FITC labeled photoreceptor outer segments for 30 minutes, 1 hour, 2 hours, 3 hours, 4 hours, or 5 hours. At each time point, the individual 96 well plate was processed for total, surface bound and engulfed photoreceptor outer segments, after which the plate was analyzed on a fluorescent plate reader. A: Percent change in photoreceptor levels after APP knockdown when compared to negative control siRNA * = Significantly different ($p < 0.05$) from paired negative siRNA control as determined from percent control data previously normalized to background fluorescence from 6 experiments and analyzed statistically in Systat 13 by paired t-test, with SEM.

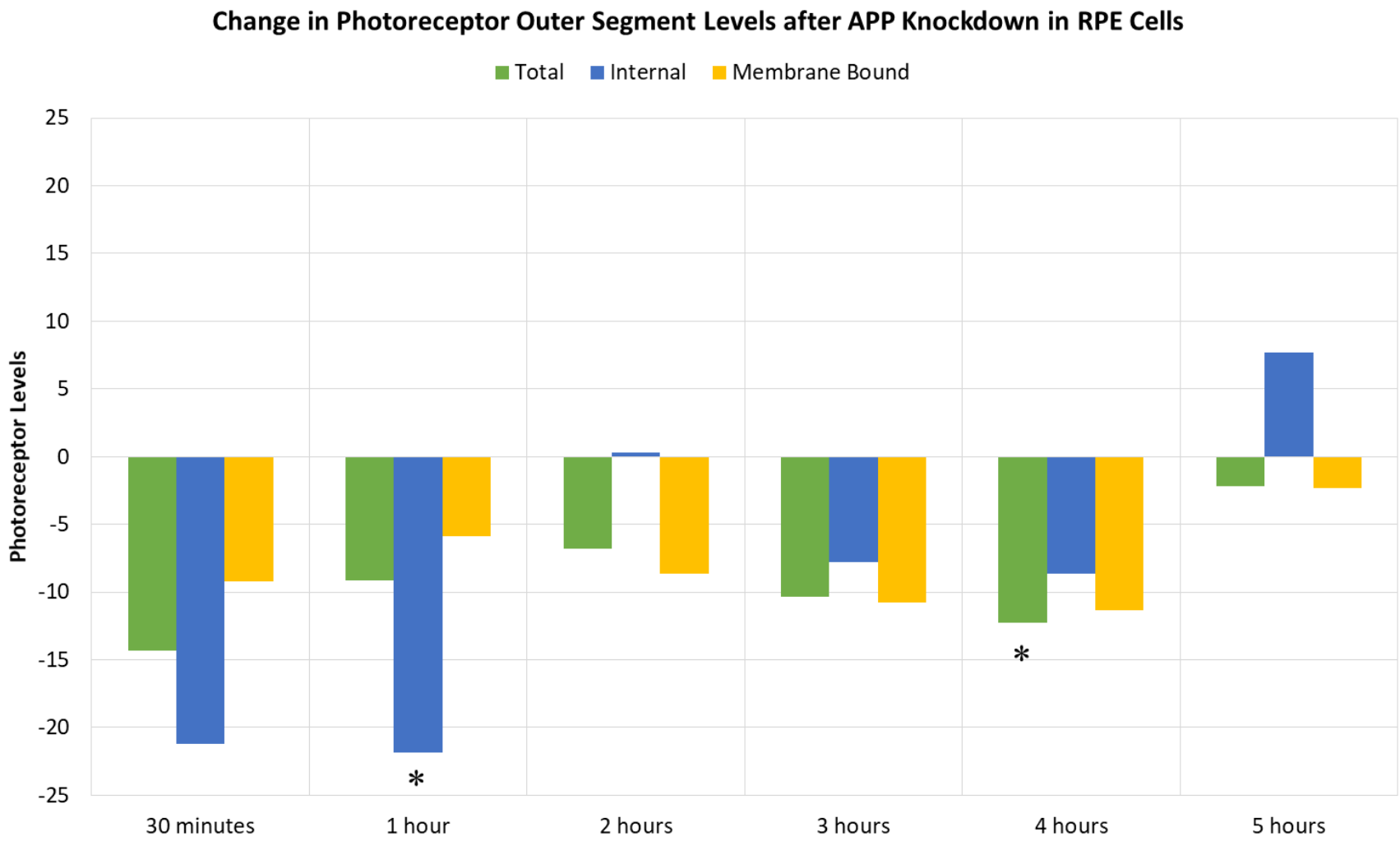
Change in Photoreceptor Outer Segment Levels after APP Knockdown in RPE Cells
Total
Internal
Membrane Bound
Photoreceptor Levels
25
20
15
10
5
0
-5
-10
-15
-20
-25
*
*
30 minutes
1 hour
2 hours
3 hours
4 hours
5 hours

CHAPTER 4

Glycosylation and Levels of the Amyloid Precursor Protein in Retinal Pigmented Epithelial Cells are Altered by Loss of Iron

Abstract

Amyloid precursor protein (APP) gives rise to amyloid beta which is implicated as pathogenic in both Alzheimer's disease and age-related macular degeneration (AMD). Our studies demonstrate that retinal pigmented epithelial cells (RPE) contain an immature as well as a mature, glycosylated form of APP, while they secrete only the mature form. In the RPE, both forms of APP are lowered intracellularly as a consequence of oxidative stress due to hypoxia. The secreted form of APP is also less due to hypoxia. The mature form of APP is formed by glycosylation, with serial addition of mannose, n-acetylglucosamine (GlcNAc) and sialic acid residues. Since APP can alter iron levels and can interact, stabilize, and be co-immunoprecipitated with the iron export protein ferroportin at the cell surface, we investigated the effect of iron chelation on APP levels in and secretion by RPE, as well as continuing our investigations into hypoxia's effect on APP levels. APP levels were determined by immunoblot analysis. Hypoxia reduced the levels of APP, both intracellular and secreted. Iron chelation reduced the size of the mature intracellular form of APP, while having no effect on the size of the immature form. Iron chelation also blocked secretion of the mature form of APP and resulted in secretion of APP of a size similar to the immature form. We determined by combinatorial enzymatic digestion that mature APP treated with sialidase was reduced in size and matched the size of the new smaller APP found after iron chelation. Additionally, the total levels of APP after iron chelation are also reduced, and this is also the case after sialidase treatment. Probing for sialic acid levels on APP showed that the reduction in size of the mature band of APP after iron chelation was due to the absence of sialic acid. This indicates an iron dependent mechanism for the addition or removal of sialic acid. Probing for sialic acid in hypoxia showed that hypoxia did not alter the amount of sialic acid on APP. The involvement of

iron in protein glycosylation is a novel and significant finding with important ramifications for this essential cellular process.

Introduction

The retinal pigmented epithelium (RPE) lies between the neural retina and the choroidal vasculature and makes up the outer part of the blood retinal barrier. Tight junctions between RPE cells provide a barrier to movement of molecules and ions and separate the RPE apical and basolateral surfaces, allowing for appropriate directional movement of nutrients and wastes into and out of the retina. Photoreceptor cells of the retina lie directly above and interdigitate with the microvilli on the apical surface of the RPE. The RPE participates in the visual cycle and is responsible not only for the nutrition of these cells but for phagocytosis and resultant turnover of photoreceptor outer segments [1]. The interplay of RPE and photoreceptor cells creates a rich environment for oxidative damage as it has high lipid, oxygen and iron content [2].

The amyloid precursor protein (APP) and iron metabolism are tightly intertwined as APP regulates iron efflux, iron regulates APP synthesis, and excess iron increases Aβ in the retina under experimental conditions [3-5]. In the presence of iron, one of the byproducts of APP cleavage, sAPPα, stabilizes ferroportin, the only known mammalian iron exporter [3, 4, 6]. This may regulate iron levels within the RPE and prevent the harmful effects of iron overload. APP mRNA also has an iron-regulatory element (IRE) [7]. IREs are RNA stem loops that control the translation of iron regulatory proteins, including APP, and thus balances cellular iron storage and transport. Increased iron within the eye has been associated with patients who have age-related macular denervation [8]. Excess iron also causes photoreceptor degeneration, further showing why iron levels must be tightly regulated [9]. Even though elaborate control mechanisms for

both iron and APP have been defined, there have been no studies done to better understand how iron depletion affects APP levels in and APP's secretion from cells.

Protein glycosylation is essential for proper protein folding and movement to the cell membrane for insertion or secretion. It is also essential for the polarized placement of many proteins in epithelial cells [10]. APP is present in both an immature and a glycosylated mature form and the glycosylation pathway for APP is well documented [11]. Like all proteins, APP glycosylation begins as a cotranslational process in the endoplasmic reticulum (ER), before transiting to the Golgi for final post translational modifications. Addition of sialic acid is an important final modification of APP. Post-translationally modified proteins are recognized and moved to their proper intracellular, plasma membrane, or secretory vesicle locations.

Once properly glycosylated, APP is moved to the membrane and cleaved by either α- or β-secretase to release soluble APP (sAPPα or β, respectively). γ-secretase then acts on the remaining protein to release Aβ from sAPPβ. The processing pathway taken by APP through the maturation process determines which route it takes. The importance of glycosylation for APP's functional localization is illustrated by the finding that the membrane protein TMEM59 causes a decrease in APP glycosylation, or maturation of APP [12]. This results in sequestration of APP in the Golgi and its inability to move to the membrane for processing to soluble sAPPβ and Aβ. On the other hand, increased sialylation of APP in Neuro-2a cells caused a 2-3 fold increase in the secretion of Aβ and sAPPβ [13]. sAPPs have several important cellular activities including maintaining inner retinal circuitry and rod and cone pathways and have been implicated in iron metabolism [4, 14].

Oxidative stress in the form of hypoxia has dramatic effects on iron levels in the RPE. We have previously shown that hypoxia induces a large increase in basolateral iron efflux from

RPE, i.e. away from the retina [15]. As hypoxia is known to cause iron catalyzed oxidative damage, this efflux is likely a protective response to this pathological condition. Since iron regulates APP levels as described earlier, the level of iron and its availability in cells may profoundly alter the fate of APP and its cleavage products. Therefore, changes in the iron state of the cell due to hypoxia may also alter the state of APP within the cell.

Previous studies showed that iron chelation altered the glycosylation of proteins in APRE-19 cells [16]. The purpose of this study was to determine if iron depletion plays a role in the processing, glycosylation or secretion of APP from RPE cells. The iron chelator Dp44mT was used in this study for that purpose. Dp44mT is highly membrane permeable, and once internalized by a cell, chelates iron with high affinity and prevents the uptake of iron from transferrin [17, 18]. Indeed, by utilizing Dp44mT, we found that iron plays a significant role in the post translational modification of APP.

Materials and Methods

Tissue culture

RPE were isolated and grown as previously described in Chapter 2.

Hypoxic treatment

For all experiments involving hypoxia, cells were placed under hypoxic (0.5% O_2) or normoxic conditions (21% O_2) conditions for 24 or 48 hours as previously described in Chapter 2.

Iron chelation of RPE cells

Non-polarized RPE cells were grown to confluence on 60mm tissue culture plates. Cells were rinsed three times with serum free, glutamine free minimum essential media, after which 30µl DMSO (vehicle) was added to control plates and 30µM Di-2-pyridylketone-4,4,-dimethyl-

3-thiosemicarbazone (Dp44MT) was added to plates that were to undergo iron chelation. Plates were incubated for 24 or 48 hours in normoxic or hypoxic conditions. After 24 or 48 hours, cell conditioned media was collected. Cells were then rinsed twice with PBS and then lysed with RIPA buffer with protease inhibitors added for 5 minutes on ice. Cells were collected and vortexed for 20 seconds, after which they were spun at 14,000 x g for 15 minutes at 4°C. The resulting supernatant was stored, with aliquots reserved for protein quantification.

Sialic acid detection

Non-polarized RPE cells were grown to confluence. Prior to treatment cells were washed two times with MEM and then placed in MEM. For all experiments examining sialic acid levels, the sialic acid label was added 6 hours before further treatments to allow sialic acid to be labeled without being affected by further experimental conditions. 35μM of the azide-modified mannosamine (tetraacetylated N-Azidoacetyl-D-Mannosamine, ManNAz) (Thermo Fisher, Waltham, MA; cat. # C33366) was added to label sialic acid. To examine the effects of iron chelation on sialic acid levels, 30μM of the iron chelator Dp44MT was also added, with control cells only receiving 35μM of the ManNAz. The azido-sugar (sialic acid label) is metabolically incorporated into sialic acid-containing glycoproteins through the permissive nature of the oligosaccharide biosynthesis pathway. Cells were then incubated in normoxic (21% O_2) for 24 hours. To examine the effects of hypoxia on sialic acid levels confluent RPE cells were washed twice with MEM and then placed in MEM, after which 35M of ManNAz was added. Cells were then incubated in normoxic (21% O_2) or hypoxic (0.5% O_2) conditions for 48 hours. For both the iron chelation and hypoxia experiments, cells were washed twice in ice-cold PBS (Corning, Tewksbury, MA) and incubated on ice for 10 minutes in 200ul RIPA buffer (Thermo Fisher, Waltham, MA) with protease inhibitors added, with periodic mixing. The resulting homogenate

was centrifuged for 10 min at 13,000 x g at 4°C, after which the lysate supernatant was collected. Protein concentrations were then measured by the BCA assay. 250µg of cell lysate was combined with the Y188 antibody for APP (Abcam, Cambridge, MA; cat. # ab32136) at a 1:30 dilution of antibody to cell lysate, after which the antibody/lysate solution was diluted to 500µl with RIPA buffer. The solutions were incubated at 4°C overnight with mixing to form the immune complex. The next day, 25µl of protein A/G magnetic beads (Thermo Fisher, Waltham, MA) were placed into low protein binding microcentrifuge tubes, to which 175µl of RIPA buffer was added and the beads were vortexed to mix. The tubes were placed into a magnetic stand to collect the beads and the supernatant was removed. This was repeated twice. The antibody/lysate solutions from the day before were added to the pre-washed beads and incubated at room temperature for one hour with mixing. After one hour, the beads were collected with a magnetic stand and the unbound sample was removed. The beads were then washed five times in 500µl RIPA buffer. The washed beads were then used in the Click-IT™ biotin protein analysis detection kit (Thermo Fisher, Waltham, MA; cat. # C33372) to label the azide modified proteins with the alkyne-biotin complex according to the manufactures instructions (steps 1.1 through 2.7 only). After labeling, the beads were collected on a magnetic stand and the excess labeling solution was removed. The beads were then washed twice in 500µl RIPA buffer. 50µl of 2x SDS-PAGE loading buffer (1M Tris/HCl pH 6.5, 10% glycerol, 200mM SDS, 150µM bromophenol blue, 70mM DTT) was added to the beads, after which they were heated at 75°C for 15 minutes to elute and denature the labeled APP from the beads. The eluate was placed on a magnetic stand to capture the beads after which equal volume (25 µl) of eluate was subjected to 8% SDS-PAGE and the proteins were transferred to a nitrocellulose membrane. APP immunoblotting was carried out as described below using the KPI antibody for APP. For

detection of the biotin tag, membranes were blocked with 1X Carbo-Free blocking solution (Vector Labs, Burlingame, CA; cat. # SP-5040). The transferred proteins were probed with horseradish peroxidase (HRP) conjugated streptavidin (2µg/ml; Pierce, Rockford, IL; cat. # 21126), washed three times with tris-buffered saline with tween (TBST) (50mM Tris, 150mM NaCl, 1% tween 20, pH 7.4) and once with tris-buffered saline (TBS) (50mM Tris, 150mM NaCl, pH 7.4). Proteins were visualized using an enhanced chemiluminescence detection system (GE Healthcare Life Sciences, Pittsburgh, PA) according to manufacturer's protocol and the blot was imaged using a ChemiDoc^{TM} MP System (BioRad, Hercules, CA) and normalized using the total protein detection method.

Enzymatic Protein Deglycosylation

Prior to enzymatic deglycosylation, RPE cells were treated with the iron chelator Dp44MT for 24 hours in normoxic conditions and the CCM and lysates were collected as described above. 33µg of total protein from the RPE lysate was transferred into microcentrifuge tubes and treated with a enzymatic protein deglycosylation kit (Sigma, St. Louis, MO; cat. #EDEGLY) according to the manufactures directions for deglycosylation under denaturing conditions utilizing 5 U PNGase F, 5mU sialidase, and 1.25 mU O-glycosidase, and following the layout shown in Figure 4.2, with the only alteration being that before analysis by immunoblotting, tubes were incubated for 18 hours at 37°C.

Immunoblotting for identification of APP

RPE lysates and cell conditioned media were immunoblotted for APP as previously described in Chapter 2.

Statistics

The data were analyzed by ANOVA with Tukey's HSD test for multiple comparisons and SEM for all experiments except the sialic acid experiments examining iron chelation and hypoxia. This data were analyzed by paired t-test and SEM. All data were analyzed in SYSTAT 13 (San Jose, California). Results were considered significant when $p < 0.05$.

Results

Effects of iron chelation on APP expression and secretion in RPE cells in normoxic or hypoxic conditions

RPE cells were exposed to normoxic (21% O_2) or hypoxic (0.5% O_2) conditions in the presence or absence of the iron chelator Dp44MT for 24 or 48 hours. Immunoblots done on RPE lysates for APP have two bands. The lower band is the immature, non-glycosylated form, and the upper band is the mature, highly glycosylated form. Rat brain was used as a positive control for APP detection. Rat brain is predominantly APP_{695}, so its two bands are slightly lower than the APP_{770} found in the RPE. Interestingly, the secreted form of APP is almost completely the mature form under both normoxic and hypoxic conditions. Treatment with the iron chelator Dp44mT caused a reduction in the size of the mature band of APP at 24 and 48 hours (Figure 4.1 A and B). Additionally, after 24 hours of iron chelation in normoxia, the amount of APP in the lysates was significantly reduced ($p<0.05$, 48%) when compared to normoxia alone (Figure 4.1 C). Hypoxic conditions also caused APP expression and secretion to be lower, but only after 48 hours, similar to the previously reported results in Chapter 2. Hypoxic conditions with iron chelation caused both intracellular and secreted APP to be almost undetectable.

Effects of enzymatic deglycosylation on APP expression in RPE cells

APP is a heavily glycosylated protein, and its glycosylation sites are known. A minority of APP is N-glycosylated, while the majority of APP is O-glycosylated, with sialic acid serving

as the terminal glycan for O-glycosylated APP (Figure 4.2A). To study the effects of iron chelation on sialic acid levels, RPE cells were exposed to normoxic conditions in the presence or absence of Dp44mT for 24 hours, after which lysates were subjected to glycosidase digestion and subsequently immunoblotted for APP. Both the immature and mature forms of APP were visible on the immunoblots for APP. While glycosidase digestion decreased the amount of APP in the lysates, it had no effect on the size of the bands (Figure 4.2B). However, in the presence of sialidase, the mature band decreased in size. When O-glycosidase is added with sialidase, only the immature band remains. PNGase F, which cleaves N-linked glycans, slightly lowered the size of both the mature and immature forms of APP.

Effects of iron chelation and hypoxia on sialic acid levels on APP in RPE cells

Because sialidase caused the size of the mature band of APP to decrease similar to that seen with iron chelation, we next examined whether sialic acid levels were affected by iron chelation, and/or hypoxia. RPE cells were pretreated for six hours with the sialic acid labeling compound, after which cells were placed in normoxic or hypoxic conditions with or without the iron chelator Dp44mT. After 24 or 48 hours, cells were lysed, APP was immunoprecipitated, and immunoblots were probed for APP and sialic acid. After 24 hours of iron chelation in normoxic conditions, sialic acid levels on APP were significantly reduced (57%) (Figure 4.3). There was a concomitant decrease in the size of the mature band of APP. After 48 hours in hypoxia with no iron chelation, sialic acid levels on APP were unaffected (Figure 4.4).

Discussion

Iron is an essential element involved in numerous metabolic processes throughout the cell. The retina and retinal pigmented epithelium (RPE) contain all of the iron regulatory proteins thus far known for other cell types in the body. An important specific role for iron in the RPE is

as an essential component of the RPE65 enzyme, a key player in the rhodopsin cycle [19]. Iron has additional key metabolic functions that have recently being discovered, such as control of glutamate secretion and glutathione levels in cells [20, 21]. However, because iron can also catalyze damaging free radical reactions, its levels are tightly regulated. Despite elaborate control mechanisms, iron dysregulation still occurs from events like sub retinal hemorrhage and contributes to numerous pathologies including retinal degenerations such as age related macular degeneration (AMD) [22, 23].

Within the eye, RPE cells contain and secrete the amyloid precursor protein (APP). APP and its cleavage products have been implicated in the pathology of AMD as well as Alzheimer's disease [24]. The soluble form of APP, sAPPα, is able to stabilize the iron exporter ferroportin [4]. By stabilizing ferroportin, sAPPα helps to regulate iron levels within the RPE by aiding in the export of excess iron from the cell and preventing the harmful effects of iron overload. Additionally, iron regulatory elements on APP mRNA control APP synthesis in response to cellular iron levels, demonstrating the interplay of iron and protein metabolism [5, 7].

Now we have evidence of an additional role for iron in cellular metabolism, namely post translation modification of APP. Our results clearly show that iron chelation with Dp44mT caused a significant decrease in the size of the mature APP band in RPE lysates (Figure 4.1A, B). The total amount of APP within lysates from RPE that had been treated with Dp44mT was reduced by 48% (Figure 4.1C). This reduction in the total amount of APP and the data showing that iron depletion by chelation interferes with the maturation of APP suggests that APP is being processed incorrectly. In order to prove that Dp44mT's effects were due to iron chelation and not some off target effect, iron ($FeCl_3$) was added to Dp44mT treated RPE cells. In

confirmation, the mature band of APP remained at its normal size on immunoblots (data not shown).

Over 50% of proteins are glycosylated, and APP's glycosylated state has been well studied [25]. There is significant posttranslational modification of APP as it transits from the ER through the Golgi to the endosomes. These modifications result in a heavily glycosylated mature APP, with an example of one branch shown in Figure 4.2A. These mature forms are secreted from cells. The O-glycosylated predominant form of mature APP has an outer coat of glycans covered with sialic acid. Addition of sialic acid to the outer most sugars is believed to protect the underlying sugars from removal, thereby maintaining the mature form. APP also undergoes N-glycosylation, where no sialic acid is added. In this study, only upon removal of sialic acid was O-glycosidase effective in removing all sugars from APP, causing only the single immature APP band to be visible on immunoblots (Figure 4.2B). The reduced size of the band resulting from iron chelation is similar to that of APP in the samples treated with sialidase, indicating that iron has a role in the glycosylation of APP. From these enzymatic digestion studies, it is apparent that the presence of sialic acid protects the glycosylated form of APP from enzymatic removal of GlcNAc and mannose residues. Therefore, since iron chelation reduces the amount of sialic acid present on APP, other sugars can also be altered. If glycosylation is necessary for the movement of APP to sites of secretion then altering its glycosylation could result in a decrease in its total secretion or it could cause the secretion of only the immature form of APP.

Iron chelation has been shown to alter the glycosylation of proteins. Specifically, silybin (also known as silibinin) is an iron chelator which regulates both N-linked and O-linked glycosylation in ARPE-19 cells and reduced iron overload in patients with the chronic hereditary β-thalassemia disease [16, 26-28]. In the present study, we investigated to see if the iron chelator

Dp44mT was altering the levels of the sialic acid glycan on APP. To do so, we utilized biorthogonal chemistry to monitor the levels of sialic on APP after iron chelation. We found that sialic acid levels on APP were reduced by 57% when iron was chelated with Dp44mT (Figure 4.3). We have previously shown that hypoxic conditions increased iron efflux from RPE cells [15]. Additionally, hypoxia reduced the amount of total APP in RPE cells as seen in Chapter 2. However, hypoxia did not alter the levels of sialic acid on APP in RPE lysates (Figure 4.4). This could suggest that hypoxia and iron chelators are able to affect different intracellular pools of iron, with hypoxia increasing iron efflux from a pool not susceptible to iron chelation and the chelatable pool of iron available to modify protein glycosylation [29]. It is known that iron regulates at least one enzyme in sialic acid metabolism. CMP-Neu5Ac hydroxylase is an iron dependent enzyme which converts the acetylated form of sialic acid to the hydroxylated form, Neu5Gc. These 2 forms of sialic acid are the most common sialic acids in mammalian cells [30]. This could be the step that the iron chelator Dp44mT is altering. Therefore, iron could play a role in the proper sialyation of APP in RPE cells by limiting sialic acid availability.

Protein glycosylation controls the ability of proteins to be sorted correctly and their ability to be inserted into membranes and properly cleaved. Little is known about the regulatory effects that glycosylation confers to APP as part of the RPE blood retinal barrier and its functional significance to iron homeostasis in the eye. Within this study, we have shown that iron alters the ability of APP to be properly glycosylated. A decrease in APP sialylation caused by iron chelation clearly demonstrates that the fate of APP is altered, with a decrease in its size and secretion. The focus of future investigation will be to determine the mechanism by which iron chelation exerts its effects and how this may alter the production of APP's enzymatic byproducts.

REFERENCES

1. Mazzoni F, Safa H, Finnemann SC. Understanding photoreceptor outer segment phagocytosis: use and utility of RPE cells in culture. Exp Eye Res 2014; 126:51-60.

2. Nowak JZ. Oxidative stress, polyunsaturated fatty acids-derived oxidation products and bisretinoids as potential inducers of CNS diseases: focus on age-related macular degeneration. Pharmacol Rep 2013; 65(2):288-304.

3. Wong BX, Tsatsanis A, Lim LQ, Adlard PA, Bush AI, Duce JA. beta-Amyloid precursor protein does not possess ferroxidase activity but does stabilize the cell surface ferrous iron exporter ferroportin. PLoS One 2014; 9(12):e114174.

4. McCarthy RC, Park YH, Kosman DJ. sAPP modulates iron efflux from brain microvascular endothelial cells by stabilizing the ferrous iron exporter ferroportin. EMBO Rep 2014; 15(7):809-15.

5. Guo LY, Alekseev O, Li Y, Song Y, Dunaief JL. Iron increases APP translation and amyloid-beta production in the retina. Exp Eye Res 2014; 129:31-7.

6. McCarthy RC, Kosman DJ. Mechanisms and regulation of iron trafficking across the capillary endothelial cells of the blood-brain barrier. Front Mol Neurosci 2015; 8:31.

7. Rogers JT, Randall JD, Cahill CM, Eder PS, Huang X, Gunshin H, Leiter L, McPhee J, Sarang SS, Utsuki T, Greig NH, Lahiri DK, Tanzi RE, Bush AI, Giordano T, Gullans SR. An iron-responsive element type II in the 5'-untranslated region of the Alzheimer's amyloid precursor protein transcript. J Biol Chem 2002; 277(47):45518-28.

8. Hahn P, Qian Y, Dentchev T, Chen L, Beard J, Harris ZL, Dunaief JL. Disruption of ceruloplasmin and hephaestin in mice causes retinal iron overload and retinal degeneration with features of age-related macular degeneration. Proc Natl Acad Sci U S A 2004; 101(38):13850-5.

9. Doly M, Bonhomme B, Vennat JC. Experimental study of the retinal toxicity of hemoglobinic iron. Ophthalmic Res 1986; 18(1):21-7.

10. Dick G, Akslen-Hoel LK, Grondahl F, Kjos I, Prydz K. Proteoglycan synthesis and Golgi organization in polarized epithelial cells. J Histochem Cytochem 2012; 60(12):926-35.

11. Schedin-Weiss S, Winblad B, Tjernberg LO. The role of protein glycosylation in Alzheimer disease. FEBS J 2014; 281(1):46-62.

12. Ullrich S, Munch A, Neumann S, Kremmer E, Tatzelt J, Lichtenthaler SF. The novel membrane protein TMEM59 modulates complex glycosylation, cell surface expression, and secretion of the amyloid precursor protein. J Biol Chem 2010; 285(27):20664-74.

13. Nakagawa K, Kitazume S, Oka R, Maruyama K, Saido TC, Sato Y, Endo T, Hashimoto Y. Sialylation enhances the secretion of neurotoxic amyloid-beta peptides. J Neurochem 2006; 96(4):924-33.

14. Ho T, Vessey KA, Cappai R, Dinet V, Mascarelli F, Ciccotosto GD, Fletcher EL. Amyloid precursor protein is required for normal function of the rod and cone pathways in the mouse retina. PLoS One 2012; 7(1):e29892.

15. Harned J, Nagar S, McGahan MC. Hypoxia controls iron metabolism and glutamate secretion in retinal pigmented epithelial cells. Biochim Biophys Acta 2014; 1840(10):3138-44.

16. Chen YH, Chen CL, Liang CM, Liang JB, Tai MC, Chang YH, Lu DW, Chen JT. Silibinin inhibits ICAM-1 expression via regulation of N-linked and O-linked glycosylation in ARPE-19 cells. Biomed Res Int 2014; 2014:701395.

17. Chen Z, Zhang D, Yue F, Zheng M, Kovacevic Z, Richardson DR. The iron chelators Dp44mT and DFO inhibit TGF-beta-induced epithelial-mesenchymal transition via up-regulation of N-Myc downstream-regulated gene 1 (NDRG1). J Biol Chem 2012; 287(21):17016-28.

18. Li P, Zheng X, Shou K, Niu Y, Jian C, Zhao Y, Yi W, Hu X, Yu A. The iron chelator Dp44mT suppresses osteosarcoma's proliferation, invasion and migration: in vitro and in vivo. Am J Transl Res 2016; 8(12):5370-85.

19. Moiseyev G, Takahashi Y, Chen Y, Gentleman S, Redmond TM, Crouch RK, Ma JX. RPE65 is an iron(II)-dependent isomerohydrolase in the retinoid visual cycle. J Biol Chem 2006; 281(5):2835-40.

20. Lall MM, Ferrell J, Nagar S, Fleisher LN, McGahan MC. Iron regulates L-cystine uptake and glutathione levels in lens epithelial and retinal pigment epithelial cells by its effect on cytosolic aconitase. Invest Ophthalmol Vis Sci 2008; 49(1):310-9.

21. McGahan MC, Harned J, Mukunnemkeril M, Goralska M, Fleisher L, Ferrell JB. Iron alters glutamate secretion by regulating cytosolic aconitase activity. Am J Physiol Cell Physiol 2005; 288(5):C1117-24.

22. Chowers I, Wong R, Dentchev T, Farkas RH, Iacovelli J, Gunatilaka TL, Medeiros NE, Presley JB, Campochiaro PA, Curcio CA, Dunaief JL, Zack DJ. The iron carrier transferrin is upregulated in retinas from patients with age-related macular degeneration. Invest Ophthalmol Vis Sci 2006; 47(5):2135-40.

23. Song D, Dunaief JL. Retinal iron homeostasis in health and disease. Front Aging Neurosci 2013; 5:24.

24. Ohno-Matsui K. Parallel findings in age-related macular degeneration and Alzheimer's disease. Prog Retin Eye Res 2011; 30(4):217-38.

25. Apweiler R, Hermjakob H, Sharon N. On the frequency of protein glycosylation, as deduced from analysis of the SWISS-PROT database. Biochim Biophys Acta 1999; 1473(1):4-8.

26. Borsari M, Gabbi C, Ghelfi F, Grandi R, Saladini M, Severi S, Borella F. Silybin, a new iron-chelating agent. J Inorg Biochem 2001; 85(2-3):123-9.

27. Gharagozloo M, Moayedi B, Zakerinia M, Hamidi M, Karimi M, Maracy M, Amirghofran Z. Combined therapy of silymarin and desferrioxamine in patients with beta-thalassemia major: a randomized double-blind clinical trial. Fundam Clin Pharmacol 2009; 23(3):359-65.

28. Moayedi B, Gharagozloo M, Esmaeil N, Maracy MR, Hoorfar H, Jalaeikar M. A randomized double-blind, placebo-controlled study of therapeutic effects of silymarin in beta-thalassemia major patients receiving desferrioxamine. Eur J Haematol 2013; 90(3):202-9.

29. Goralska M, Nagar S, Fleisher LN, Mzyk P, McGahan MC. Source-dependent intracellular distribution of iron in lens epithelial cells cultured under normoxic and hypoxic conditions. Invest Ophthalmol Vis Sci 2013; 54(12):7666-73.

30. Chou HH, Takematsu H, Diaz S, Iber J, Nickerson E, Wright KL, Muchmore EA, Nelson DL, Warren ST, Varki A. A mutation in human CMP-sialic acid hydroxylase occurred after the Homo-Pan divergence. Proc Natl Acad Sci U S A 1998; 95(20):11751-6.

Figure 4.1 Effect of iron chelation on APP levels in RPE RPE cells were grown to confluence then exposed to normoxic or hypoxic conditions in the presence or absence of the iron chelator Dp44mT for 24 (A) or 48 (B) hours. Cell conditioned media (CCM), lysates, and 75 µg of whole rat brain tissue lysate were probed with the APP antibodies 3E9 (CCM), KPI (lysates) or actin. **A:** Effects of iron chelation on RPE CCM and lysates after 24 hours in normoxia and hypoxia. **B:** Effects of iron chelation on RPE CCM and lysates after 48 hours in normoxia and hypoxia. **C:** APP levels in non-polarized RPE lysates after 24 hours in normoxia with iron chelation. * = significantly different ($p = 0.000$) from control from four experiments analyzed statistically in Systat 13 by ANOVA and post-hoc Tukey's HSD.

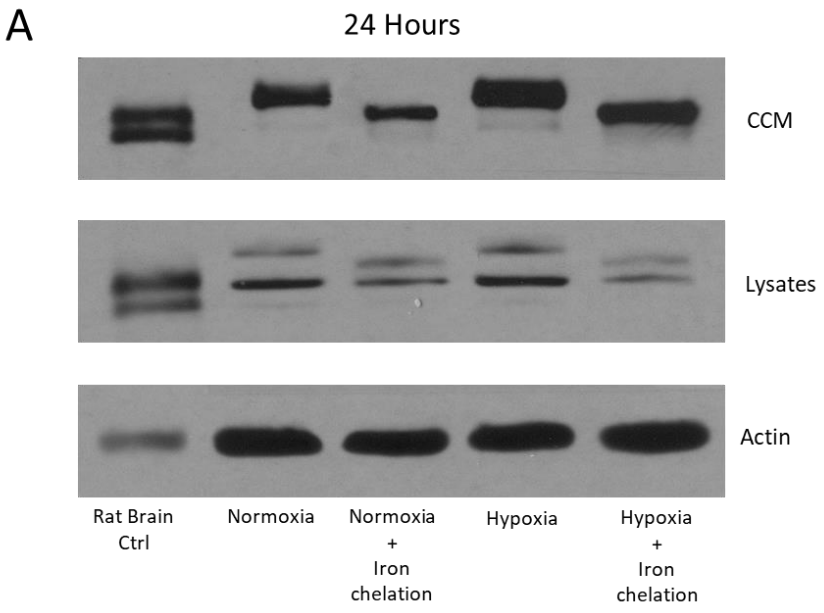
A
24 Hours
CCM
Lysates
Actin
Rat Brain Ctrl
Normoxia
Normoxia + Iron chelation
Hypoxia
Hypoxia + Iron chelation

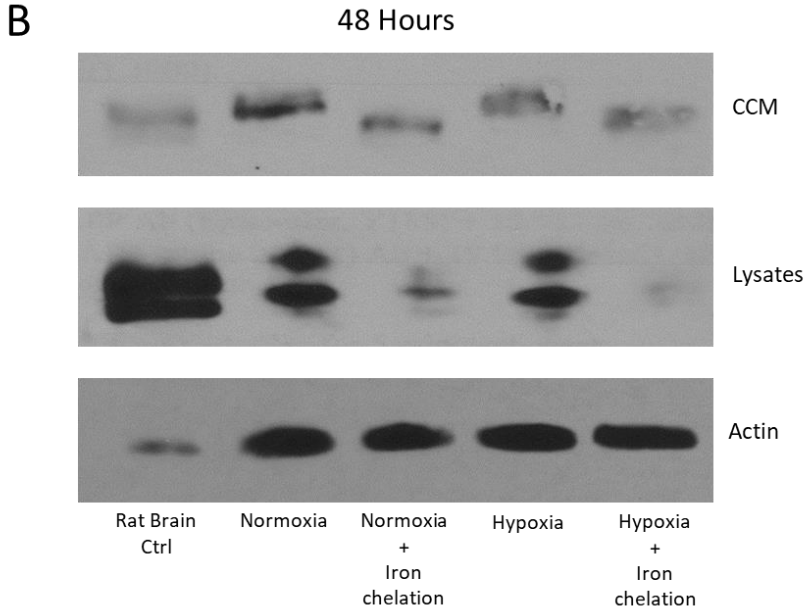
B
48 Hours
CCM
Lysates
Actin
Rat Brain Ctrl
Normoxia
Normoxia + Iron chelation
Hypoxia
Hypoxia + Iron chelation

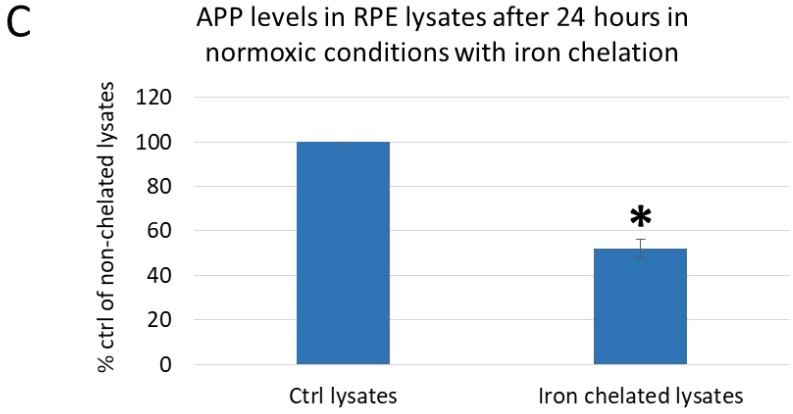
C
APP levels in RPE lysates after 24 hours in normoxic conditions with iron chelation
% ctrl of non-chelated lysates
120
100
80
60
40
20
0
*
Ctrl lysates
Iron chelated lysates

Figure 4.2 Effect of enzymatic deglycosylation and iron chelation on APP levels RPE cells were grown to confluence then exposed to normoxic conditions in the presence or absence of the iron chelator Dp44mT for 24 hours. Lysates were subjected to glycosidase digestion. Digest products were then probed with the APP KPI domain antibody. **A:** Simplified schematic drawing of hypothetical APP glycosylation and sites of enzymatic cleavage. **B:** Enzymatic deglycosylation of APP in RPE lysates after 24 hours in normoxia and iron chelation.

A

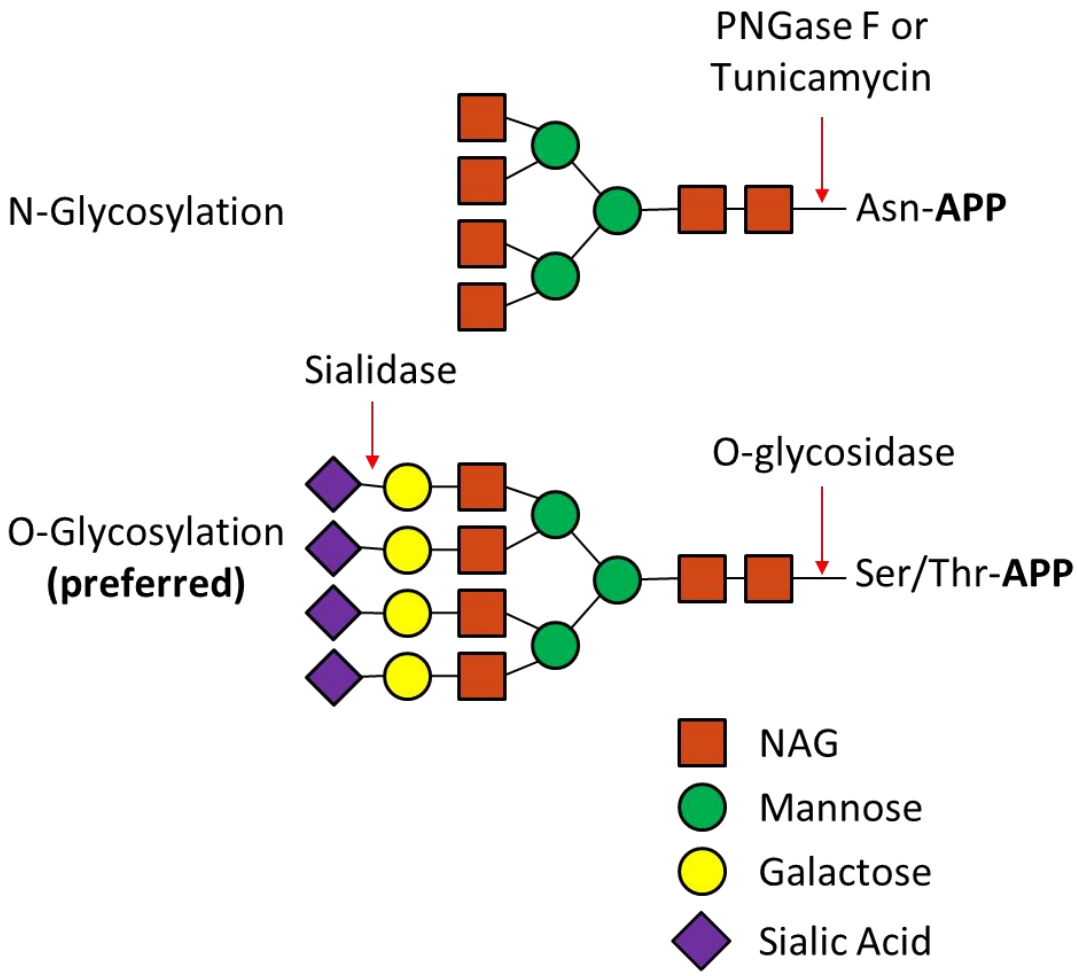

B

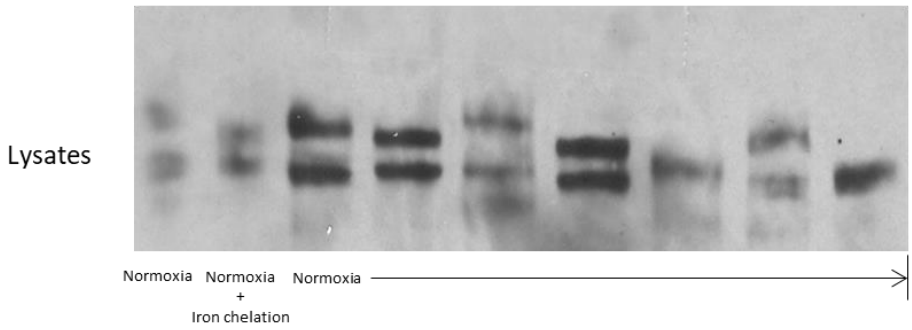

Lane	1	2	3	4	5	6	7	8	9
PNGase F	-	-	+	-	-	+	-	+	+
Sialidase	-	-	-	+	-	+	+	-	+
O-glycosidase	-	-	-	-	+	-	+	+	+

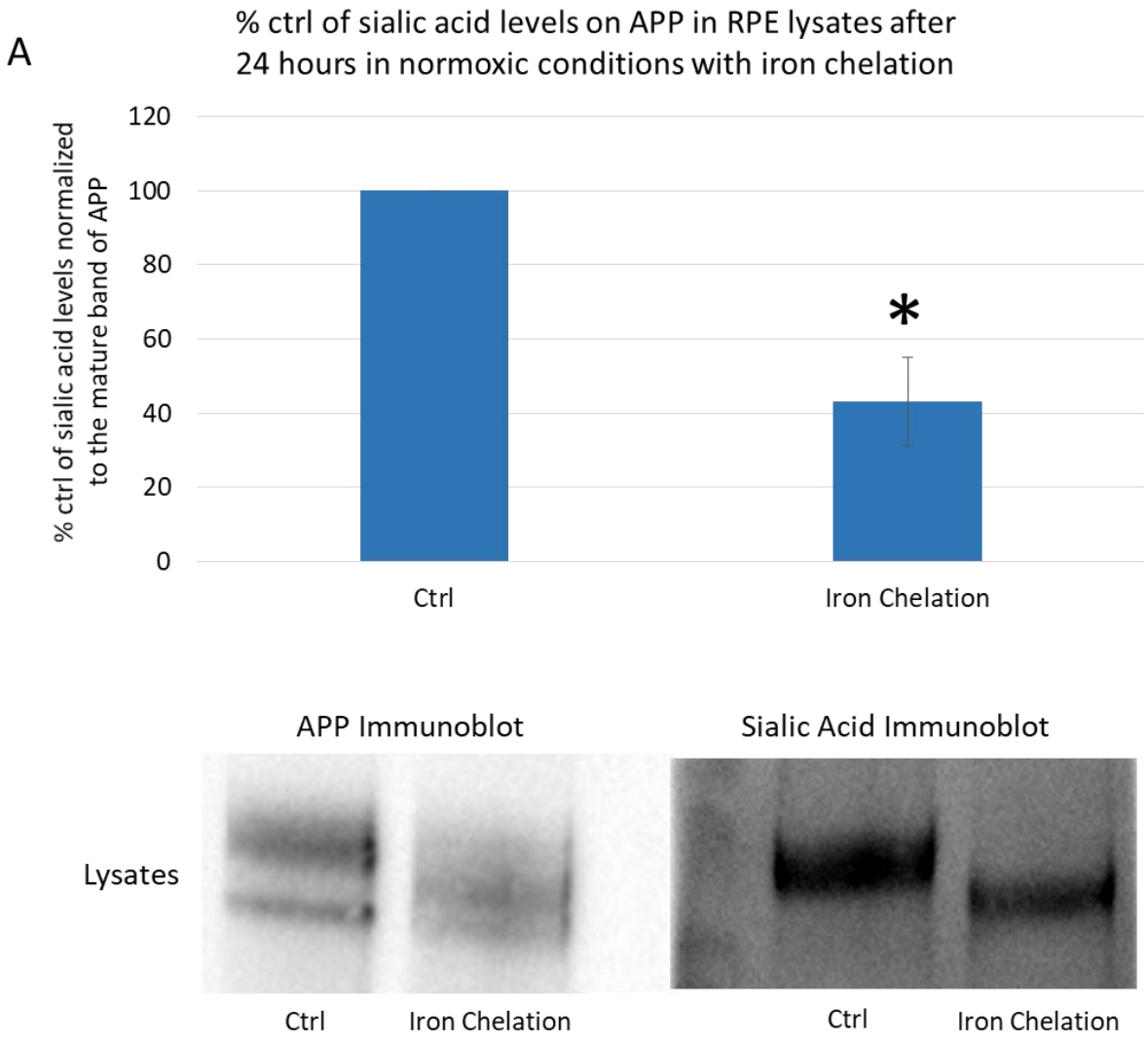

Figure 4.3 Iron chelation alters sialic acid levels on APP RPE cells were grown to confluence. Sialic acid was labeled 6 hours ahead of the application of the iron chelator Dp44mT for 24 hours in normoxic conditions. Lysates were collected and APP was immunoprecipitated, after which immunoblots were probed for APP and sialic acid levels. **A:** Sialic acid levels on APP in RPE lysates after iron chelation in normoxic conditions, with representative APP and sialic acid immunoblots below the graph. * = significantly different from control from four experiments analyzed statistically in Systat 13 using percent control data by paired t-test and SEM.

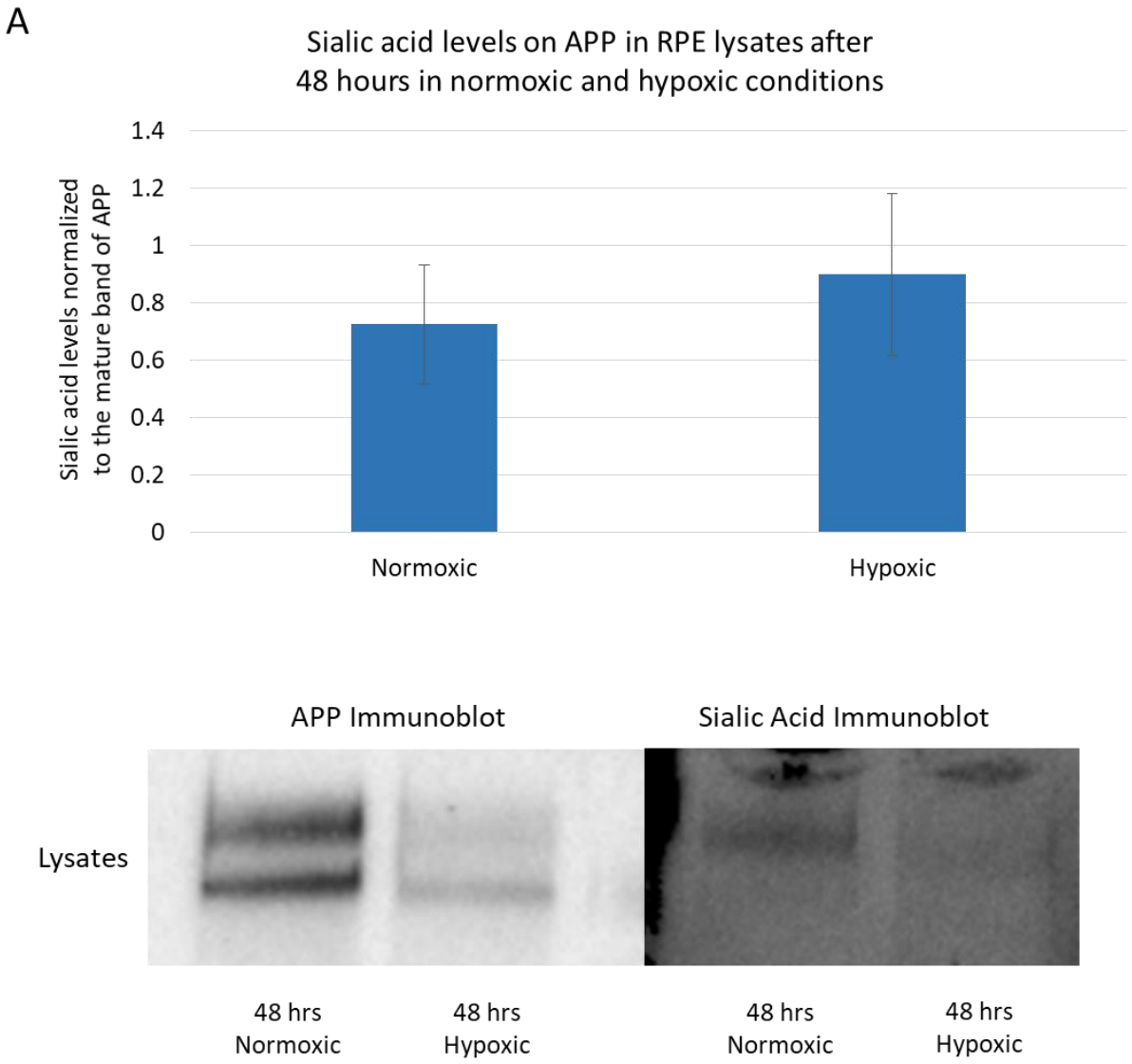

Figure 4.4 Hypoxia does not alter sialic acid levels on APP RPE cells were grown to confluence. Sialic acid was labeled 6 hours ahead of the cells being placed in normoxic or hypoxic conditions for 48 hours. Lysates were collected and APP was immunoprecipitated, after which immunoblots were probed for APP and sialic acid levels. **A:** Sialic acid levels on APP in RPE lysates after 48 hours in normoxic or hypoxic conditions, with representative APP and sialic acid immunoblots below the graph.

CHAPTER 5

Conclusions and Future Directions

The work described in this dissertation demonstrated that the metabolism of the amyloid precursor protein (APP) within retinal pigmented epithelial (RPE) cells is susceptible to changes in both the oxygen and iron environment within the eye. Hypoxia was first shown to lower intracellular levels and secretion of APP. We determined if the lowered amount of APP in RPE cells was due to a decrease in synthesis or an increase in degradation of APP. Alterations in the lysosomal and proteasomal degradation pathways were not found to be the cause of the reduction in intracellular APP levels. Specifically, inhibition of the lysosomal and proteasomal pathways did not reverse the hypoxia induced decrease in APP levels. Overall, the finding that hypoxia decreases the synthesis of APP is what is believed to be altering the levels of APP within the RPE. This finding was also in line with studies that have shown that hypoxia is able to decrease the synthesis of proteins within the brain [1]. Since the eye is an extension of the brain, conditions that affect the brain should have similar effects on the eye. Also, since APP aids in iron export, a reduction in APP levels during hypoxia likely impairs the ability of the RPE to properly metabolize iron, thus contributing to deleterious effects on the RPE. It would be advantageous to investigate the specific mechanism by which hypoxia is altering the synthesis of APP. Is it at the transcriptional level, or is there a post translational mechanism that is causing APP levels to be altered?

As mentioned above, the levels of APP in RPE lysates were lowered in hypoxia, and its apical secretion was severely diminished as well. The mechanism by which hypoxia alters APP's secretion is still to be elucidated. Is APP being improperly sorted in hypoxia? This may be possible, as APP secretion was also affected when the protein transporter complex retromer was knocked down with siRNA. Since hypoxia also lowered retromer expression, it may be that APP is not able to be properly sorted within the cell to the correct domain when retromer is not

present, thus explaining its diminishment in apical secretion. There is precedent for the idea that hypoxia can alter the directionality of protein secretion, since vascular endothelial growth factor has been shown to be secreted more in the basolateral direction in hypoxic conditions [2]. Alternatively, hypoxia may alter the ability of APP to be properly modified as it transits through the ER and Golgi. Improper modification could result in improper sorting signals being attached to APP, leading to an alteration in its secretion.

Our lab has shown that hypoxic conditions cause a vast efflux of iron from the cell, specifically in the basolateral direction [3]. One might then expect that since iron chelation caused a significant change in the maturation of APP, specifically due to altering the sialyation of APP, that hypoxia might have a similar effect. However, under hypoxia, APP maturation was not affected. Iron is thought to exist within the cell in multiple discrete labile iron pools that can be differentially utilized by the cell when iron is needed [4]. However, it is not known how or where these pools of iron exist and how they are regulated within the cell. This may be one way to explain how hypoxia did not alter APP glycosylation, but iron chelation did.

One limitation on the above mentioned oxygen studies were the oxygen levels that the RPE were placed in to simulate normoxia. While we did determine that the 0.5% oxygen level was inducing hypoxic stress on our RPE cells, we now know that the normoxic levels we utilized are not the true physiologic levels of oxygen that the RPE, and the eye as a whole, are normally exposed to [5, 6]. Future studies should be done with the RPE cells placed in a more physiologically relevant oxygen level when simulating normoxic conditions.

Our studies imply that a lack of iron may be limiting the addition, or causing the removal, of sialic acid to APP. Additionally, it should be investigated how a loss of iron affects the underlying sugars that form before the addition of sialic acid. Is it possible for a loss of iron to

alter the levels of other sugars on APP, thereby limiting sialic acid addition? If so, this could further alter the subcellular localization and secretion of proteins by altering the signaling pathways that are often define by glycans that are added to proteins. Also, at what levels of iron depletion are these changes in glycan levels on proteins seen? Is a total loss of iron necessary for alterations to occur in the glycosylation pathway, or does a certain threshold of iron loss need to occur before the cell will have its ability to properly glycosylate proteins altered?

This change in the levels of sialic acid on APP also has implications for APP's localization. Sialic acid is involved in the localization of proteins within the cell by acting as a signal that can be read to determine where that protein should be localized within the cell and which domain of the cell that protein should be secreted from [7]. By causing a decrease in sialic acid on APP, APP could be improperly localized, thus impairing its processing and section from the RPE. This improper localization could cause ocular pathologies.

Further study is warranted to determine how specifically iron is affecting the glycosylation of APP. One enzyme that regulates sialic acid metabolism, CMP-Neu5Ac hydroxylase, is an iron dependent enzyme which converts the acetylated form of sialic acid to the hydroxylated form, Neu5Gc. These two forms of sialic acid are the most common sialic acids in mammalian cells [8]. Additionally, the iron chelator silibinin regulates N- and O-linked glycosylation in the ARPE-19 cell line [9]. Our prevailing hypothesis for the changes that we saw in sialic acid levels on APP is that the enzyme responsible for the addition of sialic acid to proteins, sialyltransferase, may be iron dependent. To test this theory, it would be necessary to carry out enzyme activity assays on sialyltransferase in the presence and absence of iron. Additionally, non-sialylated APP could be tagged and tracked within the RPE to determine how a lack of sialic acid affects the localization of APP. Both of these experiments would help to

further elucidate the importance of sialic acid, not just for APP, but for other sialylated proteins throughout the body. However, it may be that other parts of the glycosylation pathway are being altered by iron loss. It would be beneficial to study the activity of numerous glycosylation enzymes to see if they are iron dependent.

RPE cells are unique in that their apical surface is in direct contact with the photoreceptor outer segments of the retina [10]. To study this unique relationship between the RPE and the photoreceptors, we utilized a quantitative fluorescent assay coupled with siRNA knockdown of APP. This assay showed that APP may have a role as either a membrane receptor or cell adhesion molecule in the phagocytosis of photoreceptor outer segments. This is a remarkable novel finding that begins to shed light on the important roles that APP may have in degenerative diseases of the eye. Improper photoreceptor phagocytosis could lead to a buildup of waste material at the apical domain of the RPE, impeding their ability to properly function, and ultimately causing vision loss. Future studies will need to be done to confirm in what capacity APP is involved in the photoreceptor phagocytosis pathway. Building upon the APP siRNA knockdown study, it would be beneficial to see within our RPE system how photoreceptor phagocytosis is impaired when the classical proteins involved in the pathway are knockdown down, specifically the αvβ5 integrins and MerTK. A widespread proteomics study to compare the properties of APP to the classical phagocytosis proteins would also be helpful in elucidating how APP may factor into this pathway.

REFERENCES

1. Preedy VR, Smith DM, Sugden PH. The effects of 6 hours of hypoxia on protein synthesis in rat tissues in vivo and in vitro. Biochem J 1985; 228(1):179-85.

2. Blaauwgeers HG, Holtkamp GM, Rutten H, Witmer AN, Koolwijk P, Partanen TA, Alitalo K, Kroon ME, Kijlstra A, van Hinsbergh VW, Schlingemann RO. Polarized vascular endothelial growth factor secretion by human retinal pigment epithelium and localization of vascular endothelial growth factor receptors on the inner choriocapillaris. Evidence for a trophic paracrine relation. Am J Pathol 1999; 155(2):421-8.

3. Harned J, Nagar S, McGahan MC. Hypoxia controls iron metabolism and glutamate secretion in retinal pigmented epithelial cells. Biochim Biophys Acta 2014; 1840(10):3138-44.

4. Goralska M, Nagar S, Fleisher LN, Mzyk P, McGahan MC. Source-dependent intracellular distribution of iron in lens epithelial cells cultured under normoxic and hypoxic conditions. Invest Ophthalmol Vis Sci 2013; 54(12):7666-73.

5. Beebe DC, Shui YB, Siegfried CJ, Holekamp NM, Bai F. Preserve the (intraocular) environment: the importance of maintaining normal oxygen gradients in the eye. Jpn J Ophthalmol 2014; 58(3):225-31.

6. Caprara C, Grimm C. From oxygen to erythropoietin: relevance of hypoxia for retinal development, health and disease. Prog Retin Eye Res 2012; 31(1):89-119.

7. McFarlane I, Georgopoulou N, Coughlan CM, Gillian AM, Breen KC. The role of the protein glycosylation state in the control of cellular transport of the amyloid beta precursor protein. Neuroscience 1999; 90(1):15-25.

8. Chou HH, Takematsu H, Diaz S, Iber J, Nickerson E, Wright KL, Muchmore EA, Nelson DL, Warren ST, Varki A. A mutation in human CMP-sialic acid hydroxylase occurred after the Homo-Pan divergence. Proc Natl Acad Sci U S A 1998; 95(20):11751-6.

9. Chen YH, Chen CL, Liang CM, Liang JB, Tai MC, Chang YH, Lu DW, Chen JT. Silibinin inhibits ICAM-1 expression via regulation of N-linked and O-linked glycosylation in ARPE-19 cells. Biomed Res Int 2014; 2014:701395.

10. Mao Y, Finnemann SC. Analysis of photoreceptor outer segment phagocytosis by RPE cells in culture. Methods Mol Biol 2013; 935:285-95.

APPENDICES

Appendix 1

Nascent Synthesis Analysis of APP Utilizing ^{35}S Methionine

In Chapter 2, we found that hypoxia dramatically decreased APP levels and secretion in retinal pigmented epithelial (RPE) cells. Chapter 3 explained the mechanisms used to investigate how hypoxia was affecting APP levels and secretion. We investigated whether increased degradation, decreased synthesis, or both contributed to the decrease in APP due to hypoxia. Prior to the methods used in Chapter 3, we first investigated the effects of hypoxia on nascent APP synthesis by employing radioactive metabolic labeling of APP [1].

To carry out the radioactive labeling of APP, RPE cells were grown to confluence, and then starved of methionine for 30 minutes to deplete the cells methionine reserves. After 30 minutes, fresh methionine free media was added to the cells, along with ^{35}S labeled methionine. This radioactive methionine is able to incorporate into all proteins being synthesized within the cell. After 16 hours in normoxic or hypoxic conditions, cells were harvested. Before the lysates were immunoprecipitated for APP, some lysate was reserved for the trichloroacetic acid (TCA) assay and for measuring total radioactive levels. The TCA assay allows for the normalization of radiolabeled proteins [2]. In brief, radiolabeled proteins are precipitated with TCA and quantitated by scintillation spectroscopy. This quantitation can be normalized to the total radioactivity measured in the reserved lysate that was not precipitated with TCA. This normalization step shows how much protein was labeled by the radiative tag, with a higher percentage labeled ensuring that most proteins within the cell were effectively labeled.

Immunoprecipitated samples not utilized for normalization were run on a gel and the radiolabel APP was imaged with a personal molecular imager from Bio-Rad. A representative image of radiolabeled APP is shown in Figure App 1.1. Though the efficiency of protein

radiolabeling was generally very high, visualizing the radioactive bands clearly was difficult. This made quantitation of the changes in APP synthesis difficult. Because of this challenge, the decision to use biorthogonal chemistry to label methionine to study the synthesis of APP was employed as explained in Chapter 3.

REFERENCES

1. Esposito AM, Kinzy TG. In vivo [35S]-methionine incorporation. Methods Enzymol 2014; 536:55-64.

2. Pollard JW. The in vivo isotopic labeling of proteins for polyacrylamide gel electrophoresis. Methods Mol Biol 1994; 32:67-72.

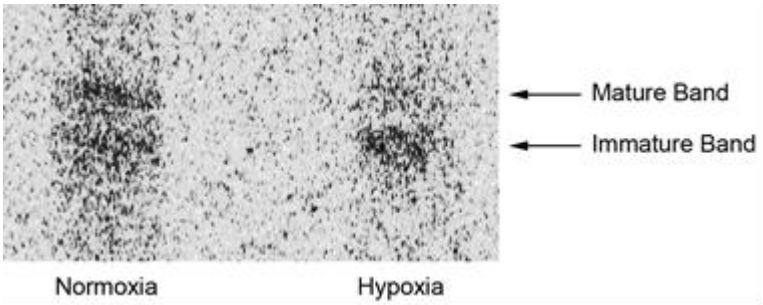

Figure App 1.1 APP levels after incorporation of ^{35}S methionine RPE cells were grown to confluence, after which media was switched to methionine free media for 30 minutes to deplete methionine reserves. After methionine depletion, ^{35}S methionine was added and cells were incubated for 16 hours in normoxic or hypoxic conditions. After 16 hours, cells were harvested, immunoprecipitated for APP, run on a gel, and imaged for the radioactivity of ^{35}S to determine the synthesis of APP under the experimental conditions.

Appendix 2

Mass Spectrometry and Lectin Blotting for Analysis of APP Glycosylation

Diverse structures of glycoproteins are involved in a variety of biological events including functional maintenance of tissues and the polarized movement of intracellular proteins [1]. Analysis of such glycan structures is, therefore, essential for understanding protein function. In order to obtain information about the structures of glycans on glycoproteins, common forms of analyses are high-performance liquid chromatography, nuclear magnetic resonance, mass spectrometry, as well as lectin blotting [1]. To study the glycosylation profile of APP, mass spectrometry and lectin blotting were employed in this work, in addition to the biorthogonal chemistry used in chapter 3.

APP exists primarily as 3 different splice variants, APP_{695} is found mainly in the brain, whereas most tissues contain APP_{770} [2]. As described in Chapter 2, we found that the form of APP in retinal pigmented epithelial (RPE) cells is APP_{770} because it contains the KPI motif, not found in APP_{695}, and the OX-2 motif, not found in either APP_{695} or APP_{751}. After synthesis, APP undergoes extensive glycosylation as discussed in Chapter 1. The glycosylation of APP was investigated to determine how alterations in glycan structure caused by altered iron levels impacted APP function within the RPE.

Previous work from this lab demonstrated that iron chelation with Dp44mT significantly lowered the size of the mature band of APP (Figure App 2.1). The results presented in Chapter 4 helped to explain how the maturation of APP in the RPE may be affected by iron. Enzymatic digest studies indicated that sialic acid levels were likely being altered on APP because treatment with sialidase resulted in a decrease in size of the mature band to that found in chelator treated samples (Figure App 2.1). It is possible that iron chelation either inhibited sialic acid addition or

caused its removal from APP. Subsequent work shown in Chapter 4 utilizing biorthogonal chemistry to label sialic acid on APP then showed that sialyation of APP is altered when iron is chelated in RPE cells. Mass spectroscopy and lectin blotting were first used to study the sialic acid content of APP in normal conditions and upon iron chelation treatment.

Mass spectrometry was employed because of its ability to analyze protein structure in extreme detail, potentially at a resolution capable of uncovering individual glycan additions. The ultimate aim was to understand which glycans were being affected by iron chelation in order to confirm our enzymatic analysis data. As the cells used in this work come from the canine eye, it was extremely beneficial that that amino acid sequence of canine APP had been determined. Canine APP and human APP have been shown to have 97% amino acid identity, and an overall similarity of 98% [3]. Similarity refers to residues that although different among sequences, belong to the same chemical family of amino acids. Because of this high similarity and amino acid identity, and because APP's N- and O- linked glycosylation sites have been defined on human APP, the mass spectrometry analysis of canine APP can be guided by the human data, simplifying a determination of glycosylation state changes. It was believed that utilizing mass spectrometry would allow for superb resolution and quantification of the glycosylation state changes in APP that occur in RPE cells due to iron chelation.

Dr. Michael Bereman, an expert in liquid chromatography tandem mass spectrometry at North Carolina State University, analyzed APP protein samples that I provided to him to uncover the discrete glycosylation changes that occur after iron chelation. RPE samples were immunoprecipitated for APP, utilizing the Thermo Scientific™ Pierce™ MS-Compatible Magnetic Immunoprecipitation Kit (Protein A/G) and a monoclonal antibody for APP (Y188 clone). Dr. Bereman utilized a state of the art mass spectrometer for these proteomic studies, in

addition to using an assortment of exo- and endoglycosidases to analyze the changes in APP glycosylation caused by iron chelation. The results of the mass spectrometry analysis of the APP samples were then blasted against the known and almost identical canine and human sequences of APP.

The analysis of APP samples provided yielded 38.3% sequence coverage against the known APP sequence, and included twenty peptide fragments within that sequence coverage (Figure App 2.2). There is a large number of possible glycosylation modification on APP, therefore specialized bioinformatics software was used to identify glycopeptides. On the twenty peptides found, two were found to be O-linked glycopeptides. However, it was not possible to obtain high enough resolution to observe the terminal glycans found on these glycopeptides. The resolution needed to observe sialic acid using mass spectrometry was not possible. Because of this we decided to try another type of specific analysis of sialic acid residues called lectin blotting.

Lectin-probed western blot analysis is a useful method to yield basic information on the glycan structures of glycoproteins, based on the carbohydrate-binding specificities of lectins [4]. By lectin blot analysis, glycan structures on proteins can be analyzed without releasing the glycans from glycoproteins. Lectin blot analysis is a simple and useful method based on western blot analysis, wherein lectins are utilized to bind to sugars and do so with a high affinity for glycopeptides in particular. The combination of glycosidase digestion and lectin blotting provides information regarding the carbohydrate structures at the nonreducing termini, types of N-glycan subgroups, and presence or absence of O-glycans in individual glycoproteins [4]. The glycosylation patterns between the control and test group can then be compared by lectin blot analysis.

To study the sialyation of APP after iron chelation, biotinylated *Sambucus nigra* elderberry bark lectin (SNA) was used. The SNA lectin was chosen because it has a strong affinity for glycoproteins with the terminal sequence Neu5Acα6GalNAc [4, 5]. N-Acetylneuraminic acid (Neu5Ac) is also known as sialic acid, and it is the terminal glycopeptide on APP. N-Acetylgalactosamine (GalNAc) is the glycopeptide sialic acid is bound to. The link binding these two glycopeptides together on APP is known to be present in the α6 confirmation [6]. This means that on the nine carbon backbone found on sialic acid, the second carbon on sialic acid forms a bond with the six carbon on the backbone of GalNAc. This α6 linkage that occurs between sialic acid and GalNAc is a common linkage found on APP. However, an α3 linkage can also form between sialic acid and GalNAc [6, 7]. This linkage can be detected by the *Maackia amurensis* (MMA) lectin. Both SNA and MMA were tested, but SNA gave a stronger signal upon blotting.

Lectin blotting of APP immunoprecipitated from lysates of Dp44mT treated RPE cells appeared to show a reduction in the intensity of the mature APP band, indicating that there is reduced sialic acid on APP after iron chelator treatment (Figure App 2.3). However, the APP bands on these lectin blots were very hard to differentiate from the background on the blot, and were deemed not sufficient enough to provide evidence that sialic acid levels were being altered on APP due to iron chelation. Therefore, since mass spectroscopy or lectin blotting did not give enough detail and resolution to understand sialic acids interactions with APP, biorthogonal chemistry was ultimately used to study changes in sialic acid levels on APP. That work, described in Chapter 4, showed that sialyation of APP is altered when iron is chelated in RPE cells.

REFERENCES

1. Moremen KW, Tiemeyer M, Nairn AV. Vertebrate protein glycosylation: diversity, synthesis and function. Nat Rev Mol Cell Biol 2012; 13(7):448-62.

2. Zheng H, Koo EH. Biology and pathophysiology of the amyloid precursor protein. Mol Neurodegener 2011; 6(1):27.

3. Sarasa L, Gallego C, Monleon I, Olvera A, Canudas J, Montanes M, Pesini P, Sarasa M. Cloning, sequencing and expression in the dog of the main amyloid precursor protein isoforms and some of the enzymes related with their processing. Neuroscience 2010; 171(4):1091-101.

4. Zuber C, Li WP, Roth J. Blot analysis with lectins for the evaluation of glycoproteins in cultured cells and tissues. Methods Mol Med 1998; 9:159-66.

5. Shibuya N, Goldstein IJ, Broekaert WF, Nsimba-Lubaki M, Peeters B, Peumans WJ. The elderberry (Sambucus nigra L.) bark lectin recognizes the Neu5Ac(alpha 2-6)Gal/GalNAc sequence. J Biol Chem 1987; 262(4):1596-601.

6. Schedin-Weiss S, Winblad B, Tjernberg LO. The role of protein glycosylation in Alzheimer disease. FEBS J 2014; 281(1):46-62.

7. Ulloa F, Real FX. Differential distribution of sialic acid in alpha2,3 and alpha2,6 linkages in the apical membrane of cultured epithelial cells and tissues. J Histochem Cytochem 2001; 49(4):501-10.

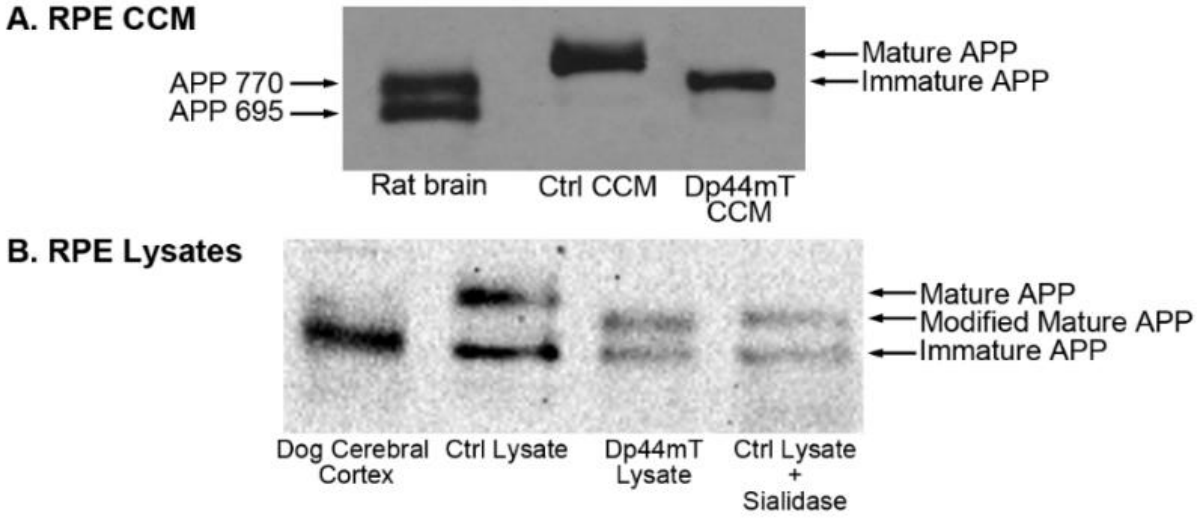

Figure App 2.1 Effect of iron chelation on APP expression in RPE RPE cells were incubated for 24hrs in the presence or absence of Dp44mT and the resulting CCM (A) and lysates (B) were immunoblotted for APP. Additional control lysates were treated with 5mU sialidase prior to immunoblotting. CCM, cell conditioned media; Ctrl, control; Dp44mT, 2,2'-Dipyridyl-N,M-dimethylsemicarbazone

Figure App 2.2 Peptide Analysis of APP Mass Spec Samples RPE cells were incubated for 24hrs and the resulting lysates were immunoprecipitated for APP and then analyzed by mass spectroscopy, resulting in 38.3% sequence coverage. More green lines under the sequence shows that sequence was identified multiple times and had multiple mass spectrums produced. Two O-linked glycopeptides sites are identified in the red boxes.

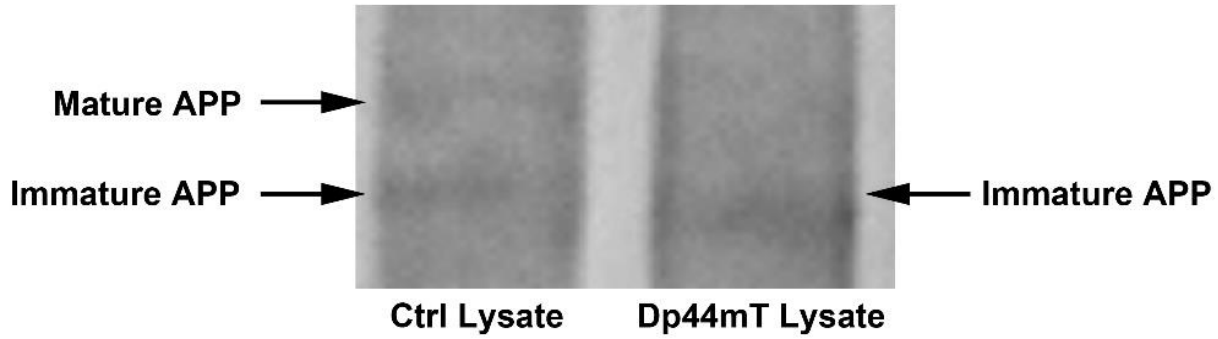

Figure App 2.3 Iron affects the sialyation of APP RPE cells were treated with either DMSO (vehicle control) or 30µM of Dp44mT. Lysates were collected and immunoprecipitated for APP. The immunoprecipitated lysates were run on a lectin blot utilizing the *Sambucus nigra* lectin which preferentially binds α-2,6 sialic acid. The control lysate displays one band each for the mature and immature form of APP and the Dp44mT lysate displays only the immature form of APP.